Division of Biomedical Engineering

Department of Human Biology

University of Cape Town

Optimisation of insertion point during latissimus dorsi tendon transfer

Dissertation

In fulfilment of the requirements for the degree:

MSc in Biomedical Engineering

Seth Thompson (THMSET001)

Supervisor: Dr. Sudesh Sivarasu

Co-supervisors: Dr. Stephen Roche

27 May 2018

DECLARATION

I, *Seth Thompson* hereby declare that the work on which this dissertation/thesis is based is my original work (except where acknowledgements indicate otherwise) and that neither the whole work nor any part of it has been, is being, or is to be submitted for another degree in this or any other university.

I empower the university to reproduce for the purpose of research either the whole or any portion of the contents in any manner whatsoever.

Signature: Signed by candidate

Date: ……28/05/2018…….

Name: Seth Thompson

Student Number: THMSET001

Course: Masters Dissertation

Declaration

I know that plagiarism is wrong. Plagiarism is to use another's work and pretend that it is one's own.

I have used the APA convention for citation and referencing. Each contribution to, and quotation in, this dissertation from the work(s) of other people has been attributed and has been cited and referenced.

This dissertation is my own work.

I have not allowed, and will not allow, anyone to copy my work with the intention of passing it off as his or her own work.

Signature Signed by candidate

Date 27/05/2018

Contents

List of Figures

Abstract

Problem and Motivation

Posterior rotator cuff injuries are common (Yamaguchi et al., 2006), (Neri et al., 2009) and often debilitating and irreparable (Sim et al., 2001). Latissimus dorsi (LD) tendon transfers have been shown to be an effective treatment for these massive or irreparable tears (Habermeyer, 2006), (De Casas et al., 2014). This procedure can have unpredictable outcomes (Ling et al., 2009). This is partially caused by discrepancies in the suggested insertion site for the LD tendon during transfers. The current literature is composed of *in-silico* studies which ignore the practicalities of the human body (Magermans et al., 2004), *in-vivo* studies which use subjective pain scores, and small scale cadaver trials. For these reasons, a study is needed that uses the power of *in-silico* modeling in a way that is verified using *in-vitro* testing on cadavers.

Aims and Objectives

The aim of this study is to determine the effects of varying the insertion point of the LD tendon on the humeral head to treat posterior rotator cuff tears in terms of the effects on strength, primarily in rotation and in flexion over a range of motion. The objectives are to use an *in-silico* model to define the effects of various insertion points and validate this model using a cadaver trial before presenting the final findings.

Methods

In-silico Model

The Upper Extremity Model (Holzbaur et al., 2005) was used to simulate tendon transfers. The moment arms in flexion and rotation were measured and recorded at angles of 0° and 90° of forward

elevation. The moment arms at each point were then projected onto humeral maps to display the results.

Cadaver Trial

Four fresh frozen cadaver torsos (eight shoulders) were mounted into a specifically designed rig. The LD was transferred to 7 points illustrative of the humeral head. The strain generated by the humerus in rotation on the clamps was measured at 0° and 90° of forward flexion for each point. These were then compared.

Results

In-silico Model

- The *in-silico* moment arm maps were generated and analysed. The optimal point for external rotation at 0° of flexion was the lesser tuberosity. Moment arms to produce external rotation were found over the entire greater tuberosity. Flexion was only generated on the posterior edge of the greater tuberosity.
- At 90° of flexion, little to no rotation generating moment arms were found in the lesser tuberosity and the anterior ridge of the greater tuberosity. Rotation generating moment arms were not significantly different between the posterior edge and the face of the greater tuberosity. No areas generated flexion moment arms.

Cadaver Trial

- At 0° of flexion, the lesser tuberosity (point 1) generated the most flexion, with the greater tuberosity (points 2-7) also generating external rotation, but at reduced levels.
- At 90° of flexion, the lesser tuberosity and the anterior ridges of the greater tuberosty (points 1-3) generated no significant rotation. The posterior ridge and face of the greater tuberosity generated similar amounts of flexion, greater than points 1-3

Conclusions

The *in-silico* model was validated in rotation by the cadaver trials and this validation was extended to flexion. For maximum rotation strength at 0° of flexion and no flexion strength, the

lesser tuberosity is the optimal point. For maximum rotation strength and no flexion throughout the motion of flexion, the middle of the face of the greater tuberosity is the optimal area. For maximum rotation throughout the motion of flexion, points 4 and 5 (the posterior edge of the greater tuberosity) represent the optimal area for insertion. This area represents the optimal compromise in terms of range of motion and strength.

Chapter 1

Introduction

1.1 Background Overview of the Research Project

Posterior rotator cuff injuries can severely limit a patient's ability to complete activities of daily living such as eating, brushing teeth,grooming hair, and reaching for objects above shoulder height. These activities are limited by an inability to externally rotate the humerus against gravity, which is caused by massive* tears in either of the teres minor, supraspinatus or infraspinatus muscles. If these tears are considered to be irreparable then a latissimus dorsi (LD) transfer can be used to restore external rotation. This procedure was first introduced by Gerber et al. (1988) in 1988 and has subsequently been modified by surgeons including being adapted for a single incision surgery by Habermeyer (2006). There is little evidence in the literature that defines the optimal insertion point of the LD tendon to restore rotation function to the joint. This project combines cadaver and biomechanical models to understand the effects of the insertion point position and predict improvements in surgical outcomes.

1.2 Problem Statement

Due to a lack of definitive research into the effects of various insertion points for the LD tendon during a transfer, it is difficult to know whether the current insertion points are the most beneficial for reducing the loss of strength caused by these tears. Many of the studies that have been carried out previously on cadavers and live patients had small sample populations or have been performed *in-silico* without any verfication of the model. Small population samples do not allow for a sufficient number of tests to be performed for any human error or human variance to be removed from the results. It is also important to note that many of these *in-vivo* studies have involved other patholo-

*See definition of massive tears in section 2.2.1 in chapter 2

gies or surgeries, such as a total reverse shoulder arthroplasty, which change the biomechanics of the shoulder joint. This problem is well described by Ling et al. (2009) where the unpredictability of the success of this procedure is described. The biomechanical studies, as mentioned above, have lacked any kind of validation from *in-vivo* (live patient) / *in-vitro* (cadaver / bench) tests. This is emphasized by Magermans et al. (2004) where the possible impracticalities such as lack of space caused by muscle volumes, which are not factored into mathematical models, are mentioned as a drawback. This research combines these two kinds of studies, *in-silico* and a cadaver trial, to provide a comprehensive solution to the problem of the effects of varying the insertion points for LD tendon transfer.

1.3 Hypothesis

It is hypothesised that there is an optimal point on the humerus for the insertion of the LD tendon in order to treat massive irreparable posterior rotator cuff tears in an otherwise healthy shoulder. It is hypothesised that this point can be found using mathematical biomechanical models comparing the muscle moment arms at certain points and ratified using cadaver testing of a limited number of motions and joint positions.

1.4 Rationale and Prevalence

Yamaguchi et al. (2006) state that, in 2006, 17 million American citizens were affected by rotator cuff disease, while Neri et al. (2009) claims it is one of the most common musculo-skeletal disorders around. Some of these tears (between 16% and 43% according to Sim et al. (2001)) can be classified as massive or irreparable.

An irreparable posterior rotator cuff tear has a drastic effect on the quality of life of the patient as the inability to externally rotate the shoulder means that the patient cannot perform activities of everyday living such as eating, brushing teeth, grooming hair or washing of the axilla Magermans et al. (2004), Bargoin et al. (2016). Gerber et al. (2006) as well as many other authors have described the positive effect that a LD tendon transfer has in reducing pain, restoring movement and improving quality of life. This has also been described by De Casas et al. (2014) and Habermeyer (2006) reporting that 78 % (De Casas et al., 2014) and 92.9 % (Habermeyer, 2006) of patients would be willing to undergo the surgery again.

The necessity of this research becomes apparent when the current literature on LD tendon transfers is reviewed. There is a lack of information describing the effects of varying the insertion point when performing a LD tendon transfer. The research that has been conducted used small sample sizes

and subjective pain measurements or unverified *in-silico* models. Bargoin et al. (2016) calls for cadaver studies to verify the computer models, as a lack of verification leads to uncertainty in the most effective insertion point. This adds to the unpredictability of the procedure described by Ling et al. (2009).

The gaps in literature mentioned in this section lead us to the conclusion that there is a need for combined *in-silico* simulation and cadaver or clinical studies to verify large ranges of possible insertion points. This study aims to have a positive effect on many patients and to improve the outcomes of LD transfers.

1.5 Aims of Research

The aim of this research is to improve the outcomes of LD transfer surgeries used to treat massive posterior rotator cuff tears by optimising the insertion point on the humerus using combined *in-silico* biomechanical and cadaver studies.

1.6 Objectives of the Study

This study has the following objectives to achieve these aims:

i) To design an *in-silico* biomechanical model to determine the effects of varying the point of insertion for LD tendon transfers.

ii) Design and build a rig to test and compare the results of tendon transfers at various points on the proximal humerus by using a cadavaric torso as a specimen.

iii) Define the effects of varying the LD insertion point to assist in surgical planning.

1.7 Expected Outcomes of the Dissertation

This dissertation has three main outcomes based on the objectives.

i) A program to simulate and analyse the outcomes from multiple LD tendon transfers in Opensim in terms of various parameters using a predefined shoulder model.

ii) A rig that can test the success of a LD tendon transfer by measuring the effect of static loads on the muscle in terms of the resulting load exerted by a cadaver shoulder at more than one humeral position.

iii) A set of conclusions outlining the effects of various insertion points on the humeral head for LD transfers to impove surgical outcomes in terms of rotation and flexion strength.

1.8 Scope and Limitations of the Research

As with any medical research, this project had the ability to be infinitely complex. To ensure the scope was controlled, this project assumed that the most appropriate surgery for the patient was a LD tendon transfer and did not attempt to define when this procedure would be most appropriate. Neither did this project seek to find a solution involving multiple tendon transfers as stated by Magermans et al. (2004).

In order to analyse the surgeries computationally, an existing shoulder model (Upper Extremity Model (Holzbaur et al., 2005)) was used. This model was not altered other than to perform the simulated surgery as well as wrapping object adjustments to ensure realistic muscle motions over bony landmarks. The parameters were measured to determine both flexion and rotation strength at a number of quasi-static, predefined, points of motion.

The cadaver study included four cadavers (eight shoulders) due to limited access to cadavers. The surgery was performed on these cadavers by Dr Daniel Henderson, a fellowship trained orthopaedic shoulder surgeon. No shoulders were excluded due to signs of unrelated deterioration such as osteoarthritis and previous shoulder surgeries. Fresh frozen cadavers were used in order to preserve the mechanical properties of the muscles and the tissue.

The motions analysed are forward flexion and external rotation. These two motions best describe the extent to which the surgery will allow the patient to resume activities of everyday living such as washing their hair, eating, brushing teeth and washing their face. Abduction is primarily performed by the deltoid muscles and as such should not be affected by a LD tendon transfer or posterior rotator cuff tear, assuming that the surgery is done on an otherwise healthy shoulder as discussed in section 2.2.1.

This chapter outlined the background and rational for the research. It defined the aims and objectives as well as describing the limitations and outlining the scope of the study. This information was informed by the study of the literature which follows in Chapter 2.

Chapter 2

Literature Review

This chapter contains a review of the current literature on the topics related to latissimus dorsi (LD) tendon transfers. This literature was used to inform the research described in this report.

To start with, this chapter describes the relevant anatomy and biomechanics of the shoulder joint. This is followed by a review of the indications and techniques that have been described for the transfer of the LD in order to treat irreparable rotator cuff tears. The current recommendations of the most effective insertion point on the humeral head are then discussed for simulation tests (*in-vivo* research) and *in-vitro* (cadaver) or *in-vivo* (live patient) trials. This chapter also delves deeper into the use of *in-silico* models to asses the biomechanics, particularly in relation to kinematics, of the shoulder. This chapter concludes by discussing the literature used to inform the instrumentation of the cadaver rig.

2.1 Relevant Shoulder Anatomy and Biomechanics

In order to inform the basics of the research, a good understanding of the anatomy, kinematics, and biomechanics of the shoulder joint is needed. This will provide an understanding of the needs that are to be fulfilled by the LD transfer as well as outlining some of the design specifications required to carry out the study. The relevant morphometrics of the torso and upper extremities are also listed.

2.1.1 Shoulder Anatomy

The shoulder is one of the most complex joints in the human body, comprising of three bones, only one of which, the clavicle, articulates directly with the axial skeleton. This makes the shoulder

joint the most mobile joint, with decreased stability. The bony anatomy of the shoulder joint, viewed from an anterior (left) and posterior (right) viewpoint, is shown in Figure 2.1. The different articulations that combine to make up the shoulder joint are listed after the figure.

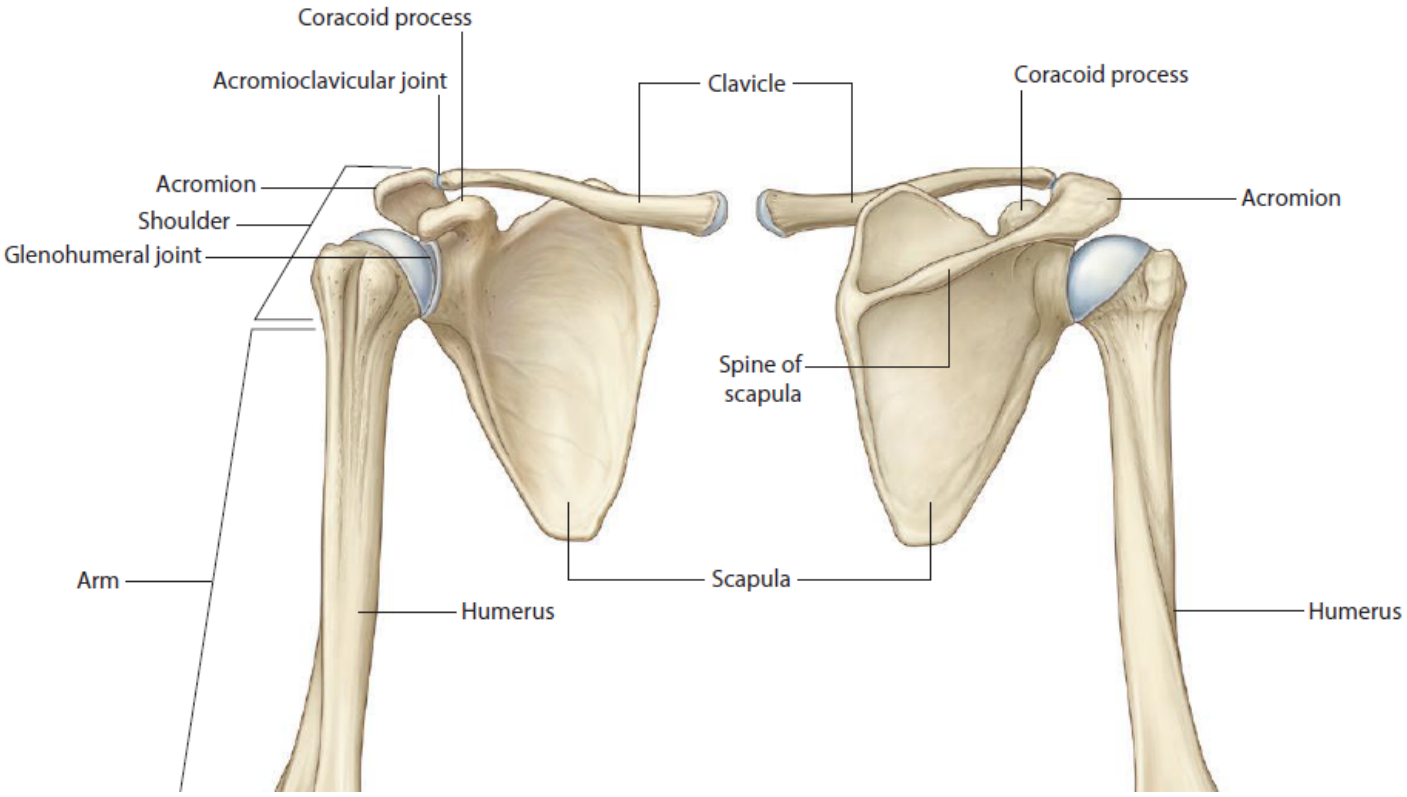

Figure 2.1: The bony anatomy of the shoulder joint from Grey's Anatomy (Drake et al., 2012)

i) The manubrio-clavicular joint - Attaches the upper limb to the axial skeleton through a fibrocartilaginous joint. This allows for a small amount of rigid motion in the clavicle.

ii) The Acromio-clavicular joint - Attaches the scapula to the clavicle. This is a plane joint, which is heavily restricted by a number of ligaments. This allows for some planar sliding allowing the scapula to rotate relative to the clavicle. The scapula is held against the thorax by muscles from the rotator cuff and back.

iii) The gleno-humeral joint - Attaches the humerus to the scapula. This is a mobile ball and socket joint that allows for a wide range of motion. It is constrained by a combination of muscles, ligaments and the cartilaginous labrum.

The muscles that surround and activate across the shoulder joint are listed in Table 2.1 to demonstrate the muscular complexity of the shoulder joint. Each of these muscles plays a role in the

various motions of the shoulder joint as well as in stabilising the joint throughout it's wide range of motion.

Muscle	Origin	Insertions	Actions
		Rotator Cuff	
Supraspinatus	Scapula	Greater Tuberosity	Abduction
Infrspinatus			External Rotation
Teres Minor			External Rotation, Adduction
Subscapularis		Lesser Tuberosity	Internal Rotation
		Deltoids	
Anterior	Clavicle (Latter third)	Deltoid Tuberosity	Flexion, internal rotation, adduction
Middle	Acromion		Abduction
Posterior	Scapular spine		Extension, external rotation, adduction
Coracobrachialis	Coracoid process	Below Lesser Tuberosity	Flexion, internal rotation, adduction
		Thoracic Muscles	
Lattisimus Dorsi	Thoracolumbar Fascia, T7-T12, 9th - 12th ribs, scapula (inferior angle), Iliac crest	Floor of intertubercular groove	Internal rotation, adduction, extension, respiration
Pectoralis Major	Medial Clavicle, sternum, costal cartilage,rectus sheath	Crest of greater tuberosity	Adduction, internal rotation
Pectoralis Minor	3rd -5th ribs	Coracoid process	Rotates glenoid inferiorly, lowers scapula
Trapezius	Occipital bone, spinous processes of C1-T12	Clavicle, Acromion, scapula spine	Raises scapula obliquely, rotates glenoid superiorly
Levator Scapulae	C1-C4	Superior angle of scapula	Raises scapula
Rhomboids	C6-T4	Medial scapular border	stabilise and raise scapula
Serratus anterior	Ribs 1 - 9	Medial scapular border	Rotates scapula laterally, adducts abducted arm.

Table 2.1: Table describing the muscles that make up the shoulder joint (Gilroy and Ross, 2009)

2.1.2 Humeral Anatomy

The LD transfer moves the tendon of the LD from the medial humeral shaft, at the base of the inter-tubercular groove (Gilroy and Ross, 2009), to a lateral point on the humeral head in order

to treat deficiencies in the rotator cuff. For this reason, it is important to understand the specific anatomy of the humeral head and the insertion points of the shoulder muscles, particularly the rotator cuff muscles, in this area.

Figure 2.2 shows the insertion sights of the postero-superior rotator cuff muscles on the humeral head. As the LD transfer seeks to use the LD to replicate the defunct rotator cuff, it is likely that one of these sights would provide an effective solution. These areas have been refered to by many studies when describing their results including: (Bargoin et al., 2016), (Ling et al., 2009), and (Magermans et al., 2004). This study also examines the effects of insertions on other areas of the humeral head to ensure all viable options are analysed.

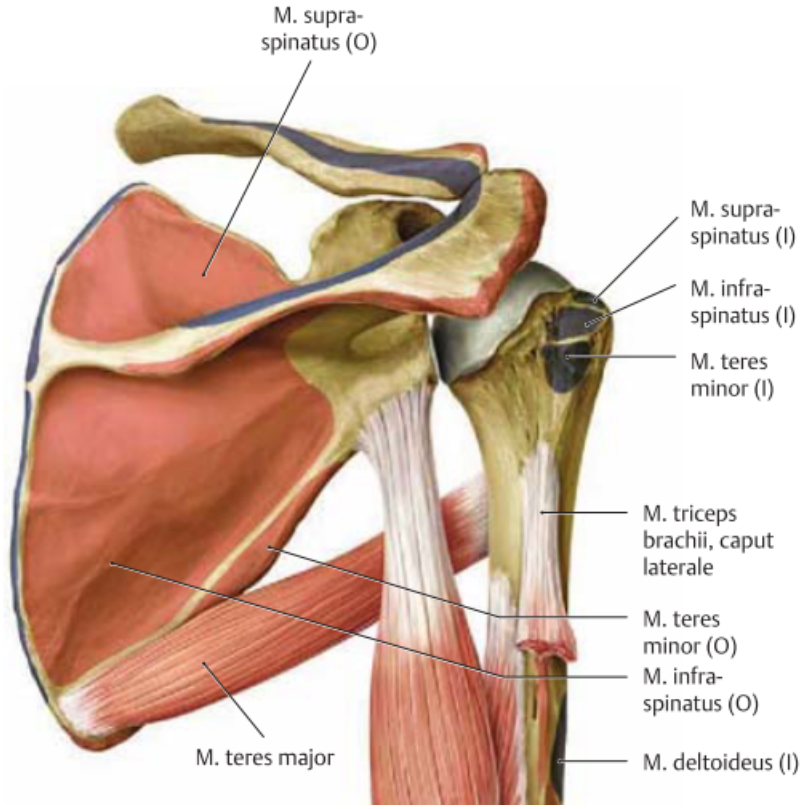

Figure 2.2: Image from (Gilroy and Ross, 2009) showing the insertion points described in Ling et al. (2009)

The flat areas marked in dark grey on Figure 2.2 are the attachment sites of the three external rotators of the rotator cuff. These are important sites to consider as they have naturally developed as points of external rotation. The results compared by the studies listed above will be discussed and compared in Section 2.2.4.

2.1.3 Shoulder and Torso Morphometries

Morphometry is the study of the varying sizes and shapes of objects, often used to describe human variance in anatomy. This is used to inform design parameters around the anthropometric variances in human populations. By designing with human morphometry in mind, it is possible to ensure that any specimen within the normal range will be able to use or be tested and alaysed using a piece of equipment.

The relevant morphometry, used as the basis for the cadaver test rig design, is listed in Table 2.2. The measurement references can be found in Figure 2.3. This is the data for an adult British male, but can be inferred to other populations for approximate dimensioning.

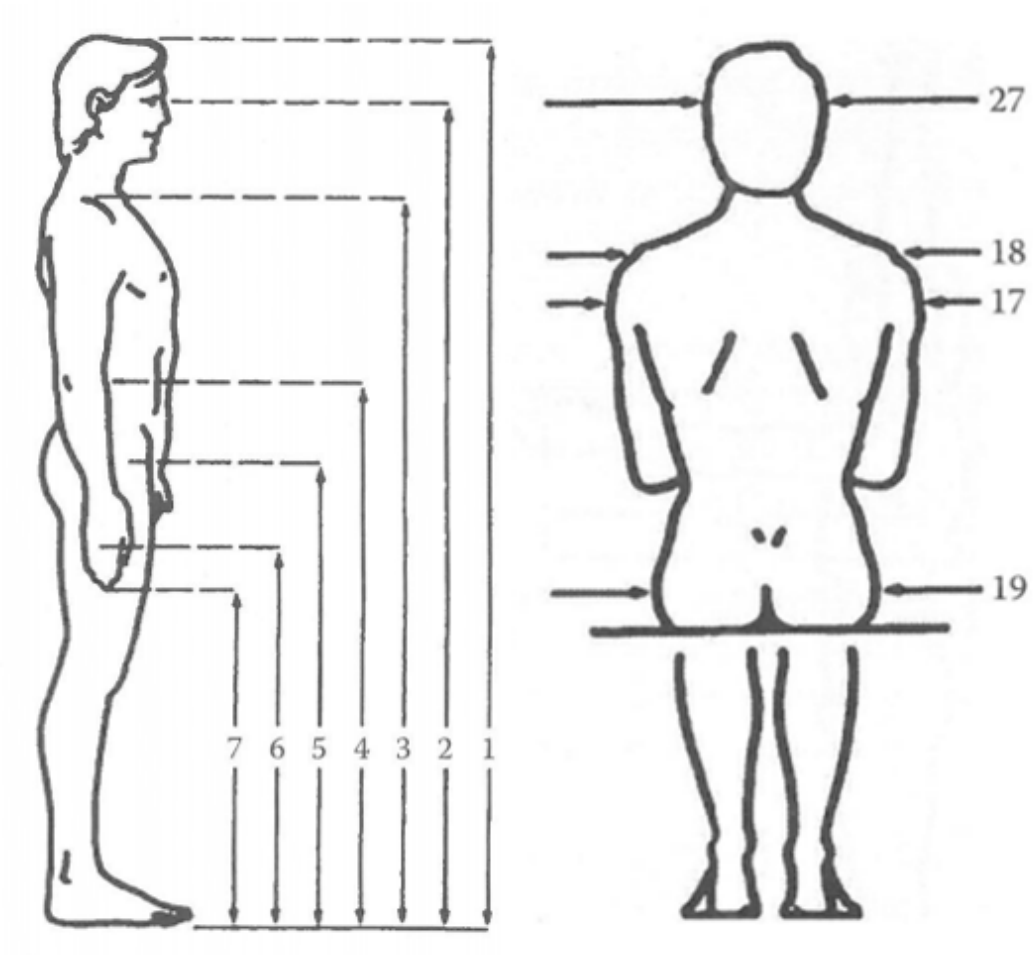

Figure 2.3: Diagrams taken from Bodyspace (Pheasant and Haslegrave, 2006) to explain the meanings of the measurements in Table 2.2

	5th %ile (mm)	50th %ile (mm)	95th %ile (mm)	Measure Reference
Shoulder Height	1330	1445	1555	3
Elbow Height	1020	1105	1195	4
Hip Height	850	935	1020	5
Bi-Acromial	370	405	440	18
Bi-Deltoid	415	465	510	17
Humerus Length	310	340	360	3 minus 4
Shoulder-Hip	480	510	535	3 minus 5
Elbow - Hip	170	170	175	4 minus 5

Table 2.2: Table of relevant morphometric data developed using Bodyspace (Pheasant and Haslegrave, 2006)

2.1.4 Biomechanics of the Shoulder

The biomechanics of the shoulder is very complex. In order to address this complexity Wu et al. (2005) suggested a set of coordinates that can be used to describe the motion in the shoulder. This coordinate system is used by the International Society of Biomechanics. The use of a standard co-ordinate system makes it easier for collaborative work, due to a common understanding, as well as making results more readily usable and comparable. The coordinate system is made up of the three rotations, as they are listed below:

- For the clavicle, the co-ordinate system is such that the origin O_c is most ventral point on the joint between the clavical and the sternum. X_c, Y_c, and Z_c are defined as shown in Figure 2.4. It is mentioned by Wu et al. (2005) that there are some errors with the X_h due to the errors that occur when defining the line between the two condyles. This can be eliminated by setting the elbow flexion to 90^o and using this as the direction of the plane.

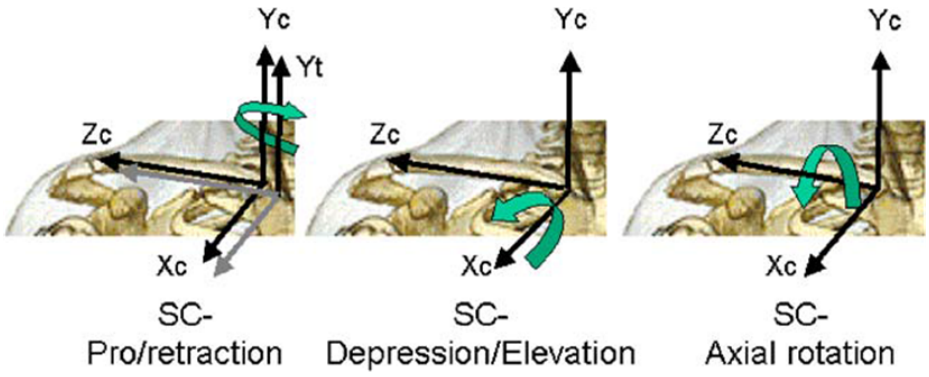

Figure 2.4: Coordinates associated with clavicular movement as described by Wu et al. (2005)

- The scapula has its origin O_s at the acromion angle where it attaches to the clavicle. From here the co-ordinates are set up similarly to those of the clavicle as shown in Figure 2.5.

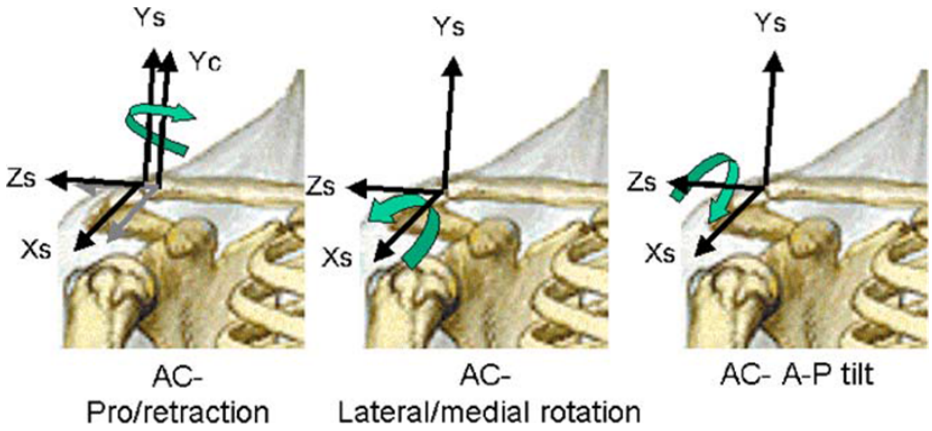

Figure 2.5: Coordinates associated with scapular movement as described by Wu et al. (2005)

- For the humerus, the origin O_h is situated at the rotational center of the gleno-humeral joint. Adduction/abduction is defined as rotation around the Z_h axis with flexion/extension around the X_h. The Y_h runs along the length of the humerus as shown below in Figure 2.6.

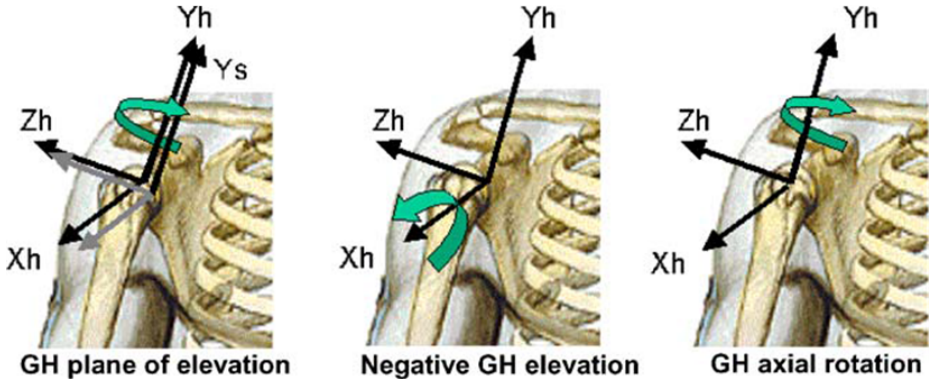

Figure 2.6: Coordinates associated with humeral movement as described by Wu et al. (2005)

These rotation coordinates are not used by all biomechanical models. Some models, including the Upper Extremity Model (Holzbaur et al., 2005) use their own coordinates to better describe the motion in terms of clinically relevant coordinates. This is done in the Holzbaur et al. (2005) Upper Extremity Model using 3 coordinates. One for elevation angle, which determines whether the elevation of the shoulder is forward flexion, abduction of anteflexion. The shoulder elevation is then made up of pre-determined combined clavicular, scapular and humeral motions that define the amount of elevation of the shoulder at the previously determined angle. Lastly humeral rotation takes place in the current, clinical reference frame.

2.2 Latissimus Dorsi Tendon Transfer Surgery

The methods that surgeons use to transfer LD tendons for the purpose of treating posterior rotator cuff tears need to be understood. This includes both the insertion points being used as well as the techniques used to fasten the tendon onto the humeral head. As this research aims to help surgeons with surgical planning and to inform their decision making processes, it is important to understand the current planning processes and techniques.

2.2.1 Indications and Contra-indications for Latissimus Dorsi Transfer

There are a significant number of publications describing the conditions under which a LD tendon transer is most likely to be successful. The success of the tendon transfer surgery depends on a number of factors including the tendon insertion point (Henseler et al., 2017). Brigham and Women's Hospital (2007) describes the care given to patients who have LD transfer procedures.

A LD transfer transfer can reduce the pain and restore some shoulder function after a 'massive posterior superior rotator cuff tear' (Brigham and Women's Hospital, 2007). Brigham and Women's Hospital (2007) describes a massive tear as a tear greater than 5 cm, a definition that is agreed upon by Oh et al. (2013) and Grimberg and Kany (2014). Grimberg and Kany (2014) mentions a second definition as a tear affecting two or more separate tendons. Massive rotator cuff tears, no matter how they have been described, appear as the leading indicator for a patient to be given a LD transfer transfer. Surgery should only be performed, after more conservative treatments including therapy and drugs have failed (Brigham and Women's Hospital, 2007).

Brigham and Women's Hospital (2007) claims that only approximately 25% of patients with massive rotator cuff tears that cannot be otherwise repaired are suitable LD transfer transfer candidates. This is because there is a large number of contra-indicative pathologies that must be taken into account before surgery. These have been discovered or described as follows.

- A damaged subscapularis has been described as a contra-indication for LD transfer transfer (Sim et al., 2001), (Werner et al., 2006).
- Patients should be below 60 years of age (Brigham and Women's Hospital, 2007).
- There should be no arthritic damage to the shoulder (Grimberg and Kany, 2014)
- There should not be any signs of deltoid palsy (lack of deltoid innervation due to nerve damage) (Grimberg and Kany, 2014)
- A complete lack of forward flexion strength (Brigham and Women's Hospital, 2007).

Reference	No. of cuff tears	No. of massive tears	Rate
Neer	340	145	42.60%
Bigliani et al.	Not listed	61	N/A
Ellman et al.	54	9	16.70%
Harryman et al.	407	146	35.90%

Table 2.3: Table of prevalence of rotator cuff tears (Sim et al., 2001)

- Pseudoparalytic shoulder, sometimes defined as the inability to abduct the arm despite there being no pain, should not be present in the patient (Grimberg and Kany, 2014).

- Iannotti et al. (2006) suggests that people with poor muscle strength prior to surgery, particularly women, were less likely to have a successful surgery.

- Grimberg and Kany (2014) claims that LD transfer is most effective when used as the primary procedure compared to a secondary procedure such as a reverse total shoulder arthroplasty.

2.2.2 Prevalence of Rotator Cuff Tears

Although rotator cuff injuries are highly common, Sim et al. (2001) claims that relatively few of these are massive or irreparable tears. A massive tear can be described as any tear of more than 2 tendons, which cannot be reattached on the greater tuberosity (Bargoin et al., 2016). Neri et al. (2009) mentions that many surgeons consider a tear of grade 3 or 4 on the Goutallier scale (those with euqal amounts of, or more, fatty tissue than muscle). Neri et al. (2009) goes on to explains that massive and irreparable cannot be used interchangeably as some massive tears are repairable. This means that there is no way to determine an exact prevalence of irreparable tears.

Neri et al. (2009) claims rotator cuff disease as one of the most common musculoskeletal disorders. Yamaguchi et al. (2006) stated that, in 2006, 17 million American citizens were at risk for rotator cuff diseases. This results in rotator cuff repair and treatment being one of the most frequent surgical solutions performed. Neri et al. (2009) lists 94% as the number of patients that fail to heal, but does not describe what level of healing is classified as failure. Rotator cuff tears are considerably more prevalent in elderly people with a 50% likelihood of bilateral tears after the age of 66 years (Yamaguchi et al., 2006).

Sim et al. (2001) lists the prevalence of rotator cuff repairs found by four studies and the rate at which these repairs were found to be “massive”. The results of this analysis is described in Table 2.3.

2.2.3 Tendon Transfer Technique

The transfer of the lattisismus dorsi was first described by Gerber et al. (1988). This technique involved inserting the tendon of the LD on the superolateral humeral head (the original insertion of the supraspinatus muscle). The results from the initial tests of 14 patients showed remarkable improvements in pain and mobility. Gerber et al. (2006) describes how the LD bundle was placed between the deltoid and the infraspinatus before being attached to the tip of the greater tuberosity. It was attached in place by a pair of braided number-3 sutures passing through holes "from the edge of the tuberosity to the lateral cortex of the humerus" (Sim et al., 2001). These sutures were knotted over the lesser tuberosity after passing through the bone at the tip of the greater tuberosity. The technique is added to by Sim et al. (2001) where the abrasion of the surface to promote attachment of the tendon is described.

Henseler et al. (2017) also describes how the single incision L'Episcopo technique which lowers the insertion point on the humerus. This technique was defined by Habermeyer (2006). Figure 2.7 shows the L shaped cut decribed by Habermeyer (2006) to gain access to the humeral head and LD tendon. It then shows the removeal of the LD, and it's replacement, over teres major and minor, to the greater tuberosity. Habermeyer (2006) proposes using three sutures, anchored into the bone as shown by the X-ray image in Figure 2.8.

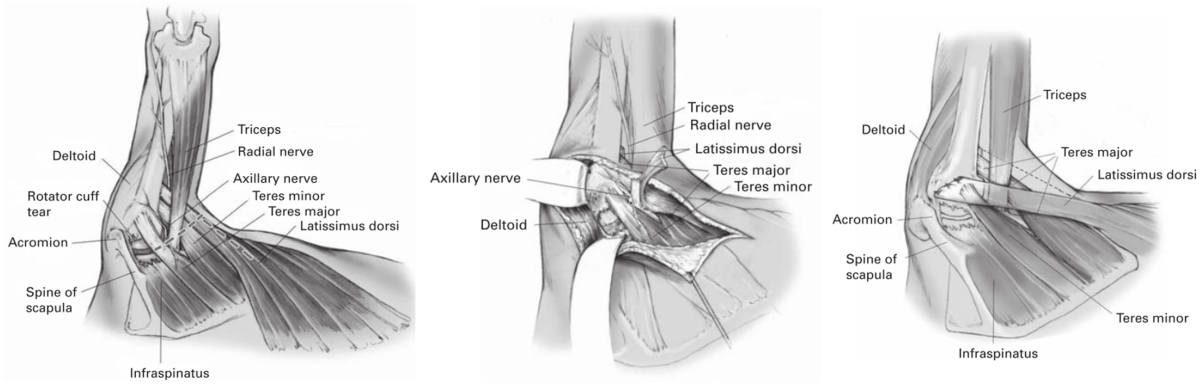

Figure 2.7: Diagrams from (Habermeyer, 2006) showing the processes used to gain access to the humerus, remove the flap, and re-attach the LD.

2.2.4 Tendon Insertion Points in the Literature

A number of studies have looked at the problem of LD transfers and tried to optimise the new tendon insertion point. This has been done experimentally using cadaver models (Hartzler et al., 2012), (Oh et al., 2013). These studies have been limited drastically by the sample size. Most commonly research has been done using live patients *in-vivo*. These studies include De Casas et al. (2014) Gerber et al. (2006) Habermeyer (2006) Iannotti et al. (2006) as well as some others.

Figure 2.8: X-ray images from (Habermeyer, 2006) showing the suture anchors in the humeral head.

These studies too were limited by there sample size with the exception of Gerber et al. (2006) who managed to review 69 patients. The main downfall of using live patients is that the surgery cannot be performed on otherwise healthy shoulders to isolate the effects. It would also be considered unethical to adjust the insertion point away from those described by Gerber et al. (2006), Oh et al. (2013) and others, as this would constitute purposefully giving substandard treatment for the purpose of research.

In order to isolate the effects of the insertion point on the outcomes of tendon transfers, some studies have used biomechanical models. Simulating the surgery and optimising for range of motion and moment arms are efficient ways of assesing surgical outcomes (Magermans et al., 2004). These computer models allow for a larger number of variables to be assessed more efficiently. This means that more information can be obtained at lower cost and in a shorter period of time. There has however been some criticism and much analysis of the accuracy of purely computer based models (Wagner et al., 2013), (Saul et al., 2014).

Physical biomechanical models have also been built as described by Favre et al. (2008) although these are limited in their accuracy due to simplifications in the biomechanics of the systems. Another common problem, which is discussed in more detail in Section 2.3 is the ability for wrapping objects to accurately and reliably recreate the movement of muscles around one another and bone. This problem is also noted by Grimberg and Kany (2014), when describing the differences between *in-silico* and *in-vitro* studies. Grimberg and Kany (2014) note that many *in-silico* studies suggest the co-transfer of multiple muscles such as LD and teres major to improve stability and strength. This is not always possible due to practicalities of space and other factors.

Biomechanical Studies

Biomechanical studies give the opportunity to test the effects of a far greater number of insertion points and their mechanical effects. Magermans et al. (2004) tested thousands of tendon transfers. It was suggested that the tendon of the LD should be transferred to the original insertion point of the supraspinatus muscle as seen in Figure 2.2. Magermans et al. (2004) mentions the possibility of this being impractical due to space, muscle volumes, and tensile properties. Favre et al. (2008) suggested an insertion posterior to the greater tuberosity of the humerus for shoulders that have undergone a simultaneous reverse shoulder arthroplasty using a mechanical testing jig.

Ling et al. (2009), however, suggested a transfer of the LD to the insertion point of the infraspinatus for shoulders with a healthy deltoid through biomechanical tests. It was also reported that, although they found this to be the optimal sight for insertion, they did see dramatic improvements with insertions at the original insertion points of the subscapularis (the lesser tuberosity) and supraspinatus. The teres minor insertion point was described as the worst option by Ling et al. (2009). These insertion points are anotated on the image from (Gilroy and Ross, 2009) in Figure 2.9.

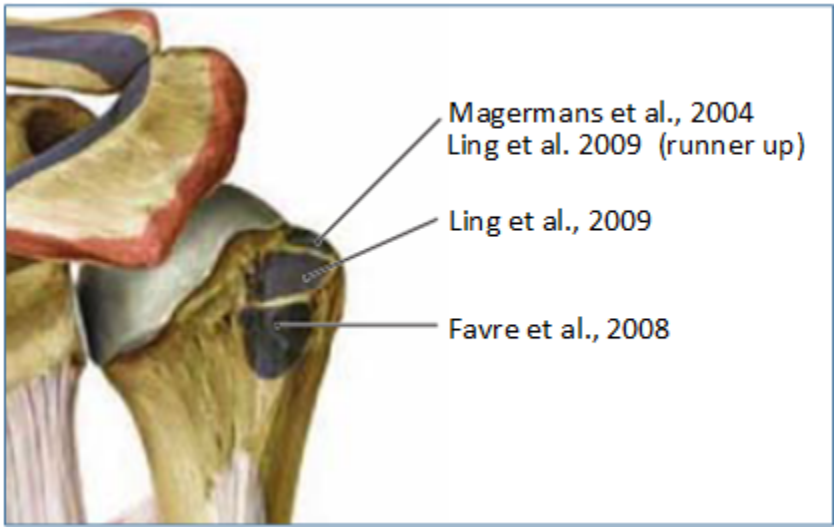

Figure 2.9: Anotated view of the humerus from (Gilroy and Ross, 2009) showing the insertion points suggested by Magermans et al. (2004), Ling et al. (2009) and Favre et al. (2008)

Figure 2.9 emphasizes the fact that the literature is inconclusive on the effects of different insertion sites during LD transfers with results ranging over the entire proximal humeral head.

In-vivo and Cadaverous Studies

Clinical studies are somewhat limited by the size of their samples as well as the fact that the surgery is often done on shoulders with other pathologies. This results in a surgery that is often affected by a range of factors other than the various insertion points, which may alter the surgical outcomes. This leads to different studies finding varying optimal insertion points.

One of the main benefits of cadaveric and in-vivo studies is that they take into account the practicalities (Magermans et al., 2004) such as space, muscle size and tensile properties. For example, Cleeman et al. (2003) used cadavers to test a number of insertion points for practicality, which can be used to advise *in-silico* models. In terms of studying the biomechanical effects of the tendon transfer Oh et al. (2013) suggest that the transfer be done in conjunction with a teres minor transfer in order to stabilise the glenohumeral joint and decrease the joint pressure. This study used the technique described by Gerber et al. (1988) with the insertion point on the posterosuperior part of the humerus. For the study done by De Casas et al. (2014) the tendon was inserted on the posterior portion of the greater tuberosity. This resulted in a statistically significant improvement in pain during activities of daily living, but had a reduced improvements in abduction strength. Bargoin et al. (2016) used a cadaver rig to measure the strength in external rotation for a series of insertion points along the distal edge of the greater tuberosity. Figure 2.12 shows how Bargoin et al. (2016) used a static load on the LD to determine the effectiveness of each point that was tested. The results for this study described point X_5 in Figure 2.10 as the most effective insertion point on the humerus. This point can be described as the insertion point of the supra-spinatus as described in Figure 2.2, which corroborates the results found by Ling et al. (2009) and Magermans et al. (2004) using a computer generated model.

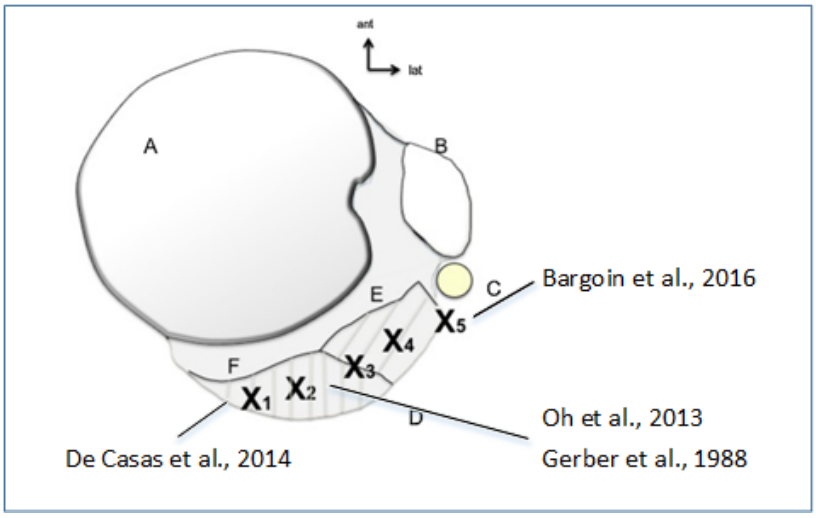

Figure 2.10: Image used by Bargoin et al. (2016) showing the flat insertion areas of the posterior rotator cuff where the area denoted E is the insertion area of the supraspinatus, and F is the infraspinatus insertion point.

2.3 Biomechanical Shoulder Models

In order to simulate a tendon transfer it is best to use a well developed shoulder model. This reduces the time costs of the project as well as making the results more easily repeatable. There are a number of widely accepted shoulder models in use in the field for a variety of studies and each of these has its own benefits and limitations. Quental et al. (2013) tested a number of models to determine the differences in results. They found that while there were some differences in force prediction using different models, the variance in muscular activity was not significant. Wagner et al. (2013) on the other hand compared eight different models across three software packages to determine the consistency between them. The differences found serve to show the importance of using another method such as a cadaver trial to ratify the results.

The available shoulder models as described in Bolsterlee et al. (2013) are:

1. The Delft Shoulder and Elbow Model (DSEM) (Magermans et al., 2004)
2. The Newcastle Shoulder Model
3. The Swedish Shoulder Model
4. Anybody Upper Extremity Model
5. Holzbaur's Upper Extremity Model (Holzbaur et al., 2005)

Bolsterlee et al. (2013) describes how the DSEM and Holzbaur's Upper Extremity Model have been used most for tendon transfer problems with positive results. Ling et al. (2009) used the Holzbaur model for a similar problem due to its ability to simulate the passive force exerted by muscles which minimises the need for and complexity of a kinematic analysis. Habermeyer (2006) also quoted the use of this model to successfully characterise other tendon transfers in the arm as well as its ability to describe the interaction between joints. The DSEM was used by Magermans et al. (2004) to simulate the effects of lattisimus dorsi transfer in conjunction with a reverse shoulder arthroplasty. The DSEM uses position inputs and then calculates the required loads from each of the 139 muscle segments to stabilise the shoulder. Both models are available online and have been used to model surgery involving the LD, the main differrence between them is the method of calculating loads and range of motion.

Lattisimus Dorsi in DSEM

The DSEM (van der Helm, 1994), has been used by a range of biomechanics studies on the upper extremity including by Magermans et al. (2004). This shoulder model has been developed using

normal muscle and joint anatomy. This means that it has not been designed to handle large changes (such as tendon transfers). This requires careful monitoring to ensure that the muscles behave as expected after transfer, without creating physically impossible geometries.

The DSEM defines the LD using 6 tendon lines that wrap around various objects to mimic the contours of the body. As the path is only defined as a begining and an end that wraps automatically around bodies, the DSEM (van der Helm, 1994) is a suitable model to simulate LD transfers.

Lattisimus Dorsi in Holzbaur's Upper Extremity Model

The Upper Extremity Model developed by Holzbaur et al. (2005) has been used to assess upper extreminty tendon stransfers before, including LD tendon transfers by Ling et al. (2009). Also developed using *normal* shoulder anatomy (with no surgical alterations), the Holzbaur et al. (2005) Upper Extremity model is not suited to all tendon transfers without adjustment.

The LD is defined in the model by 3 muscle strands comprised of 4 parts. This segmented muscle helps to simulate the narrowing of the muscle towards it's insertion point. This also helps with wrapping as any specific section of the muscle can be set to wrap, allowing more realistic wrapping around sharp corners.

2.4 Procedure Validation Parameters

In order to determine the relative success of a surgery, cadaveric or simulated, it is important to develop a set of relevant parameters. These parameters should aim to objectively measure the benefits of the surgery and should be chosen such that they show both possible improvements and well as possible weaknesses of various approaches.

The human trials such as De Casas et al. (2014), Gerber et al. (2006) and others have used subjective pain measurements as well as range of motion and strength measurements. As this study will not include live patients who are able to give pain measurements, as well as the fact mentioned by a number of authors including De Casas et al. (2014) that: "the procedure has been proven to be a valid surgical treatment... [for] chronic pain", it is not not necessary to investigate possible causes of pain with each insertion point. Sim et al. (2001) describes the moment arm as "the relative length of a muscle and its line of action relative to the center of rotation of (Sim et al., 2001)". This is directly related to the effective strength that a muscle contributes to a specific motion.

Habermeyer (2006) showed that, after transfer to the greater tubercle as shown in Figure 2.8 as well as the necessary rehabilitation, the LD acts as an active external rotator. Habermeyer (2006) also shows that the LD has no activity during internal rotation. This was shown using electromyographs

(EMG) post surgery during these motions seen in Figure 2.11. This shows that the LD should have an active effect in external rotation post surgery.

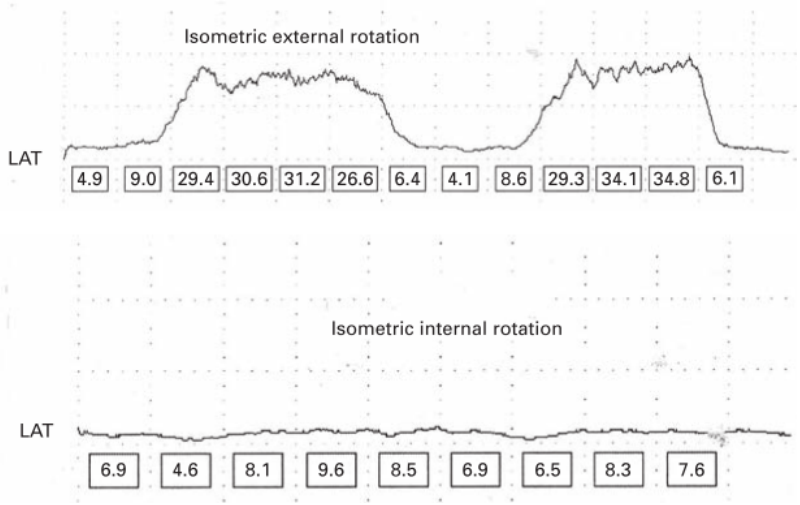

Figure 2.11: EMG from Habermeyer (2006) showing LD activation during external rotation and internal rotation to describe the active effects of the LD post transfer.

2.4.1 In-silico Verification Parameters

The most common range of motion tests involve external rotation(Magermans et al., 2004), (Gerber et al., 2006), (Ling et al., 2009) and abduction (Magermans et al., 2004), (Gerber et al., 2006), (Ling et al., 2009) as well as often including forward flexion (Magermans et al., 2004), (Gerber et al., 2006), (Ling et al., 2009) for activities such as eating and anteflextion (Magermans et al., 2004) for activities such as washing the axilla. Studies such as Magermans et al. (2004) used *percentage of successful simulations* as their comparative parameter. This was done by simulating a a range of activities of daily living and comparing moment arms, contact forces and other parameters to declare each motion as successful or unsuccessful.

The ability for the muscles to generate a load about the shoulder's center of rotation for flexion, abduction, internal and external rotation is related to the moment arms produced by the muscles as well as their relative sizes. Muscle moment arm is defined by Sherman et al. (2015) as "the 'effectiveness' of a particular muscle at generating a particular motion of interest" . This was taken into account by Ling et al. (2009). Ling et al. (2009) also took range of motion into account by measuring the strain (percentage length change) on the muscles during specific movements.

A number of other studies looked at similar parameters but it is clear that some of the most important parameters are the range and strength of abduction, flexion and external rotation. Sim et al. (2001) also describes the moment arm as a parameter that can be used to determine the effectiveness of the surgery in restoring a certain motion.

2.4.2 Cadaver Verification Parameters

The simulation study will asses the effects of various insertion points on the muscle moment arms at specific points in predefined motions. The cadaver study however, will assess the reaction load generated in the shoulder by a set loading condition in a range of positions. These static testing procedures are being used to eliminate the mass of the arms from the equation, thus reducing the number of external factors influencing the results.

In order to evaluate various insertion points, it is important that the cadaver tests track related parameters similar to those used in the simulation. As it is not possible to accurately measure tendon lengths and moment arms it is important to measure the load required to abduct rotate or extend and compare this to other similarly administered cadaver tests.

Oh et al. (2013) measured the range of motion during loading and the rotational effect of a load with the humerus set at three different angles of abduction using frozen cadavers. This was an effective way to determine the ability for the LD to exert a moment on the humerus after surgery. A similar study done by Werner et al. (2006) used tension to load the LD in different positions and recorded the range of the affected motion. This is different to Hartzler et al. (2012) who used a cadaver to simply measure the range of passive motion of the shoulder post surgery. The rig used by Werner et al. (2006) shown in Figure 2.12 could serve as a model for the cadaver tests in this project.

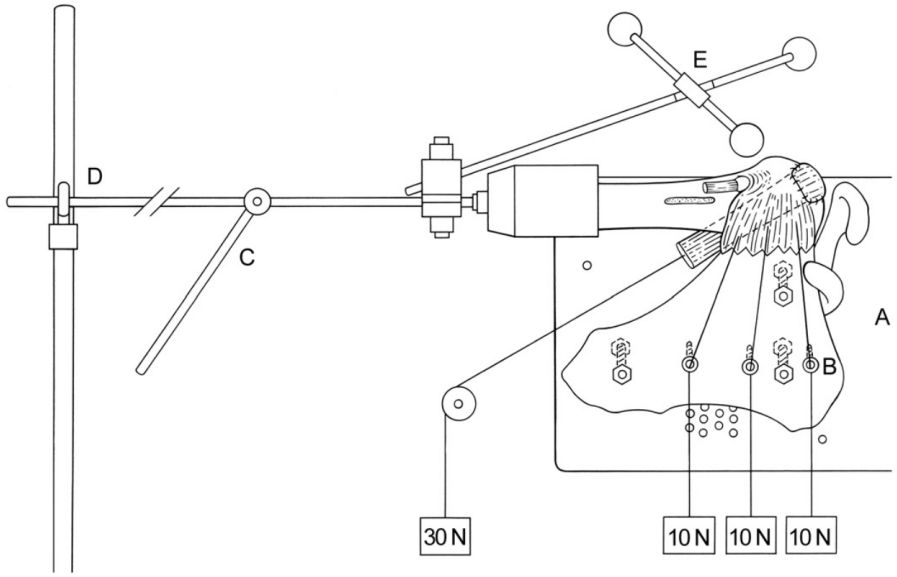

Figure 2.12: Schematic of the cadaver shoulder testing rig used by Werner et al. (2006)

A similar setup was used by Bargoin et al. (2016) to test the optimal insertion point for LD tendon transfers. This used the rig setup shown in figure 2.13 with the LD stapled to varying insertion

points. The staples were used as they allowed the insertion point to be moved without weakening the bone. Bargoin et al. (2016) used 10 N and 20 N (Approximately 1 and 2 kg respectively) to simulate the load from the LD muscle. Magermans et al. (2004), on the other hand,quotes 40 N/cm^2 as the maximum muscle force after surgery during their simulations. Similarly Oh et al. (2013) used 24 N and 48 N as the load exerted by the LD.

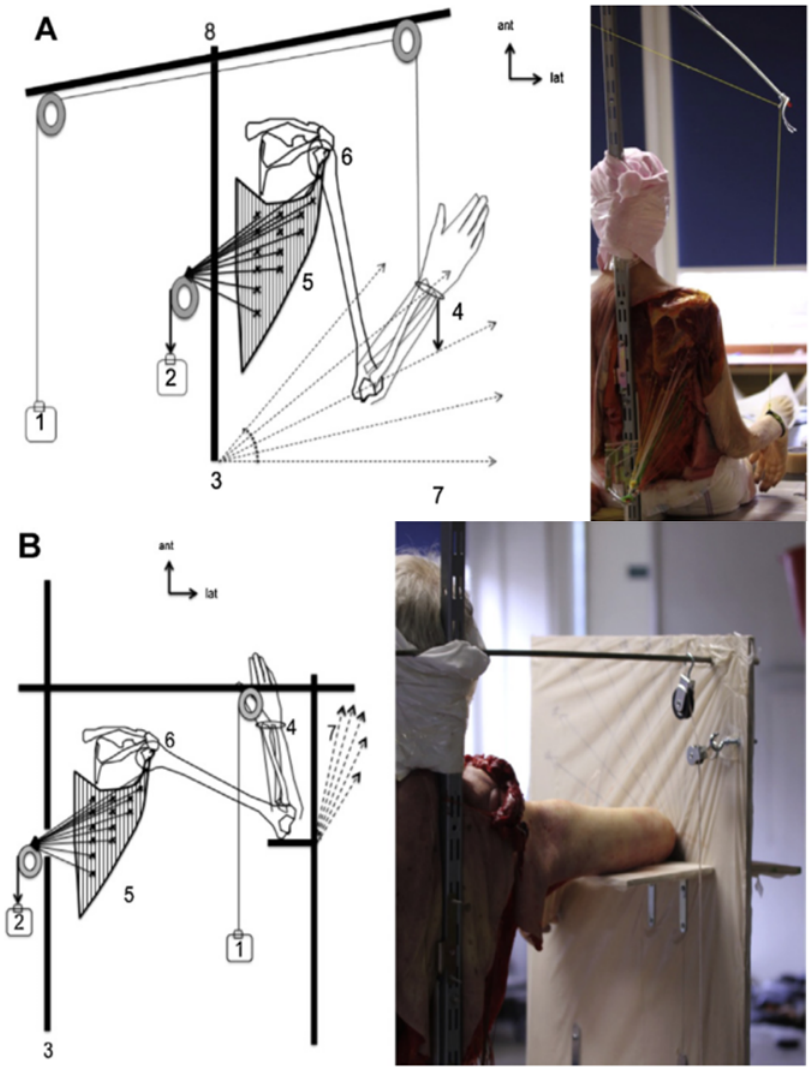

Figure 2.13: Image from Bargoin et al. (2016), showing the setup used to determine the optimal insertion point.

Favre et al. (2008) used an instrumented rig to test the best insertion points on a reverse shoulder implant. Figure 2.14 shows how wires were used to replicate the muscle loads for the LD. The problems with this rig are that the scapula is fixed, which removes the complexities of the shoulder joint, and only allows the shoulder surgery to be tested in one position. The data was automatically

stored during the tests on a computer and analysed later. This is a good way to ensure that bias is eliminated as it blinds the researcher to the results being generated.

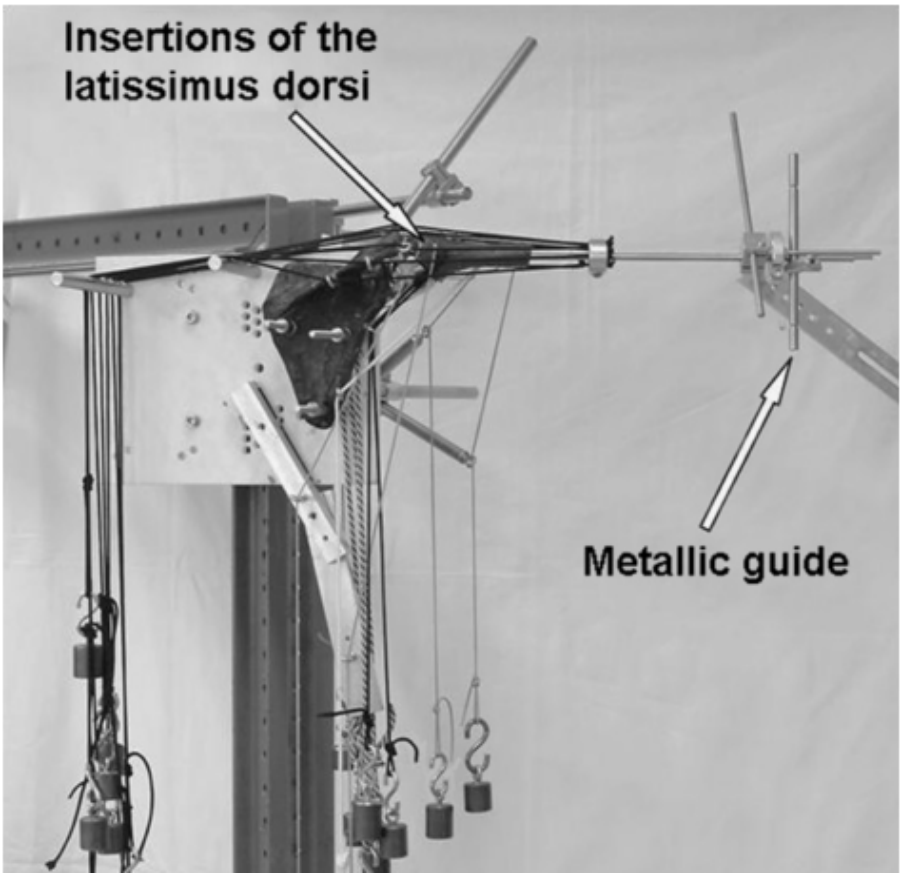

Figure 2.14: Image from Favre et al. (2008) showing the rig that was used to test LD insertion points after transfer.

Cadaver Rig Instrumentation and Measurement

Bargoin et al. (2016) used a visual comparison of the height to which the hand could be raised as a measurement of strength and range of motion from the LD. This is a simple way to compare outcomes, but conflates the parameters of strength and range of motion. Werner et al. (2006) on the other hand used an electro-mechanicaly instrumented rig to measure the resulting loads. This solution is more accurate and more repeatable. Favre et al. (2008) used an instrumented rig to test the best insertion points on a reverse shoulder implant. Figure 2.14 shows how this rig was set up.

There are a number of factors that must be considered during instrumentation. These factors include:

- Ensuring that the measurement is large enough to be read above any noise that may be introduced.
- Parameters should not be conflated and each parameter measured should be isolated from others.
- Measurements taken bilaterally and those taken at high and low angles of flexion should be directly comparable.

This chapter was a review of the literature used to inform this study. This included a review of the shoulder anatomy and biomechanics, current literature on LD transfer surgery, biomechanical shoulder models and the parameters currently used to determin the outcome of an *in-silico* or *in-vitro* LD transfer. Chapters 2 and 3 will use this body of knowledge to investigate the optimal insertion point for the LD on the humeral head during transfer.

Chapter 3

In-silico Insertion Point Optimization

3.1 Introduction to in-silico Insertion Point Optimisation

This chapter describes the *in-silico* optimisation of the surgical insertion point of the latissimus dorsi (LD) to treat posterior rotator cuff tears. It includes a full introduction to the study before describing the methodology used. The results are then discussed and conclusions are drawn. These results are later compared in Chapter 5 to those from the cadaver study in order to determine their clinical relevance.

3.1.1 Rationale and Problem Statement in-silico Study

LD tendon transfers have been shown to be an effective way of treating irreparable posterior rotator cuff tears (Gerber et al., 2006), (De Casas et al., 2014), and (Habermeyer, 2006). The most effective insertion point or area on the humerus is, however, under debate. Different studies have shown varying results as discussed in Section 2.2.4. Some of the reasons for these varying results are that simulations aren't properly verified and cadaver, or in patient, trials have too small or too diverse of a sample group. For this reason, it is necessary to set up a simulation or *in-silico* study, that can test the effectiveness of many points on a humerus with minimal conflating variables. This *in-silico* study must then be compared to a cadaver trial to determine the clinical relevance of the results.

Problem Statement

The current body of knowledge regarding the optimal placement of the LD tendon to treat posterior rotator cuff tears is undecided and insufficient. This leads to lower rates of success for the surgery and poorer outcomes for thousands of people worldwide. This needs to be remedied with

a model that describes the effects of moving the tendon placement under various conditions, which is comparable to an *in-vitro* study to ensure it's clinical relevance.

3.1.2 Aims of in-silico Insertion Point Optimisation

The aims of the simulation are to generate a clinically relevant set of results that can be used by clinicians to inform their decision making process in terms of the insertion point, and to define an optimal insertion point for the LD during transfer to treat rotator cuff tears. This will be done by informing clinicians how various insertion areas affect different clinical outcomes.

3.1.3 Expected Outcomes of in-silico Insertion Point Optimisation

This *in-silico* optimisation will provide a number of outcomes, including a comparison of the effects of various insertion points on:

1. Humeral rotation strength at low angles of flexion
2. Flexion strength in neutral rotation and low angles of flexion
3. Humeral rotation strength at high angles of flexion
4. Flexion strength in neutral rotation and high angles of flexion

These comparisons will be provided in the form of both a heat map and a numerical comparison based on the research methodology of the cadaver trial described in Chapter 4.

3.1.4 Scope and Limitations of the in-silico Simulations

The *in-silico* study assesses the kinematic moment arm in rotation and flexion of the LD in various positions of humeral flexion. It is assumed as stated by Gatti et al. (2007) that the moment arm is indicative of the strength provided by a certain muscle in a specific direction of rotation. Using this parameter, the model assesses each point on a CT scan of a humeral head to determine the optimal placement of the tendon.

The moment arms in flexion and rotation are measured as these are the motions most affected by posterior rotator cuff tears. They are assessed at 0° and 90° of forward flexion to ensure that the results are clinically relevant throughout a full range of forward flexion.

The limitations of this study include:

- This is a kinematic study which does not take into account motion and mass as these would be conflating variables to the movement of the insertion point.
- Only the relocation or transfer of the LD is considered.
- It is assumed that the premise behind the surgery is valid as it has been shown to be over years of use.
- This study does not assess the effects of the tendon placement on gleno-humeral stability as this has not been found to be an issue in previous studies.
- Only two humeral positions were tested. This was done to simplify the effects of moving the tendon placement on the humeral head.
- The model was not able to perfectly simulate the movement and wrapping of the LD tendon over the bony details of the humeral head. This is a common problem found in kinematic and biomechanical dynamics simulations.

3.2 Simulation Methods

This section describes the processes used to create the *in-silico* model. To start with, the software and the model are described. This section continues by describing the techniques used to simulate the transfer of the tendon insertion as well as how the parameters were chosen and measured. Lastly the visualisation and result processing process is laid out.

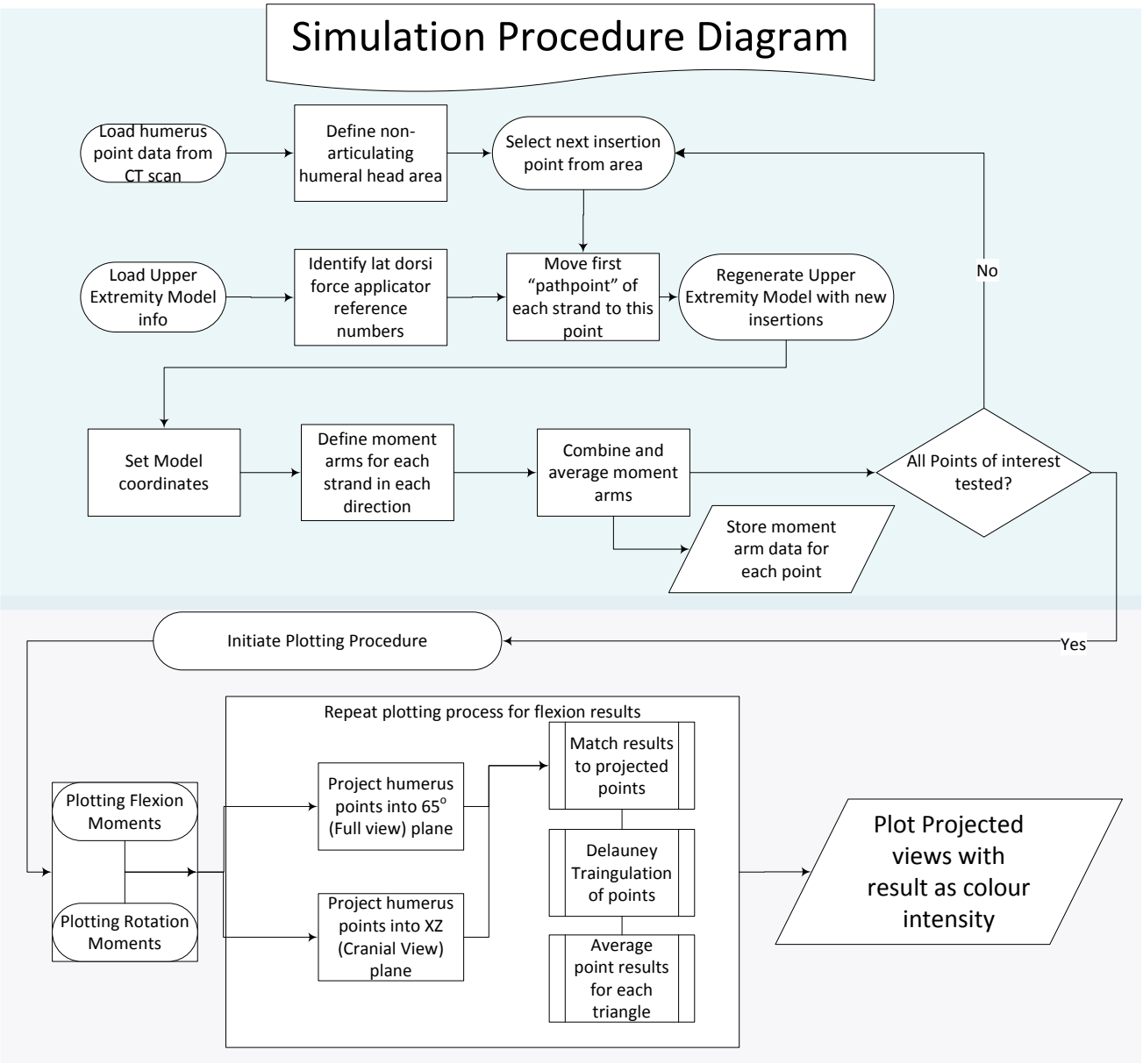

Figure 3.1: Process flow chart describing the process used to generate and assess *in-silico* surgeries.

Figure 3.1 breaks down the process used to generate simulated surgical results. The process shown

was repeated for the motion of external rotation at positions of 0° and 90° in order to ensure that the results are relevant for a range of tasks. The details of each step in this process are described in this section.

3.2.1 Models and software

Modeling Software

The biomechanics modelling software used for this research was OpenSim, an open source version of SIMM, developed by The National Center for Simulation in Rehabilitation Research at Stanford University. This software is commonly used to study the biomechanics of human joints, including the shoulder joint.

OpenSim has a graphical user interface (GUI) as well as an application programming interface (API). In order to perform the thousands of simulations needed to create a virtual map of the humerus, the API was used. The OpenSim library was synced with Matlab to allow for the simulations to be scripted and queued as well as for results and image processing. Mimics was used to segment the CT scan of the humerus that makes up the base of the humeral map.

Mathematical Shoulder Joint Representation

The generation of a useable shoulder model is extremely complex. For this reason, a previously developed and tested model was used to simulate the tendon transfer surgery. The model that was used for this simulation is the Upper Extremity Model developed by Holzbaur et al. (2005).

The Upper Extremity Model was built and tested using normal anatomy meaning that changes in geometry to simulate tendon trasfers can introduce problems. Bolsterlee et al. (2013) describes the use of wrapping objects used to mimic muscle interactions with bony structures and other muscles. A number of these wrapping objects were added and removed from the model to mimic real life motion. These alterations are described below

- Original objects TMAJ_LATHum, LAT_TMAJhh, and LAT_TMAJ2hh were removed from the wrapping lists of all three LD muscle strands. These were removed as they were used to wrap around the medial humeral shaft as they did not interact with the muscle strands after surgery.
- A new wrapping object was set for the 0 Degree tests to mimic the wrapping of the LD around the humeral head. This object was defined as a ellipse with Center $x, y, z =$

$(-0.0025, -0.028, -0.01)$ Rotation $x, y, z = (0.03805, 0.2886, -1.5067)$ in radians and Dimensions $x, y.z = (0.085, 0.023, 0.033)$ These coordinates are defined relative to the humeral reference axis as developed by Holzbaur et al. (2005) with the object shown in Figure 3.2a.

- A new wrapping object was set for the 0 Degree tests to mimic the wrapping of the scapula and rotator cuff. This object was defined as a ellipse with Center $x, y, z = (-0.0418, -0.0619, -0.02195)$ Rotation $x, y, z = (-1.59, -0.28082, -1.7635)$ and Dimensions $x, y, z = (0.03, 0.03, 0.15)$ These coordinates are defined relative to the scapula reference axis as developed by Holzbaur et al. (2005) with the object shown in Figure 3.2b.

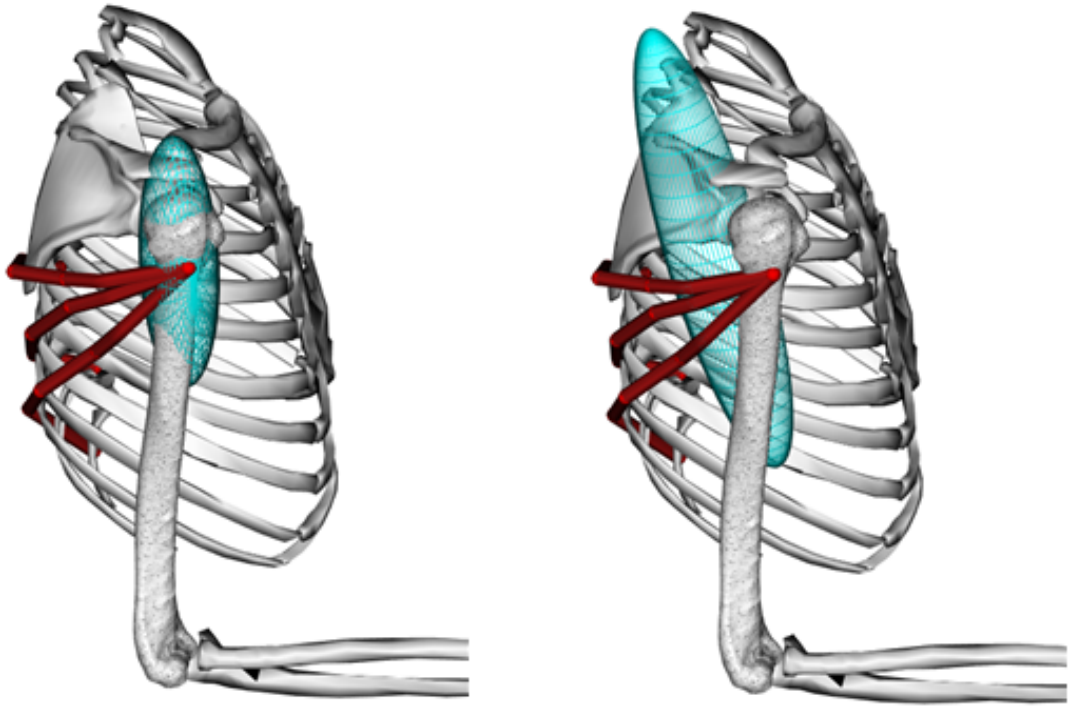

(a) Humeral wrapping object used for low angles of flexion in the altered Upper Extremity Model.

(b) Scapular wrapping object used for low angles of flexion in the altered Upper Extremity Model.

Figure 3.2: Comparison of wrapping objects at low angles of flexion in the Holzbaur Upper Extremity Models.

- A new wrapping object was set for the 90 Degree tests to mimic the wrapping of the LD around the humeral head. This object was defined as a ellipse with Center $x, y, z = (-0.002, -0.0077, -0.0051)$ Rotation $x, y, z = (0.0380482, 0.00855211, -1.40673)$ in radians and Dimensions $x, y.z = (0.032, 0.02, 0.028)$ These coordinates are defined relative to the humeral reference axis as developed by Holzbaur et al. (2005) with the object shown in Figure 3.3.

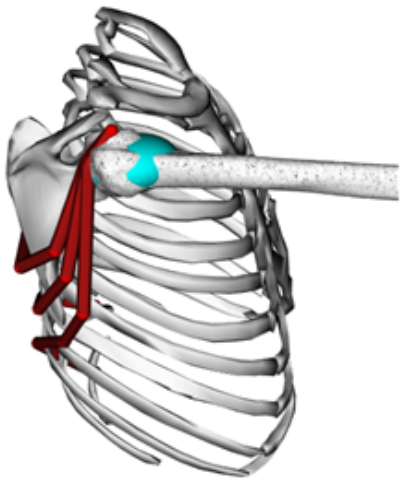

Figure 3.3: Humeral wrapping object to mimic the wrapping of the LD tendon over the humeral head at high angles of flexion, particularly 90°.

The coordinate system used by this model is described in more detail in Section 2.4. This coordinate system does not follow the International Society of Biomechanics standards in order to use more clinically relevant coordinates. The relative motion of the three bones making up the shoulder joint are hard-coded into the model to reduce complexities in motion data.

3.2.2 Tendon Placements

In order to build a 'map' of the efficacy of each point on the humeral head, a large number of tests were sequenced to measure the relevant parameters at each point. In order to do this, a relatively high resolution image of a representative humerus was generated from CT scan data. An .sti file (3D image file made of triangulated points) was generated using Mimics from this data. In order to correctly position the humerus on the axis, the center of the humeral head (found using a 15 point sphere fitting algorithm) was used as the origin for coordinates. The points of the lateral and medial epicondyles were used to rotate the humerus to the correct position in space.

The points that make up the area of interest in this study include the points around the top of the greater and lesser tuberosities. These points were defined to reduce computation time. Not all of the points which appear inside the wrapping objects (and thus have inaccurate, irrelevant results) could be removed. These points were identifiable and were ignored for the purposes of this study, the discussions and conclusions.

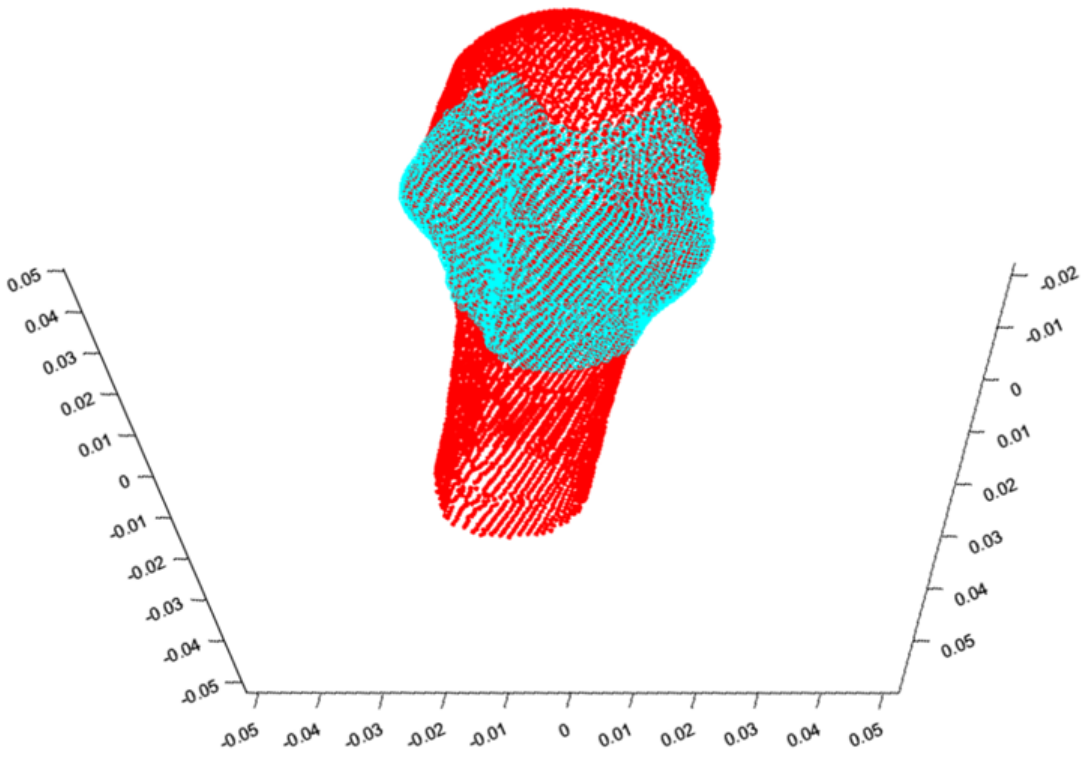

Figure 3.4: Matlab image showing each point that makes up the segmented humerus (in red) and each point in the area of interest (circled in cyan)

For each point in the area of interest, a surgery was simulated with that point as the insertion point of all 3 LD muscle strands. A vector with the results of each test on each point was built to use for comparison.

Seven points of interest were selected on the humerus. These points were selected to be used for comparison to literature and to the cadaver trial described in Chapter 4. These 7 points have coordinates as listed in Table 3.1 and their positions on the humerus are shown in Figure 3.13.

Point Num	X Pos	Y Pos	Z Pos	Area
1	0.023	0.006	0.005	Lesser tuberosity
2	0.013	0.012	0.018	Edge of sulcus
3	0	0.01	0.022	Supra-spinatus insertion
4	-0.01	0.006	0.019	Infra-spinatus insertion
5	-0.015	-0.006	0.016	Teres minor insertion
6	0.003	0	0.0021	Central greater tuberosity
7	0.003	-0.015	0.021	Greater tuberosity base

Table 3.1: Table showing the coordinates of the 7 points of interest selected to compare to literature.

3.2.3 Parameters, Measurements and Coordinate Systems

Parameter Selection

In order to compare the efficacy of one area of the humeral head to another, for LD transfer, a set of parameters must be selected for comparison. These parameters were chosen to compare the ability for the patient to perform certain motions. The motions chosen were:

- External rotation - This is the main motion performed by the posterior rotator cuff and therefore the main motion that needs to be recreated by the tendon transfer. There is a normal 180° range of motion for this action from 90° (flexed forearm rotated across the body) to -90° (flexed forearm pointing laterally).

- Forward flexion - Forward flexion is used (in conjunction with external rotation) to perform many tasks of daily living including washing the axilla, eating and brushing teeth. This motion can be affected by deltoid palsy, one of the contra-indications for LD tendon transfers. Normal range of motion for this action is 0° (arm at the side) to 180° (arm raised vertical).

- Abduction was not tested: The lat dorsi does not affect abduction/ adduction once transferred to the humeral head and for this reason it was not considered in this study.

Adduction was excluded as it is not affected by the rotator cuff. The rotation strength at various stages of adduction may be of interest in future studies. The effects of the loss of abduction strength due to the repositioning of the LD on patients abilities to complete activities of daily living has also not been studied.

In order to determine the ability for a patient to perform these motions after the surgery, the moment arms in each direction (flexion and rotation) were measured. The effective moment arm, as measured using the OpenSim API, is well known as an indicative parameter of active muscle force (Gatti et al., 2007) and (Bolsterlee et al., 2013). The parameters were measured at specific points during forward flexion to see if the position of the humerus affects the effective moment arms. They were measured at 0° and 90° of flexion. Figure 3.5 shows the model at an angle of 0° of flexion. Similarly, figure 3.6. shows the model at 90° of forward flexion.

0° was chosen as the lower angle to emulate rotation in front of the body, similar to the external rotation required when moving objects while sitting at a table or desk. This external rotation would be especially useful for using a mouse at a computer.

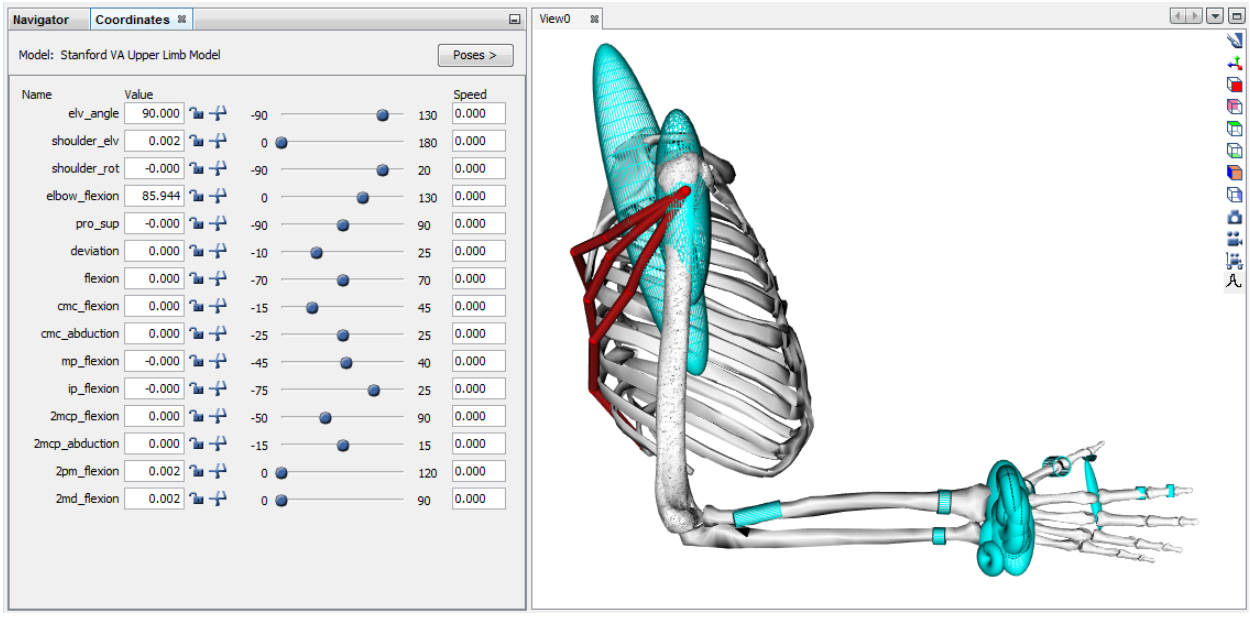

Figure 3.5: OpenSim view of Upper Extremity Model as used for the tests with the humerus at an angle of 0° of flexion.

90° was chosen as the higher angle of flexion to emulate the motion of reaching towards the head. This motion is used for every day motions of living including hair grooming, eating and facial cleaning, and lifting objects from shelves at or above head height.

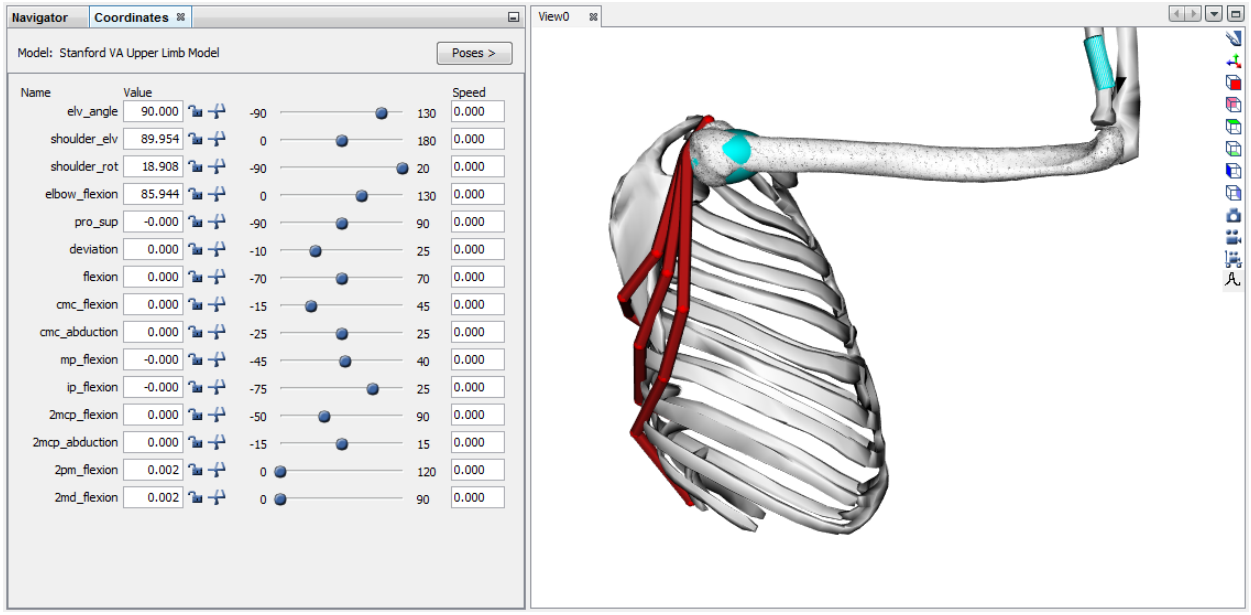

Figure 3.6: OpenSim view of Upper Extremity Model as used for the tests with the humerus at an angle of 90° of flexion.

Coordinates in the Model

Wu et al. (2005) describes the standard 9 coordinate system for shoulder motion with each coordinate representing Z, X and Y rotations (in that order) for each of the clavicle, scapula and humerus respectively. These compound rotations can complicate calculations, particularly in OpenSim as they are not always defined in clinically relevant directions as well as occasionally resulting in a gimbal-like locking. The Upper Extremity model uses 3 coordinates to describe the motion of the shoulder. The relationship between the humeral, clavicular and scapular movement is defined in the model, while the overall clinical motion is described by the coordinates of the model. These three coordinates are Elevation Angle, Shoulder Elevation and Humeral Rotation; executed in that order. This method ensures that the results are clinically relevant as the motion is described in terms of clinical parameters in the model.

These coordinates can be seen in Figure 3.7.

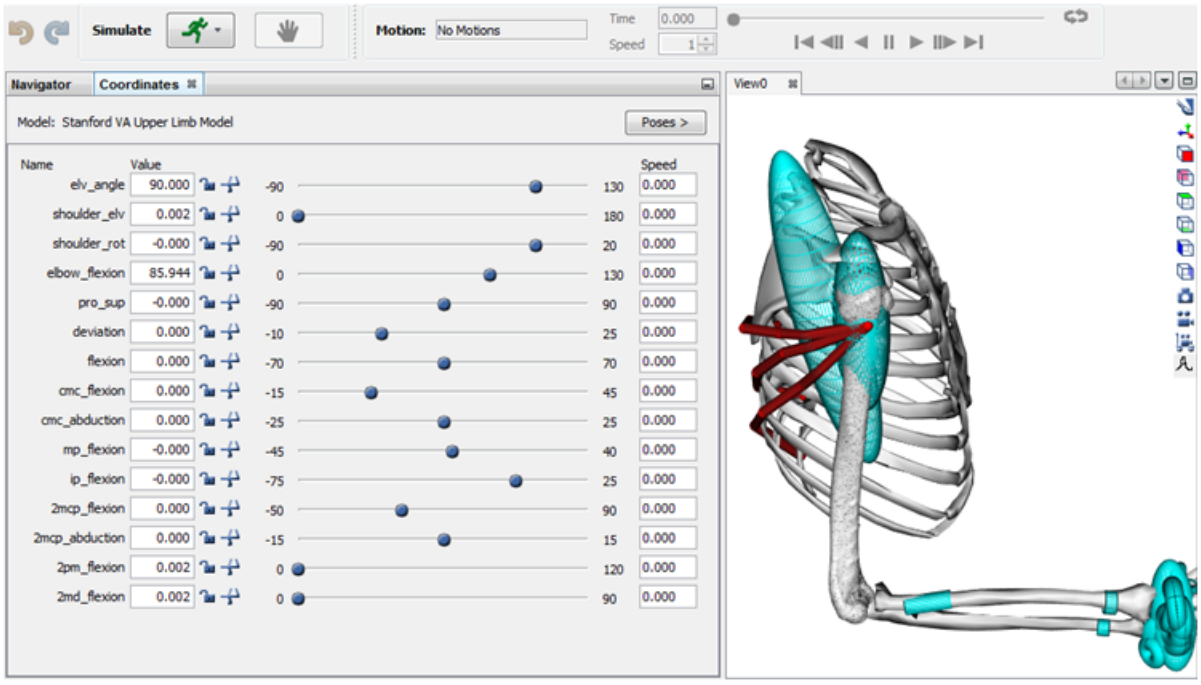

Figure 3.7: OpenSim view of the Upper Extremity Model with the coordinates listed.

The relevant coordinates are the first three coordinates listed in Figure 3.7: elv_angle, to determine whether the motion is clinical abduction, flexion or something in between; shoulder_elv; the amount of flexion or abduction of the joint; and shoulder_rot, the amount of humeral rotation. The other coordinates control the forearm, hand and phalanges.

Parameter Measurement and Storage

In order to compare the effects of various insertion points, a simulated transfer was performed to each relevant point on the humeral head. This was done using a series of matlab files and functions to iterate through each point and store all of the measured parameters for further processing. The block diagram in Figure 3.1 shows a break down of the processes used to complete this. An example of the 7 points of interest is shown in Figure 3.9 and was used to verify the automated parameter outputs.

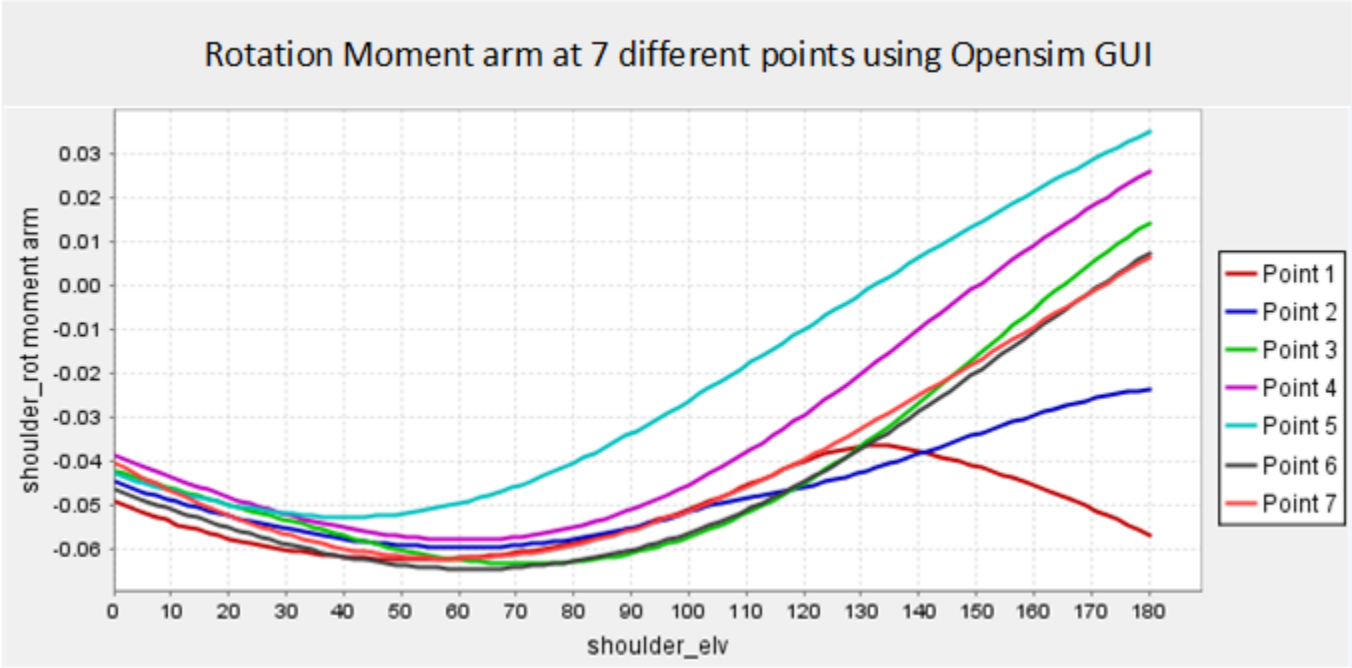

Figure 3.8: Image showing a comparison of the rotation moment arm throughout the motion of flexion with different insertion points (Using the 0 Degree model and therefore less relevant above 50 Degrees of flexion).

Figure 3.9 shows the moment arm in rotation (Shoulder_rot moment arm) as the arm is elevated through 180° using the coordinate shoulder_elv. The moment arms were measured at each point in the area of interest at both 0° and 90° of flexion. The moment arm for each strand was then averaged and saved for comparison. These values were used to generate an effectiveness map of the humeral head.

3.2.4 Visualisation and Result Processing

Once the moment arms results for each simulated surgery have been recorded, they must be processed in order to be presented in a readable form. This was achieved by projecting the humeral

points and the measured results for each point onto a 2D Plane. This gave a 2D view of the relevant part of the humeral head. This view was generated by projecting the points onto a plane that was set at an angle of 65° to the X-Y plane. This projection process is detailed in Section 3.2.4 Projections.

These projected results were then triangulated using Delauney triangulation. Once the points were triangulated, the results making up the corners of each triangle were averaged. This averaged value was then used to prescribe the colour of the projected triangle. This process is described in more detail in Section 3.2.4 Plotting and visualisation.

These projected, triangulated results are then plotted to create a visual map of the humerus describing the effects of the varying insertion points. This plotting process is clearly described in Section 3.2.4

Projections

To project the image into the relevant plane to view the non-articulating surface, the axis is rotated 65° . This is done in matlab using the following sequence of code:

```
Map = [points,zeros(length(points),1)]; %Define the 3D Map of points as all
                                        % Points on the humerus

a = tan(65*pi/180);                     %Constant to rotate through 65 Deg
b = -1;                                 %Constant b

Map = [(Map(:,1)*a + Map(:,3)*b)/sqrt(a^2 + b^2), Map(:,2), Map(:,4)];
                                        % Redefine 3D Map as 2D with X
                                        % values represented by rotated
                                        % X and Z values
```

Figure 3.9: Code projecting points into 2D 65° plane.

This shows how the points are rotated about the axis so that the X'-Y' plane represents the required viewing plane. The points are then projected onto this plane by removing the redundant Z' information.

This produces the points seen in Figure 3.10. These projected points represent the humerus as seen from the lateral angle in 2D. The third direction (Map(:,4)) represents the results that have been stored and references each of these to the point at which it was measured.

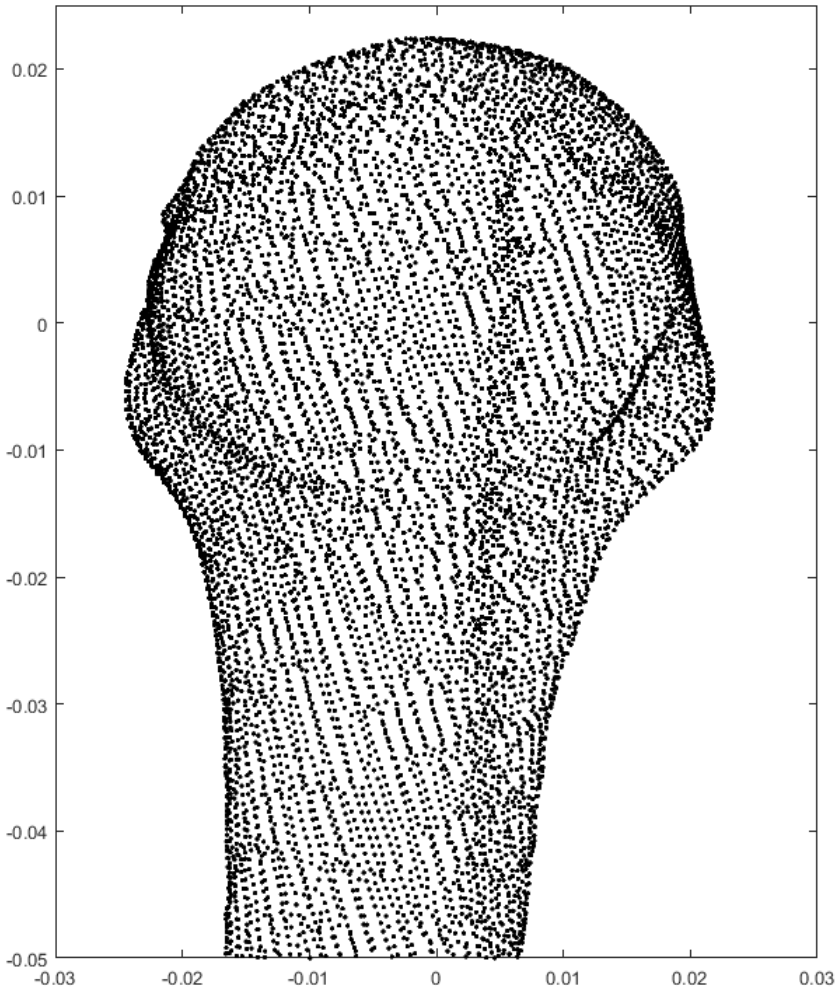

Figure 3.10: Projected view of the humerus from Matlab

Figure 3.10 accurately displays the shape of the humerus, but does not provide a framework to map the results onto this plot. This is done using triangulations described in Section 3.2.4.

Triangulation and Result Averaging

Once the points have been projected into the correct plane they provide an image as shown previously on the right of figure 3.10. This view gives an idea of the structure and shape of the humerus through point densities. In order to show the results "mapped" onto the humerus, each result needs to be referenced to a face. This was done by first triangulating the projected points that make up

the humerus using the *delauney* function in Matlab^{TM}. Figure 3.11 shows the humerus plotted as separate white patches for each triangulated piece.

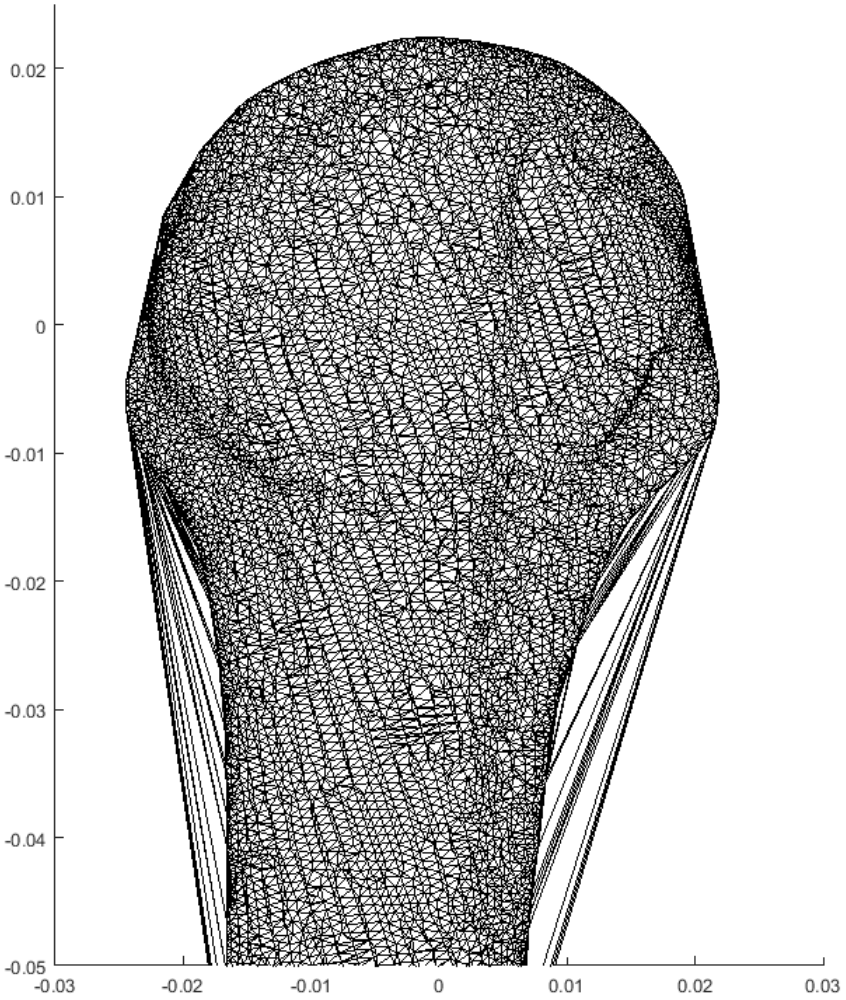

Figure 3.11: Lateral view of all points triangulated to generate faces onto which results can be mapped.

Figure 3.11 shows the humerus as it was automatically triangulated by Matlab. In order to remove the extra triangles that do not fall inside the actual humerus, a vector of the perimeter lengths for each patch was generated. Any patches that had a perimeter more than 2.4 standard deviations from the mean (found by trial and error) were removed. This "corrected" projection is shown in figure 3.12.

The results were then projected onto this image using a colour scale. The process was identical with the other projections with varying distances from the mean perimeter being used. The value for each patch was determined by finding a simple, un-weighted, mean of the results for the three points that make up the vertices. This allowed for the results to be easily visualised as described next.

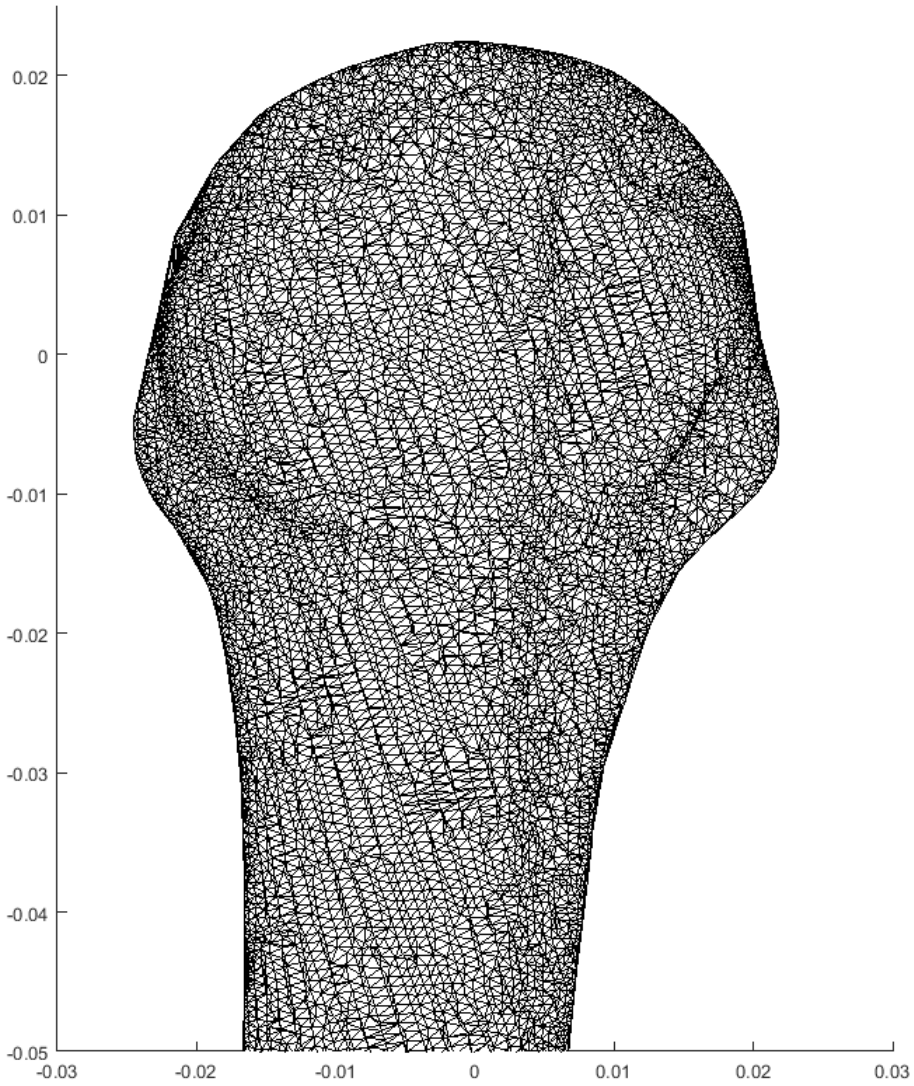

Figure 3.12: Corrected blank XZ projection to show the base onto which the map is projected.

Plotting and Visualisation

Once the results had been calculated, stored, projected, and triangulated as described above, they were plotted. First the blank projection was plotted into the figure. The results were then plotted over this. This gives the illusion of the results being projected onto a 3D humerus. The plots were done using the *patch* plotting function in Matlab^{TM}, with the patch colour described by the averaged value for that patch. A range of colour schemes were trialled to find which of them gave the most accurate impressions at first glance. The colour scheme *jet* was used for it's wide range and clear emphasis of differences.

7 'points of interest' were identified for individual testing. These points were chosen so that they could be used to describe trends in the effectiveness of the humerus as well as compared to literature, particularly Bargoin et al. (2016). These points are shown on the model in Figure 3.13

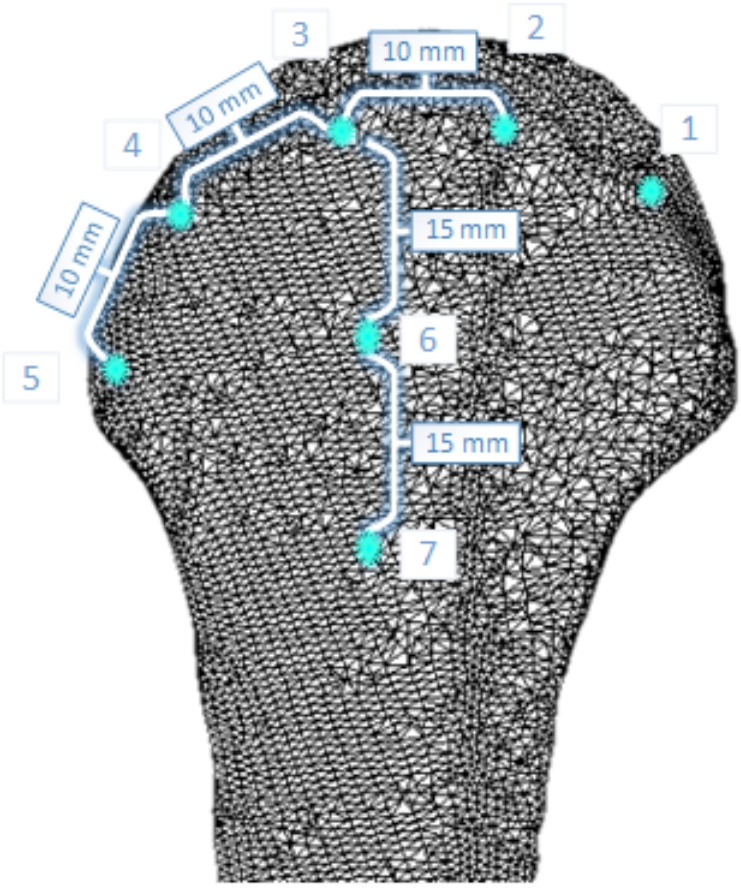

Figure 3.13: Lateral humeral view with 7 points of interest marked, with approximate distances between points.

3.3 Results of in-silico Insertion Point Optimization

The following results were generated using the methods described in the preceding section. The maps show the various moment arms for each point tested on the humerus and the results at each of the 7 points of interest are listed below in tables 3.2 and 3.3.

3.3.1 Moment arms at 0 Degrees of flexion

The following results represent the moment arms calculated for each point at 0°of flexion from the adjusted Upper Extremity model. These results, and the conclusions drawn from them are discussed in Section 3.3.

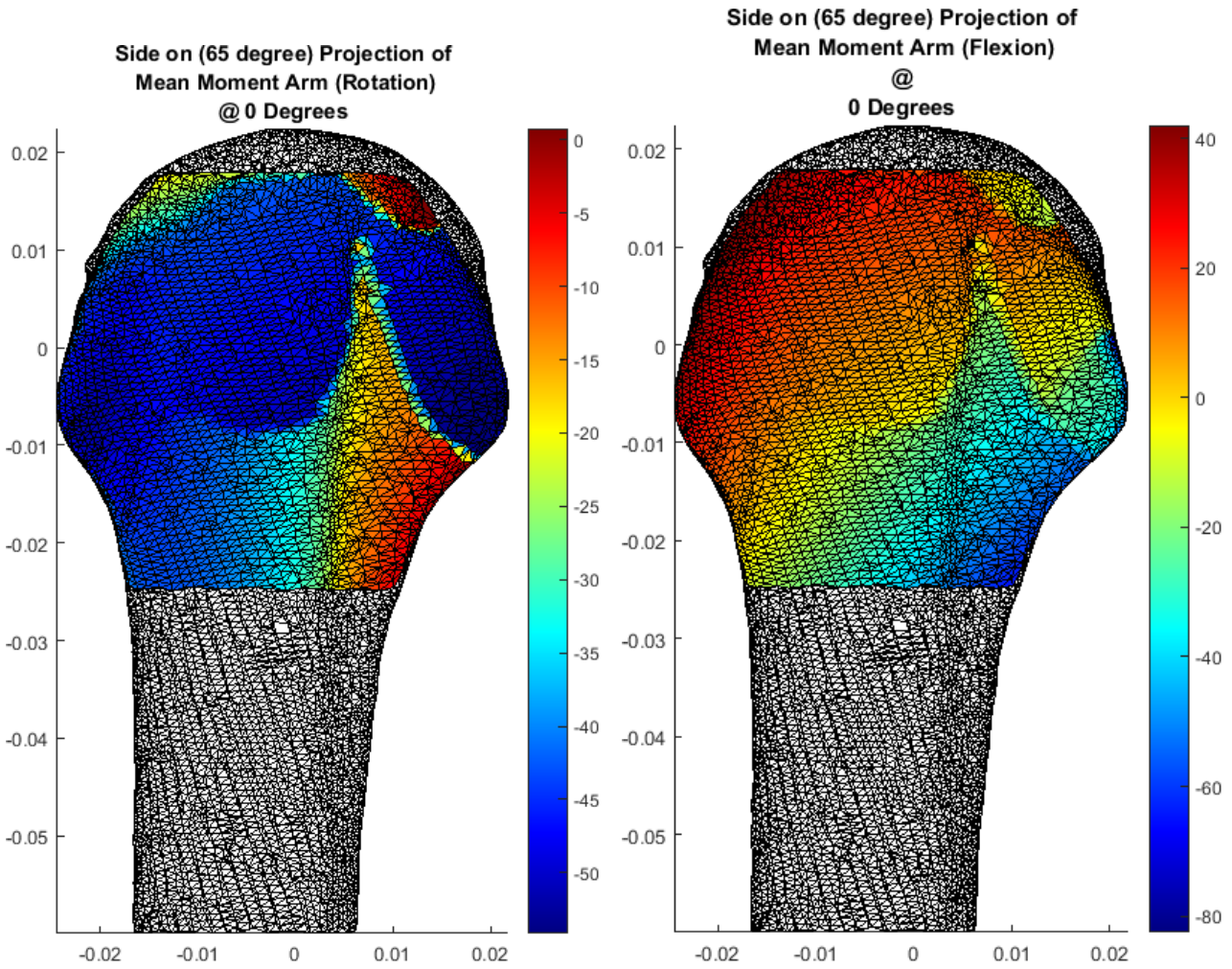

(a) Map of rotation moment arms at 0° of flexion

(b) Map of flexion moment arms at 0° of flexion

Figure 3.14: Flexion and rotation moment arms at 0° of flexion for latisimus dorsi - note, colour schemes are not consistent between maps. Bluer colours on both maps denote increases in the desired moment arm.

For example, it can be seen from Figure 3.14a that the peak of the lesser tuberosity is is the darkest blue indicating the largest negative moment arm. As external rotation is defined as a negative rotation, a negative moment arm (and the colour blue) shows a more effective insertion area. Colours tending towards red show less effective areas. This is the opposite in Figure 3.14b. Forward flexion is a positive rotation and thus larger positive values show more effective insertion points for flexion. The colour scheme was reversed for flexion meaning improvements are still denoted by bluer colours, while red denotes decreased moment arms.. Some points tested for Figure 3.14a were inside the wrapping object and were removed from the results as they were clearly not representative of a realistic moment arm at that point. From some of these points the muscles wrapped around the medial part of the humerus, and for others, simply ran straight through it.

To allow for better referencing of areas on the humeral head and for comparison with literature and other studies, 7 points of interest were defined and tested. The results for these tests as well as the positions of the 7 points in the humeral reference frame are recorded in Table 3.2.

Point Num	X Pos	Y Pos	Z Pos	Flexion moment arm (m)	Rotation moment arm (m)
Point 1	0.023	0.006	0.005	-0.039	-0.049
Point 2	0.013	0.012	0.018	0.008	-0.045
Point 3	0	0.01	0.022	0.021	-0.042
Point 4	-0.01	0.006	0.019	0.028	-0.039
Point 5	-0.015	-0.006	0.016	0.029	-0.043
Point 6	0.003	0	0.0021	0.006	-0.047
Point 7	0.003	-0.015	0.021	-0.016	-0.04

Table 3.2: Simulated results of combined moment arms at 0° of flexion for 7 points of interest.

For example, it can be seen from Table 3.2 that point 3, which is positioned at (0, 0.01, 0.022) generated a combine flexion moment arm of 21 mm and a combined external rotation moment arm of 42 mm. Point 1 had the greatest moment arm in rotation, but generate ante-flexion, while point 6 generated a combined 47 mm of flexion, while having almost no effect (just 6 mm combined between the muscle strands) on the rotation of the humerus. These results are displayed in Figure 3.15.

Figure 3.15 shows the simulated moment arms at 0° of flexion for the 7 points of interest. The blue dots denote the combined external rotation moment arm and the orange crosses denote the combined flexion moment arm. The rotation moment arms are shown as absolute values as they all have a positive effect. It can be seen that points 1 and 7 generate negative flexion, while all other points generate positive forward elevation.

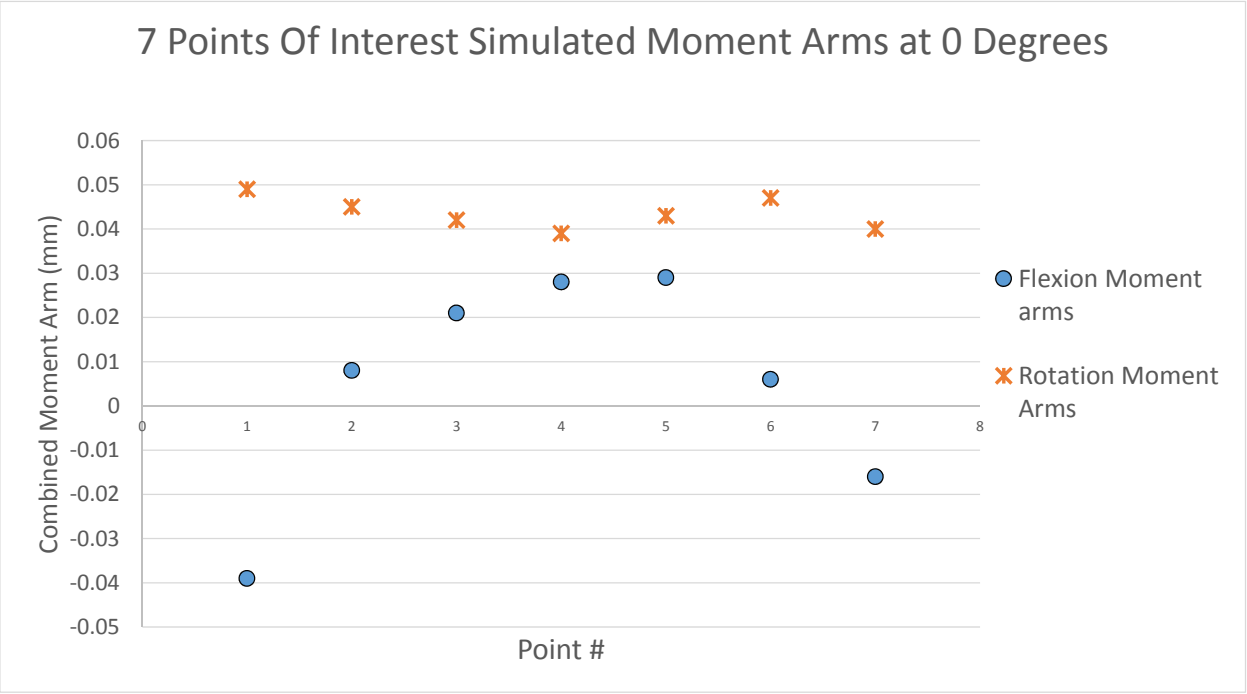

Figure 3.15: Graph comparing the moment arms results for each of the 7 points of interest.

3.3.2 Moment arms at 90 Degrees of flexion

The following results represent the moment arms calculated for each point at 90°of flexion from the adjusted Upper Extremity model. These are used to ensure that the conclusions drawn are valid for more than a single position and can be used throughout a motion.

Figure 3.16a shows the combined moment arms in rotation for each of the points on the humerus. Figure 3.16b shows the flexion moment arms in the same way.

Figure 3.16a shows clearly that the posterior edge of the greater tuberosity has a greater combine moment arm as it is a darker shade of blue. The base of the greater tuberosity shows similar values to the posterior edge, while the lesser tuberosity and surrounding areas show minimal rotation moment arms.

Figure 3.16b clearly shows that the proximal half of the humeral head provides no forward flexion and only a little extension, while the distal part of the head provides increasingly powerful extension.

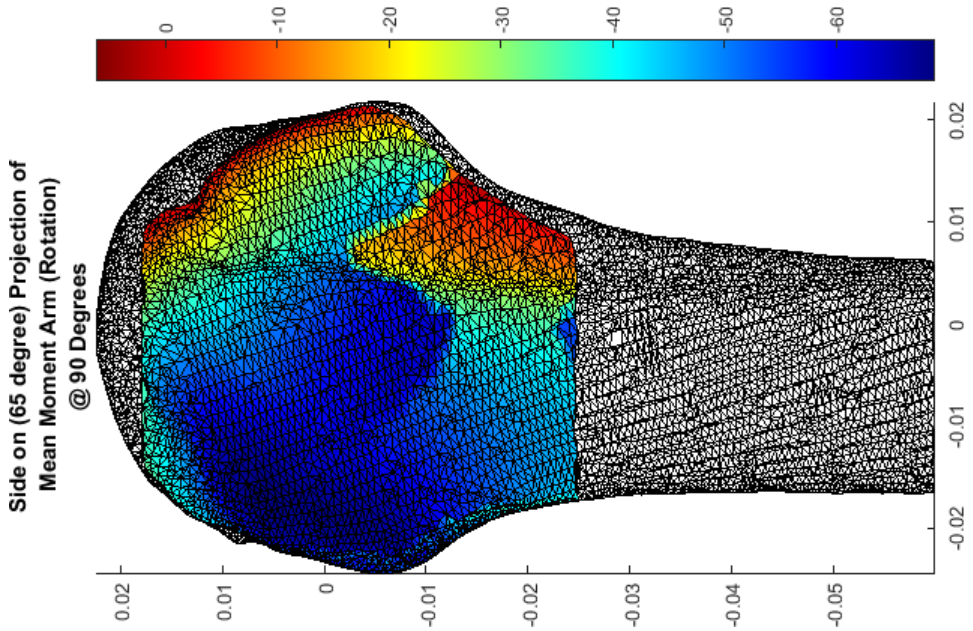

(a) Map of rotation moment arms at 90° of flexion

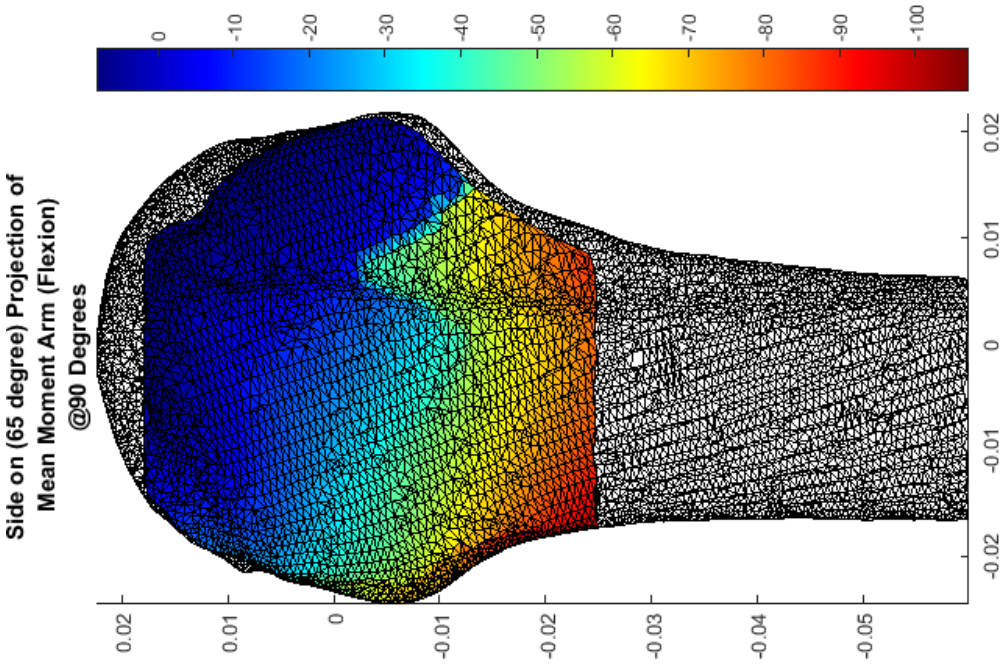

(b) Map of flexion moment arms at 90° of flexion

Figure 3.16: Flexion and rotation moment arms at 90° of flexion for latisimus dorsi - note, colour schemes are not consistent between maps.

The same 7 points were tested at 90° of flexion. The results for these tests are summarised in Table 3.3. These results are important for ensuring the automated model behaves as expected and for comparison to literature and other studies.

Point Num	X Pos	Y Pos	Z Pos	Flexion moment arm (m)	Rotation moment arm (m)
1	0.023	0.006	0.005	-0.004	-0.003
2	0.013	0.012	0.018	-0.001	-0.035
3	0	0.01	0.022	-0.008	-0.055
4	-0.01	0.006	0.019	-0.022	-0.06
5	-0.015	-0.006	0.016	-0.053	-0.057
6	0.003	0	0.0021	-0.024	-0.059
7	0.003	-0.015	0.021	-0.058	-0.048

Table 3.3: Simulated results of combined moment arms at 90° of flexion for 7 points of interest

It can be seen that points 1 and 2 generate very little rotation, while 3-7 generate far greater moment arms. points 3-7 are not easily distinguishable from one another as they are very similar in effectiveness. The table reads as would be expected in flexion in that all points have negative moment arms, ranging from negligible for points 1-3 to much larger for points 5 and 7. At this high angle of flexion, no points appear to generate any flexion load.

The results of Table 3.3 are shown in Figure 3.17.

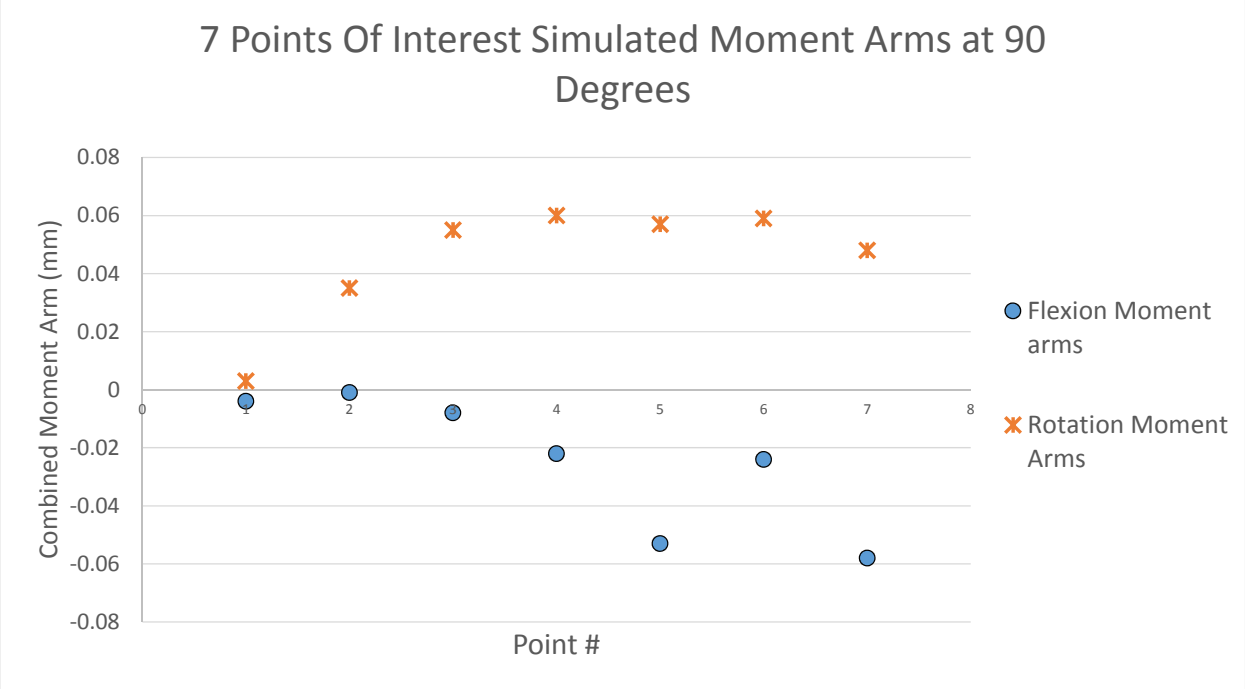

Figure 3.17: Graph comparing the moment arms results for each of the 7 points of interest.

Points 1 and 2 generate little to no rotation at 90° of flexion as shown by the orange crosses in Figure 3.17, while points 3-7 show similar, high, rotation moment arms. It can also be seen that all 7 points generate negative flexion moment arms, with points 4-7 having the most effect.

3.4 Conclusions and Discussion of in-silico Results

This section describes the conclusions that can be drawn from the result in section 3.3. These clinical relevance of these results, and the limitations, are the discussed to ensure that the results and conclusions are properly contextualised. To end, recomendations are made for possible extensions, improvements and recommendations for future research.

3.4.1 Conclusions Drawn

The following conclusions can be drawn from an analysis of the results in section 3.3 in terms of optimising the rotation strength of patients due to LD tendon transfers:

- At 0°of flexion; rotation can be optimised by using the lesser tuberosity or the anterior part of the greater tuberosity.
- At 90°of flexion; No rotation is generated on the lesser tuberosity.
- At 90°of flexion; the anterior edge of the greater tuberosity is up to 42% less effective in generating rotation than the posterior edge.
- At 90°of flexion; the rotation moment arms are negligibly different from the middle area of the greater tuberosity to the posterior edge.

Combining these conclusions that were drawn from; Figures 3.16a and 3.14a, and Tables 3.2 and 3.3 it can be seen that the posterior part of the greater tuberosity points 3-5 is far superior at high angles while being marginally inferior at low angles. The anterior part,while slightly better at low angles has little to no rotation at higher angles. Point 6 is the second largest moment arm at both angles, making it the optimal point for rotation throughout the range of motion. The posterior edge (points 3-5) is the second best when the entire range of flexion is considered. In terms of flexion, The following conclusions can be drawn from the results listed in section 3.3:

- At 0°of flexion, flexion is optimal on the distal, posterior edge of the tuberosity (points 4 and 5).
- At 90°of flexion there is no flexion generated by the LD tendons.

From this it can be seen that only points 3, 4 and 5 generate any meaningful flexion moment, and only at low angles of flexion.

Thus; if some flexion is required, points 3-5, preferably point 5, have the best flexion with good amounts of rotation throughout the motion of flexion. If no flexion is required, point 6 (on a bony landmark about 1.5 cm below the distal ridge and around 1 cm from the sulcus) has been shown by this simulation to have the best overall rotation moment.

3.4.2 Discussion of Limitations and Clinical Relevance of Results

The clinical impact that changes to insertion point may make are reduced by the patient's ability to improve muscle function. This can help make up for marginally inferior insertions as an increase in muscle strength or size can overcome slight reductions in moment arms.

For this reason it should be noted that the difference in moment arm between the 7 points at 0° of flexion is fairly small and will not have much clinical impact. However, the difference at 90° is large (when looking at points 1 and 2 compared to the others). This suggests that those points should be avoided to ensure rotation can be performed throughout a full range of flexion motion.

Similarly, it should be noted that for many patients who undergo this surgery, generating flexion is not the main aim of the transfer. For this reason, the flexion benefits derived from points 4 and 5 need only be taken into account when their are special circumstances that require additional flexion strength.

If some flexion is required, this study found points 3-5 to be the optimal areas for insertion. This complies with Ling et al. (2009) and Favre et al. (2008) as seen in Figure 2.9. If no flexion is required, and rotation is desired throughout a full range of flexion motion, point 6 was found to be optimal. This is not seen in any literature as the face of the humeral head has not been analysed by many studies. If rotation is only required at a low angle of flexion, point 1 was found to be optimal. This corroborates the secondary findings of Ling et al. (2009). This study has corroborated different other studies, depending on the required surgical outcomes. This can be used to tailor the outcomes for a specific patient.

These results are in line with parts of the literature, and extend the understanding of insertion points for LD tendon transfer by including a wider range of points. This provides surgeons with a more nuanced idea of the effect that various insertion points will have on the outcomes of their surgery.

The results and conclusions of this study are limited in 2 main ways:

1. The changes in moment arm were only examined during a flexion motion and not during

any abduction motions. There are some activities of daily living that require abduction and external rotation, and these were not taken into account.

2. The tests were done with the humerus in a neutral state of rotation. The moment arms could change for greater angles of internal rotation. As the LD would simply wrap around the bone, this should not have a drastic effect on the relevance of the results

3.4.3 Recommendations for Future Studies

The following are recommendations for future studies to improve our knowledge of the effect of tendon insertion site on the clinical outcomes of LD transfer patients.

- Future studies could compare the effectiveness of transferring various tendons (teres major, infra-spinatus etc.) to determine the optimal tendon to transplant.
- The effects of tendon insertion point on gleno-humeral stability should be analysed.
- The effects of tendon insertion point through abduction motions should be analysed.
- A dynamic model assessing joint contact forces, muscle loads and range of motion could be designed.
- The optimal insertion point for the LD (or other tendon transfers) could be studied with reverse shoulder arthroplasties.

Chapter 4

Bio-mechanical Cadaver Study

4.1 Introduction to Cadaver Insertion Optimisation

This chapter details the bio-mechanical cadaver study performed to validate the *in-silico* study done in Chapter 3. It details the rig design process as well as the research methods. Next, the results are layed out before conclusions are drawn from them. These are then discussed and will be compared to the simulation results in discussions and conclusions in Chapter 5.

4.1.1 Rational and Problem Statement for Cadaver Trial

The need for a cadaver trial that is run in parallel with kinematic/ bio-mechanical simulations is well described by Magermans et al. (2004). A simulation cannot take into account all of the factors that are present in the actual biomechanics of the human body. Simulations can also have internal errors, errors in assumptions and may break down under certain circumstances. This means that all simulations studies should be compared to *in-vitro* or cadaver literature and, if possible, to a parallel cadaver trial. Current cadaver and in-patient trials , inlcuding Cleeman et al. (2003), Oh et al. (2013), De Casas et al. (2014), and Bargoin et al. (2016) do not produce results that can be used to validate the *in-silico* model described in Chapter 3. For this reason, a new study was set up that would have comparable results to the *in-silico* study and could be more reliably compared for validation.

Problem Statement

In-silico studies should not be used without being validated by *in-vitro* testing in order to ensure that the results are clinically relevant and bio-mechanically possible. A parallel cadaver trial is the best way to do this as it allows the results from both studies to be directly compared in order for them to be verified.

4.1.2 Aims of the Cadaver Study

The aim of this study is to determine the optimal insertion point of the latissimus dorsi (LD) on the humerus for treatment of posterior superior rotator cuff tears. These results aim to validate the results found using the kinematic *in-silico* model.

4.1.3 Study Outcomes

The outcomes of this study include:

1. A comparison of the surgical outcomes with transfer to 7 points on the humeral head for LD tendon transfer at a neutral position of flexion .
2. A comparison of 7 points on the humeral head for LD tendon transfer at a high (90°) angle of flexion .
3. An optimal insertion point to promote rotation generation post LD tendon transfer.

4.1.4 Scope and Limitations of Cadaver Trial

This cadaver trial is comprised of clinical force generation assessments in rotation at 2 angles of flexion in fresh frozen cadavers. The load generation assessments are done for 7 points on the humeral head and performed bilaterally on whole cadaver torsos. The load assessment involves measuring and comparing the torque produced in rotation for each of the 7 points on the humeral head for a given load spread evenly across the broad area of the LD origin. 4 cadavers were used, providing 8 shoulders, with four measurements taken for each point on the shoulder. This gave a total of 32 data points for for each measurement, allowing for robust statistical analyses. The limitations present in this study include:

- The shoulder is a very complex joint with many muscles acting in unison. This study did not examine the effects of co-contraction of various muscles, which could affect the center of rotation and rotation force generating ability. Including co-contraction would have added many more conflating variables, making the results less statistically significant.
- The rig used was unable to measure flexion load generation as the rotation was greatly affected by the lack of co-contraction of the biceps brachialus and deltiod.
- Only male participants were tested as these were the cadavers made available by the department.
- Some data points were excluded as there were problems with cadaver decay and data recording in some tests. This was not excessive and still allowed a robust statistical comparison of the results.
- There was some sticking in rotation of the clamps used for measuring caused by congealed blood entering the mechanism. This was counteracted by taking more measurements and discarding those with obvious errors.

Steps were taken as mentioned to ensure that these limitations do not affect the reliability of the study.

This section has given an introduction to the cadaver trial which was conducted. It has motivated the need for such a trial, provided the aims and objectives and discussed the scope and limitations. The next section describes the process undertaken to design the rig used to perform conduct the trials.

4.2 Cadaver Trial Test Rig Design Process

This section details the design process and specifications for the rig used to measure the effects of various insertion points in the cadaver trials. The rig was built to fit on an original cadaver torso mount used for previous studies within the department. This eliminated the need to design a mounting system for the cadavers and provided a framework from which to work. As this rig will be used to mount cadavers in the future, all of the additions had to be removable. All of the parts drawings for this test rig can be found in Appendix C. Originally, the rig was designed to assess the post surgical-strength in both flexion and rotation. After a pilot test on one cadaver, it was found that flexion could not be assessed as the rotation in this direction is more complex and requires co-contraction of a number of shoulder muscles. This section briefly describes the efforts made to assess flexion, even though they was unsuccessful. The completed rig is shown in Figure 4.1 before use.

Figure 4.1: Image of the rig used to test the effectiveness of various insertion points using cadaver torsos.

4.2.1 Specimen Mounting

The cadaver specimen was mounted vertically in the rig. This was achieved using whole cadaver torsos. A 12 mm drill bit was used to drill through the manubrium and spinal elements T2 or T3. An M10 bolt was inserted into this hole, and mounted into the appropriate hole in the frame. The height was chosen to allow the majority of the cadaver weight to be supported by the bolt. The shoulders were also set to the correct height to reach the clamps described in Section 4.2.3.

4.2.2 Latissimus Dorsi Load Application

Once the cadaver was mounted, a system was needed to apply a load on the humerus at various points to simulate the action of the LD muscle after surgical transfers to different points. From the literature analysed in Chapter 2, this has been done in two main ways. The first way is to attach wires to each insertion site with weights on the end of each wire (Favre et al., 2008). This requires the wires to accurately mimic the broad insertion of the LD and was used successfully by Favre et al. (2008). A second method performed by Werner et al. (2006) used the end of the LD tendon with a single load at approximately 45 degrees from vertical. This method does not take into account the effects of the broad insertion. Bargoin et al. (2016) used sutures to fix the weighted wires into the muscle, mimicking the broad origin of the LD without making assumptions about tendon length and tendon wrapping around the humerus.

For this rig it was decided that multiple loaded wires as in Bargoin et al. (2016) would provide a more realistic model than the single point of Werner et al. (2006) and be more efficient than the direct wire transfer used by Favre et al. (2008). In order to achieve this, a base plate was bolted to the back of the rig with holes to guide the loading wires. The placement of these holes was based on the dimensions listed in 2.1.3. The dimensions for these are shown in Figure 4.2.

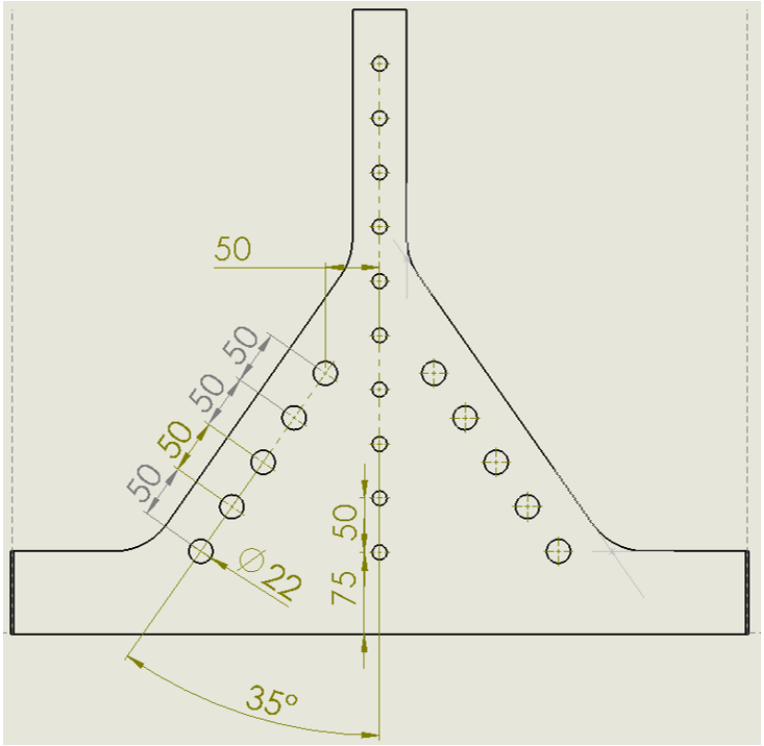

Figure 4.2: Dimensions used to ensure the load applicator wires apply a clinically relevant load, mimicking the LD muscle (in mm).

The original design included a full plate covering the back, but after an initial pilot study, this was reduced to improve access to the LD muscle from behind. In order to ensure that the wires can flow through the plate smoothly, S bends were printed and attached to bearings in the holes. This reduced friction as well as reducing wear on the wires.

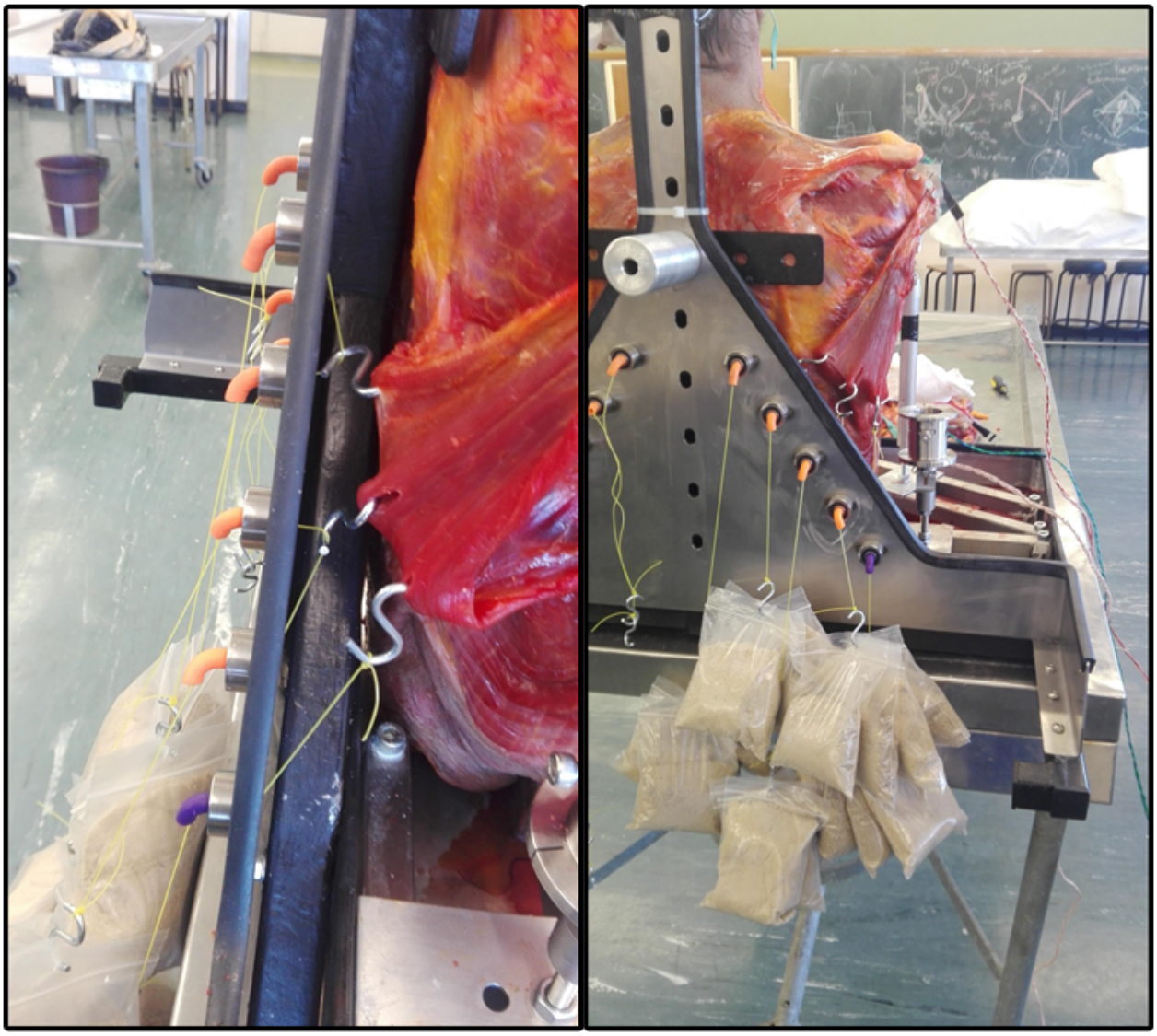

Figure 4.3: Image of the hooks in the LD muscle on specimen 1 showing how the load is transferred to the muscle.

In order to transfer the load from the wires to the muscle, hooks were attached to each set of wires as shown in Figure 4.3 on the left hand side. On either end of these loops, sandbags were used as weights to generate the load. These weights can be more clearly seen on the right hand side of Figure 4.3. Four (4) bags, exerting a load of 2 N each, were hung on each of the 5 hooks. This generated a combined load of $40 \pm 2\%N$ on the latissimus dorsi. The resulting load exerted by

the humerus determined how effective the insertion point being tested was in generating external rotation. Several cycles of loading were performed to remove slack and elasticity in they system.

In order to assess the effects of the surgery at various insertion points on the same humerus without compromising the bone, nails were placed in the humeral head. The layout of these nails is described in detail by Figure 4.16. A loop was generated at the end of the tendon using a whipstitch. The size of this loop is negligible compared to the size of the latissimus dorsi and did not affect the results. This loop was then hooked onto each nail to simulate differently placed insertions during surgery. These are shown clearly in Figure 4.4

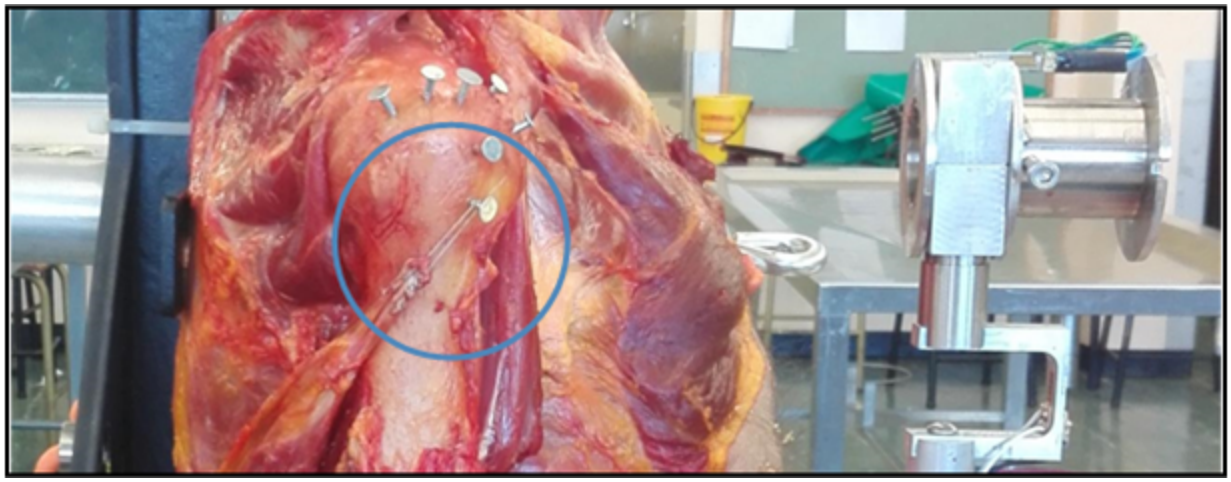

Figure 4.4: Nails placed in the humeral head for efficient changing of insertion point.

4.2.3 Load Generating Ability Measurements

Once the force was applied by the LD as described, the resultant load exerted by the humerus must be measured. This has been done in a number of ways, as described in Section 2.4.2. For this study it was decided that an instrumented clamping device would provide the most accurate and repeatable results. The results of the surgery, in terms of both flexion and rotation strength, were needed at a low angle of flexion and a high angle. This required two instrumented clamping devices.

There were a number of design iterations of these devices. The diagram in Figure 4.5 gives an overview of how the long clamp for high angles of flexion changed over time. Figure 4.6 shows the same for the shorter clamp designed to measure results at a low angle of flexion.

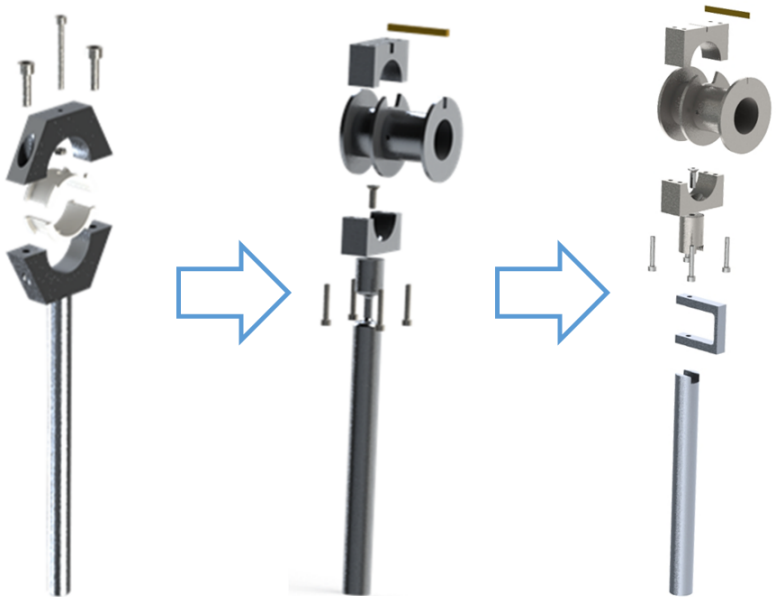

Figure 4.5: Changes in the design of the longer clamp to ensure that it can accurately and precisely measure the flexion and rotation strength for different insertion sights.

The first clamp used rosetta strain gauges on the stem. The strain directions were separated using post processing. This conflated too many variables and so a separate load cell was used for rotation in the second iteration. A load cell for flexion was then added in the third iteration to attempt to measure flexion. Unfortunately, due to the complex nature of flexion, this was not possible.

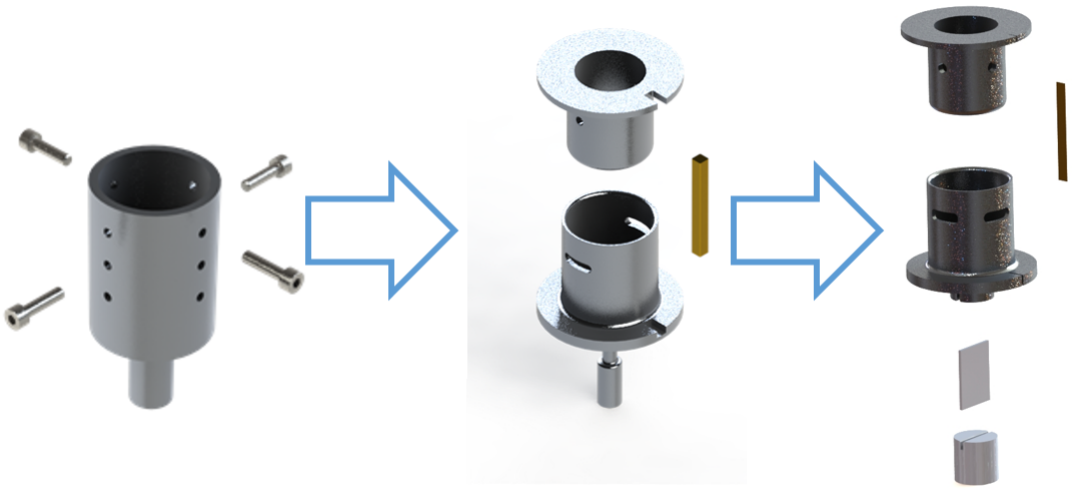

Figure 4.6: Development of the shorter clamp to measure the rotation and flexion strength at a low angle of flexion.

The first short clamp also used Rosetta strain gauges. This was upgraded using the same rotation load cell used in the long clamp, adjusted for the relative directions of rotation and clamping. The third iteration attempted to include flexion measurements, but this failed as the clamp needed to be adjusted to comfortably clamp the humerus at 0° .

In order to ensure that the humerus can be easily clamped in the load cells, it must be shortened and the epicondyles removed. It was cut at around 200 mm from the center of rotation, at the point where the epicondyles merge with the cylindrical shaft. This point is shown in Figure 4.7 for clarity.

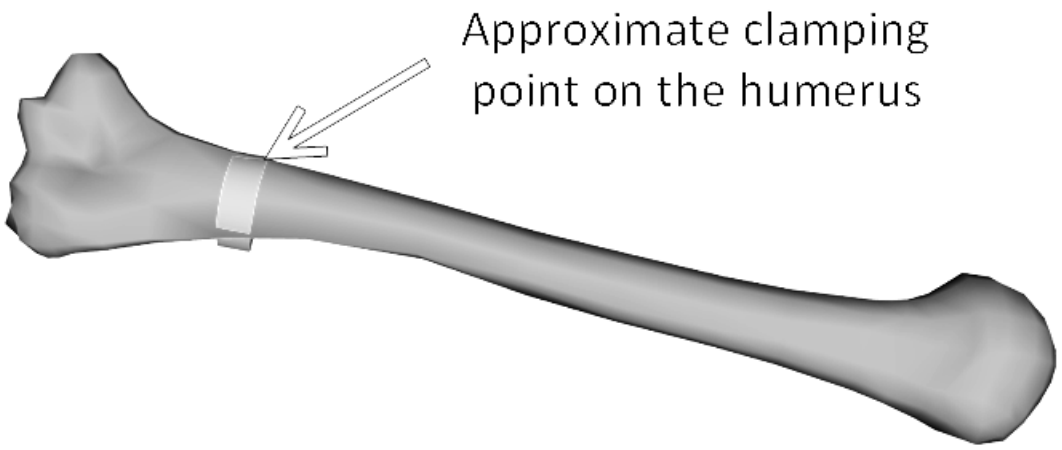

Figure 4.7: OpenSim view of a humerus highlighting the approximate point at which the condyles will be removed to allow for clamping.

The point shown in Figure 4.7 varies between specimens. The distance from the center of rotation of the humerus to the clamp was adjusted for each specimen to allow it to fit into the clamps on the rig, which did not affect the results in any way. This distance was occasionally changed between 0° and 90° tests as the clamps were not identical.

Long Clamp Specifications and Load Measurement

The long clamp was designed to measure the torsion strength in external rotation with the arm flexed to around 90° as well as to measure the strength in flexion. The clamp was made up of 3 distinct parts: The stem with adjustable height (A); the clamp that measures rotation strength (B), and the flexion load cell (C). These are labelled A, B and C respectively in Figure 4.8

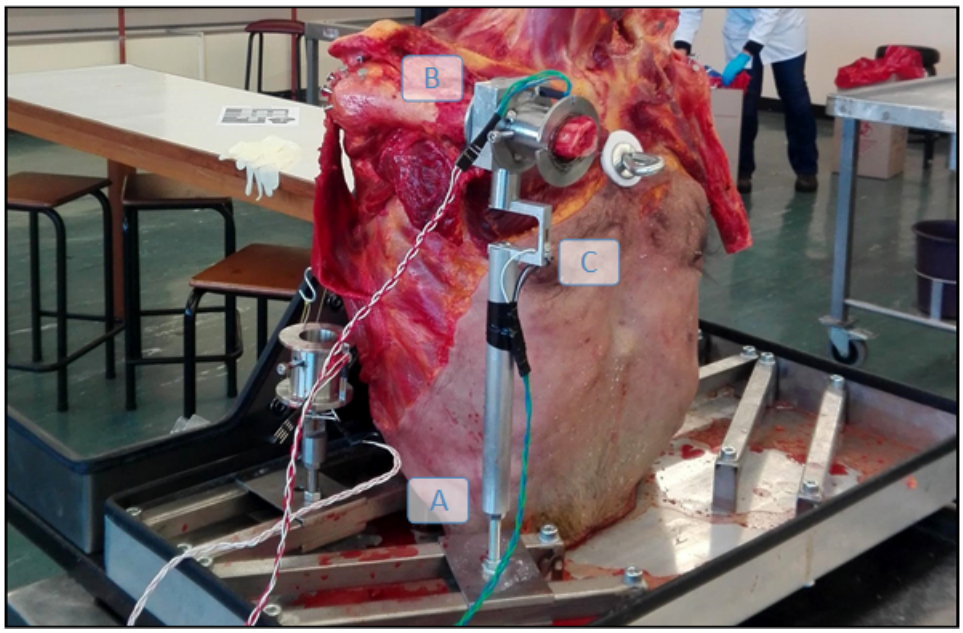

Figure 4.8: Labelled Long Clamp showing both load measuring sections as well as the adjustable height on the stem.

The height was made adjustable using a long threaded bolt and a threaded hole in the stem. This allowed for an adjustment in height of 30 mm. Once the clamp was positioned at shoulder height, it was locked in place with a locking bolt. The clamp held the humerus in place. The epicondyles were removed from the humerus and it was placed through the center of the clamp. 3 bolts were used to lock it is place (see Figure 4.8). The load cell, with a pair of strain gauges, was positioned 30 mm from the center of rotation. This was a piece of stainless steel, with strain gauges on opposite sides. The load and strain were approximated as shown in the diagram in Figure 4.10 to determine the optimal strain bar thickness t.

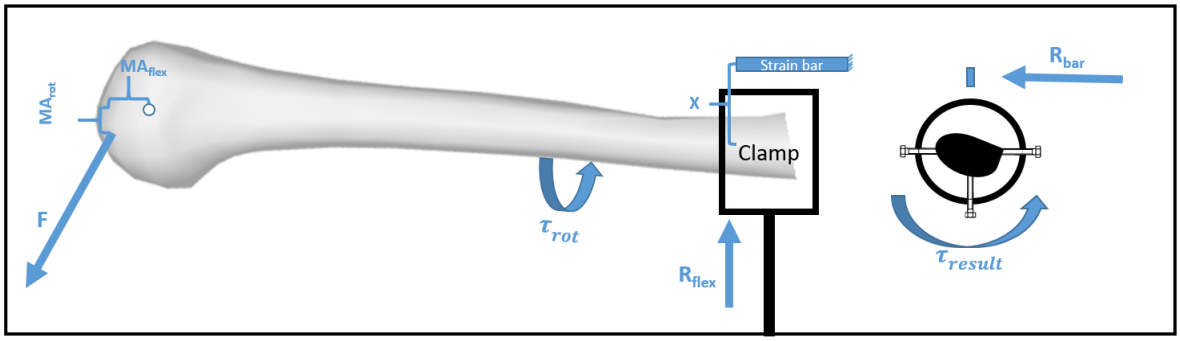

Figure 4.9: Diagram showing a simplified breakdown of the forces on the humerus in the long clamp.

Assumptions	Value	Units
Load applied by latissimus dorsi on humeral head	40	N
Maximum rotation moment arm on humeral head in rotation	20	mm
Maximum rotation moment on humeral head in flexion	15	mm
Distance from clamp to humeral center of rotation	200	mm
E (Youngs Modulus) of stainless stell	160	GPa
Yield strength of stainless steel	502	MPa
Clamp center to load cell disctance (x)	35	mm

Table 4.1: Table describing the assumptions used to design the rotation measuring load cells.

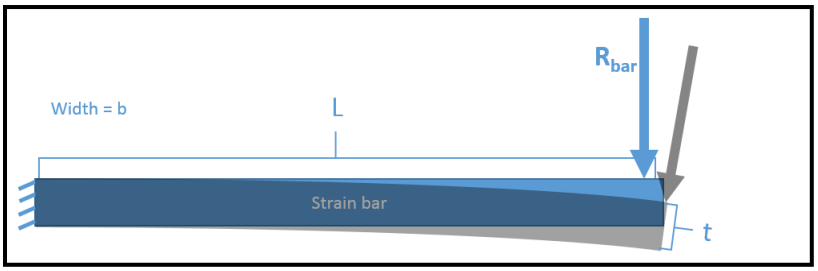

Figure 4.10: Diagram showing the simplification used to determine the strain, and thereby the stress, measured by the strain gauge.

Using this information, it was determined that the optimal thickness of the steel plate is 1 mm. Using the flexion load, basic load simulations were done in Solidworks to determine the expected stress and strain in the load cells.

Short Clamp Specifications and load measurement

The bottom clamp was designed similarly to the long clamp. Figure 4.11 shows the bottom clamp including: the stem which is adjusted by height for up to 60 mm (A); the flexion load cell (C) and the clamp, with a rotation load cell similar to that in the long clamp. The height adjustable stem is made up of a threaded bar and two locking nuts. This allows the height to be adjusted for the specimen shoulder height. The clamp is also locked in place using a third locking nut. The flexion was measured by the strain gauges on either side of the piece of sheet metal making the flexion load cell. As previously described, the strain measured here was not clinical flexion as the lack of co-contraction in the shoulder muscle did not simulate rotation around a fixed point.

The rotation load cell was designed to work exactly like that shown in the long clamp. The humerus was clamped using 3 bolts that were alternatively tightened to ensure the center of rotation was as close to the center of the clamp as possible.

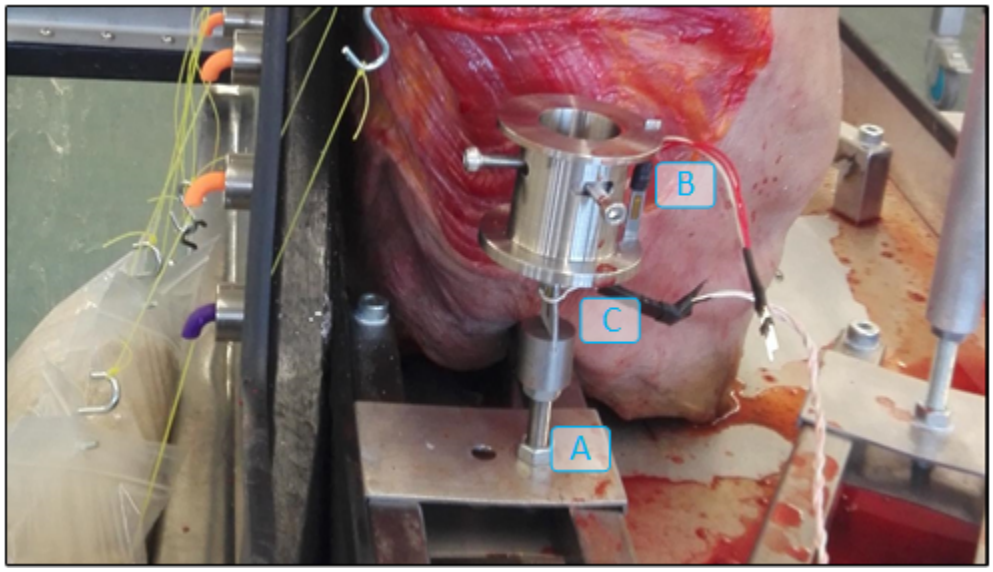

Figure 4.11: Bottom clamp with the adjustable stem (A), flexion load cell (C), and rotation cell clamp (B).

Electronics Design

To measure the loads exerted on the clamps, strain gauges were configured for the load cells. These strain gauges were set up to measure the bending stress in the materials. The change in resistance due to the change in strain is extremely small. A standard amplification circuit (half wheatstone bridge) was used to amplify the strain reading to separate the readings from the noise of the system.

The components are listed below and the connections are shown in Figure 4.12.

- $R1 = 120 \pm 1\%\Omega$ composite (aluminium foil) strain gauge
- $R2 = 120\Omega$ resistor
- $R3 = 120 \pm 1\%\Omega$ composite (aluminium foil) strain gauge
- $R4 = 120\Omega$ resistor
- $Pot1 = 500\Omega$ Potentiometer to zero / adjust signal
- $R5 = 4.7k\Omega \pm 1\%$ Resistor

- $R6 = R7 = 75k\Omega$ Resistors
- LM358 = Operational amplifier to stabilise reference signal of 2.5V
- AD8223 = Instrumentation amplifier to amplify and stabilise strain signal from the gauges and send it to Arduino
- $Pot2(0 - 500\Omega$ Potentiometer$)^*$ = Gain Resistor to set AD8223 amplifier gain

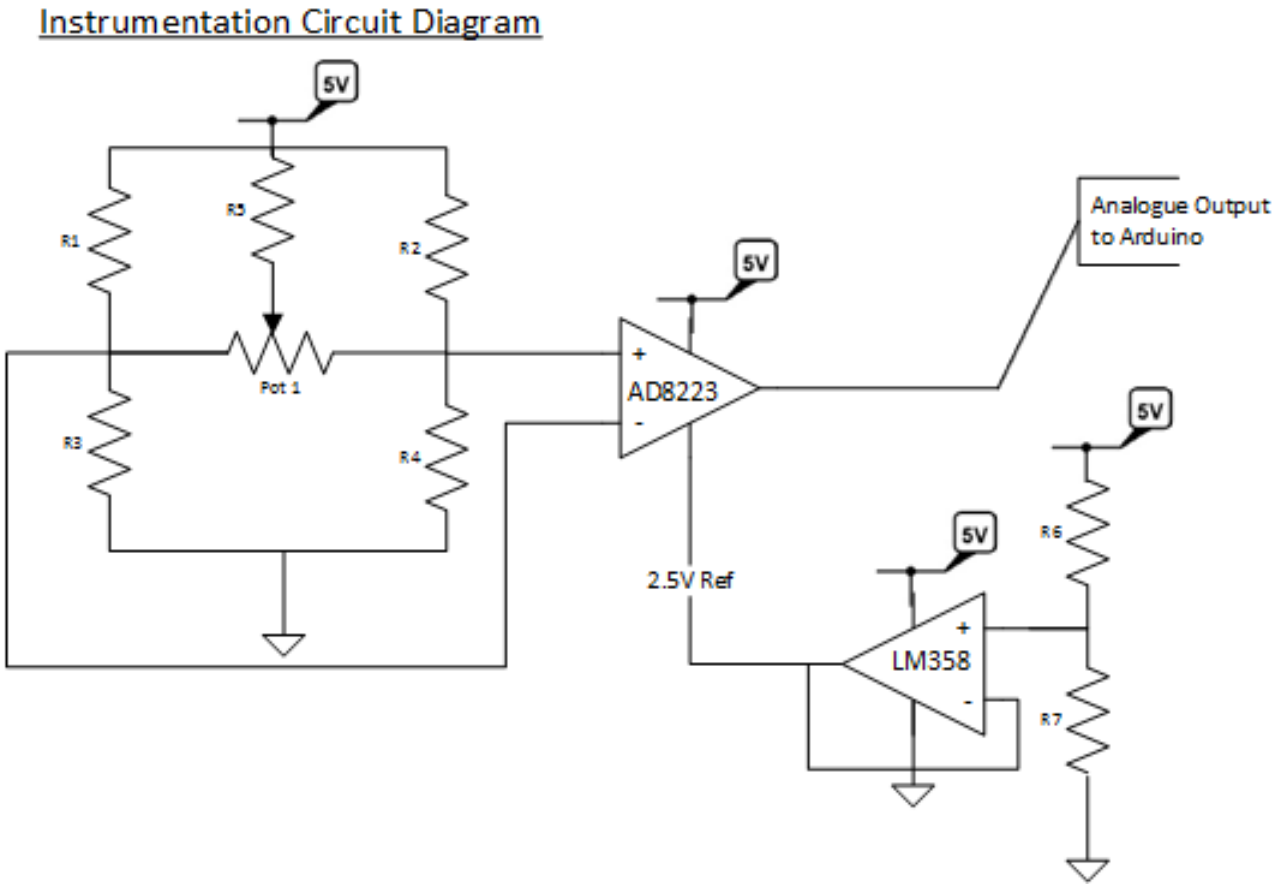

Figure 4.12: Circuit diagram and connections for strain signal requisition and amplification.

Values were read into the Arduino analogue inputs and output to excel for further analysis. There was no need to calibrate the analogue voltage signal to a specific force as they are directly proportional. This allows the signal to be compared in lieu of comparing actual forces, stresses or strains.

*Component not shown in diagram

4.3 Cadaver Trial Protocol

Due to the uncertainties in mathematical models shown by Quental et al. (2013), it is imperative that a mathematical model be ratified by a small scale biomechanical trial using cadaver specimens. This trial was set up to record similar parameters or outcomes to the mathematical model in order to directly ratify the results. This aimed to both ratify the decision to use moment arms as a measurement indicative of force application, as well as verifying the optimal insertion point.

4.3.1 Cadaver Selection and Ethics

The cadavers were sourced from the Human Biology department of the University of Cape Town. These cadaver torsos were randomly assigned. They consisted of 4 males, all with healthy shoulders. These cadavers were donated to science and were used for a number of parallel studies after this study. The protocol was outlined for the Human Research Ethics Committee (HREC) at UCT and submitted for approval. Approval was given for the research to proceed on the 24th of February 2017 under HREC reference number 048/2017. This approval is attached as Appendix D.

4.3.2 Experiment Set-up

The cadaver trial is split into 2 parts: the neutral low angle of flexion tests shown below in Figure 4.13 to verify the 0° results in Chapter 3 and the high angle tests to verify the 90° in Chapter 3 shown in Figure 4.14.

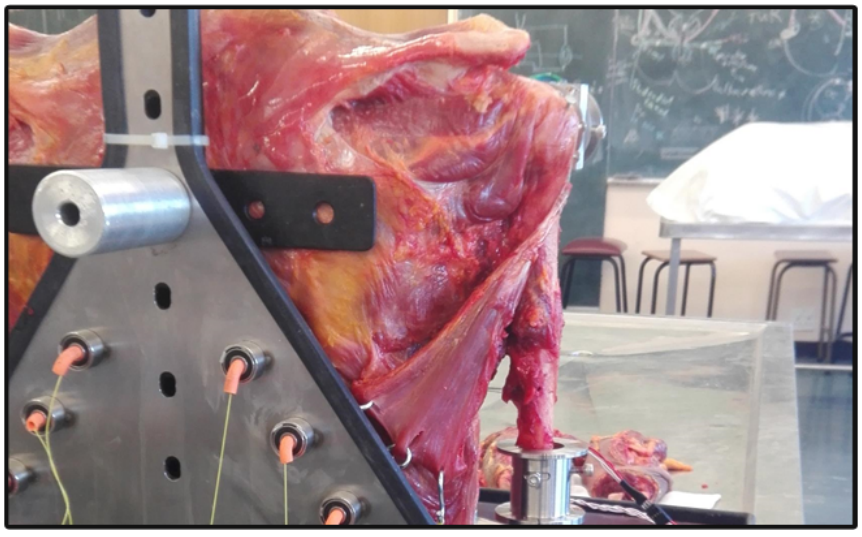

Figure 4.13: Image showing cadaver placed in the testing rig for low angled 0° tests.

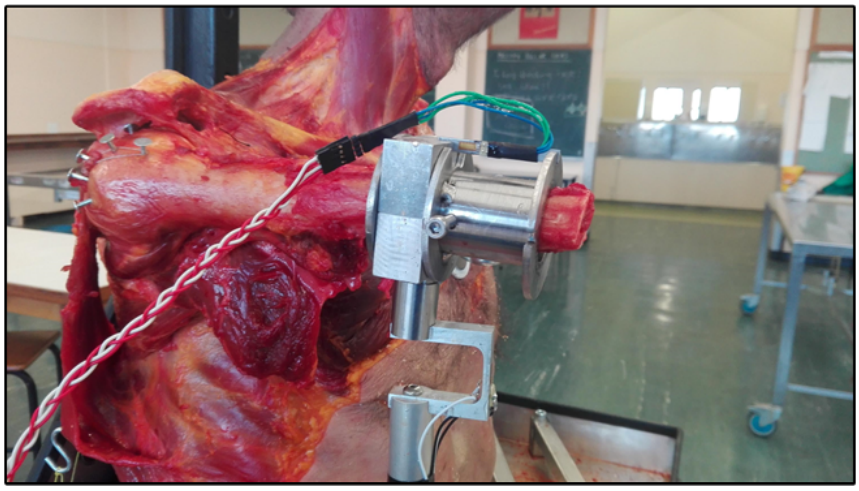

Figure 4.14: Image showing cadaver set-up for high angled 90° tests.

Multiple repititions of loading as well as repititions of pre-loading were used for each test to ensure the tests gave repeatable and reliable results. This generated a signal similar to the one seen in Figure 2.11 from Habermeyer (2006) and shown in Figure 4.15.

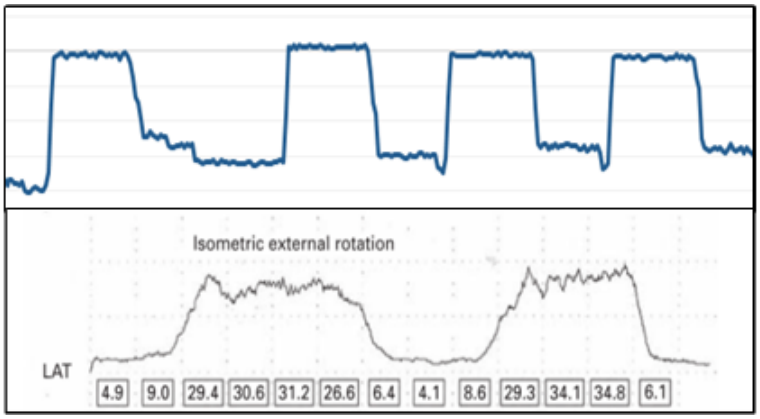

Figure 4.15: Example signal from cadaver tests for rotation compared to Habermeyer (2006) measured isometric contractions for rotation

This figure shows that the measurements taken were comparable to the active contractions measure post surgery in the literature.

The protocol used for all tests is shown below. This protocol was followed to ensure that the results were consistent and to reduce the number of conflating variables.

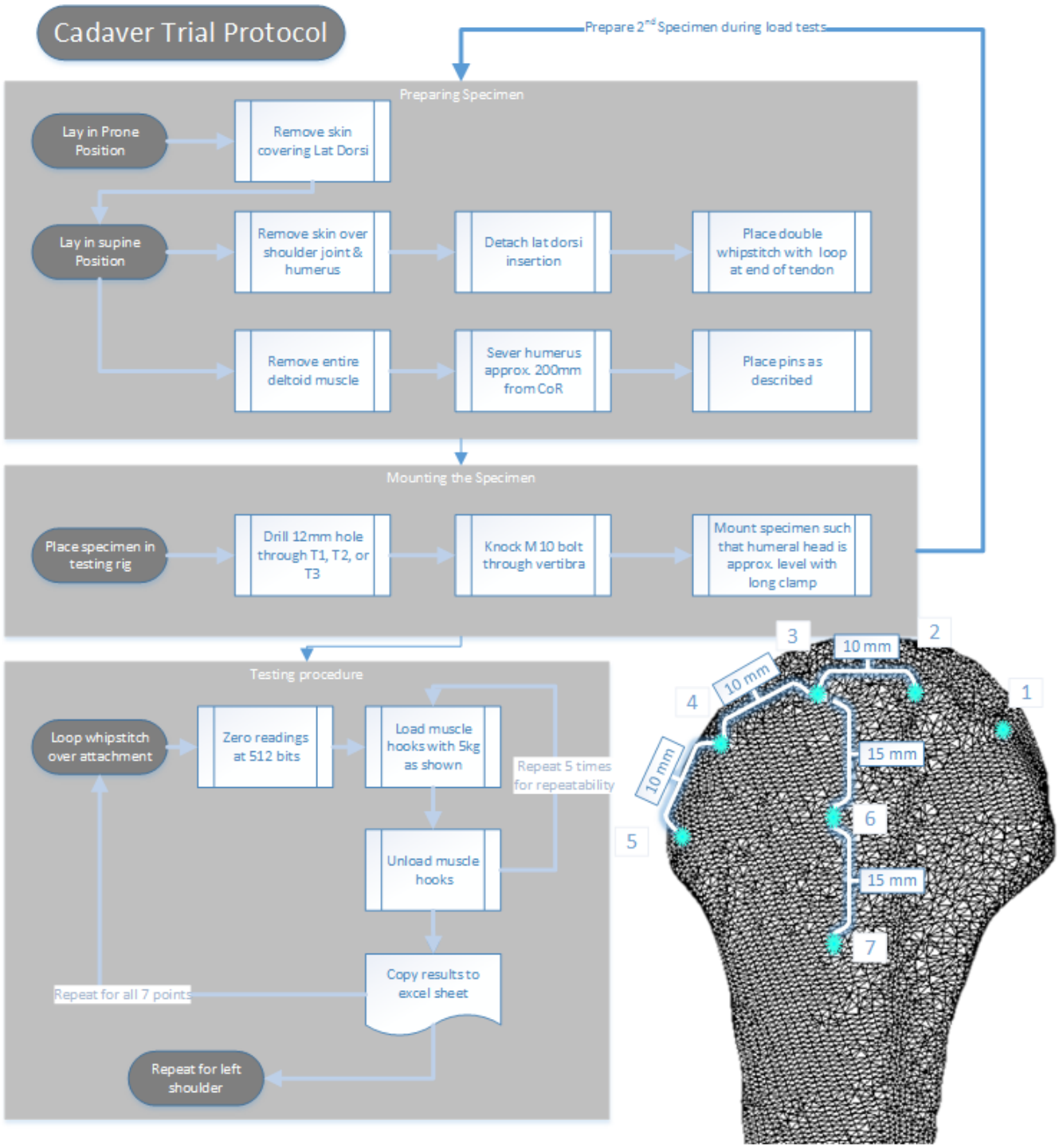

Figure 4.16: Cadaver trial protocol.

4.3.3 Data Analysis and Result Processing

For each point, on each of the 8 cadaver shoulders, applied loads were measured 4 times. This gave 32 data points for each test. These points were then statistically compared using the following process:

1. A Q-Q test was done on each set of 32 data points to ensure that they were normally distributed as would be expected of a fair trial and can be found in Appendix B.
2. Once normality was determined; a one-way anova with a post hoc tukey analysis was done to compare the 7 points to one another and to determine the statistical significance of these differences.
3. The mean, with error bars showing the 95% confidence interval, was plotted for each point to give a visual representation of the results.
4. These were then analysed and conclusions were drawn from these points.

4.4 Results of Biomechanical Cadaver Study

This section lays out the results of the cadaver trial. It is broken into two parts, one for the 0° tests and one for the 90° . The results in each part are represented by a scatter plot that shows the strain measured for each data point. The strain data is the change in the analogue reading obtained when the specimen went from a loaded to an unloaded state. The data for each point was tested for normality using Q-Q Plots which are shown in Appendix B. Once normality was confirmed, the results were compared using a one-way Anova test with a post-hoc Tukey analysis to compare the means and demonstrate statistical significance. These were then plotted on a set of axis showing the mean moment arm and the 95% confidence intervals.

4.4.1 0°Flexion Results

The 0° tests were carried out as described in Section 4.3. The results gained for all tests when the humerus was clamped at 0° of forward flexion are shown in this section. Figure 4.17 shows the strain readings gained for each of the 32 tests done on each point (some data points are missing due to bad readings and cadaver decay). These are each plotted against the point number using the data stored in the relevant table in Appendix A.

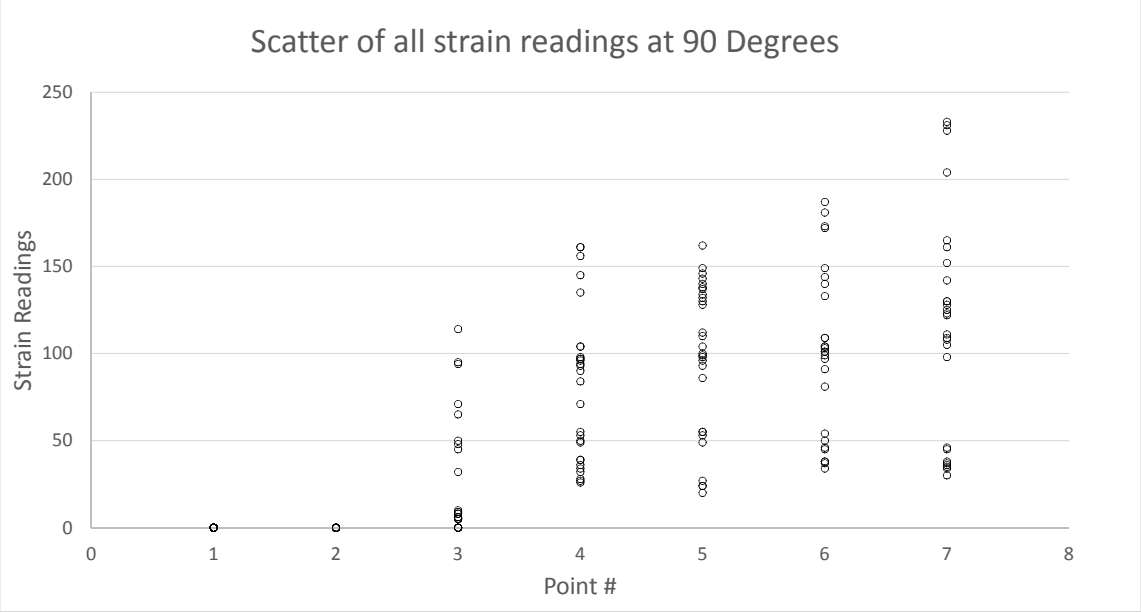

Figure 4.17: Scatter of all data points for the 0° flexion tests; The data used to populate this table can be found in Appendix A.

Using IMB SPSS statistical software one sample T-test, the mean and 95% confidence interval was defined for each point ,1 -7, shown in Figure 4.17. This is represented by a scatter plot (Figure 4.18), where the mean strain reading for each point is marked and error bars show the extent of the 95% confidence interval.

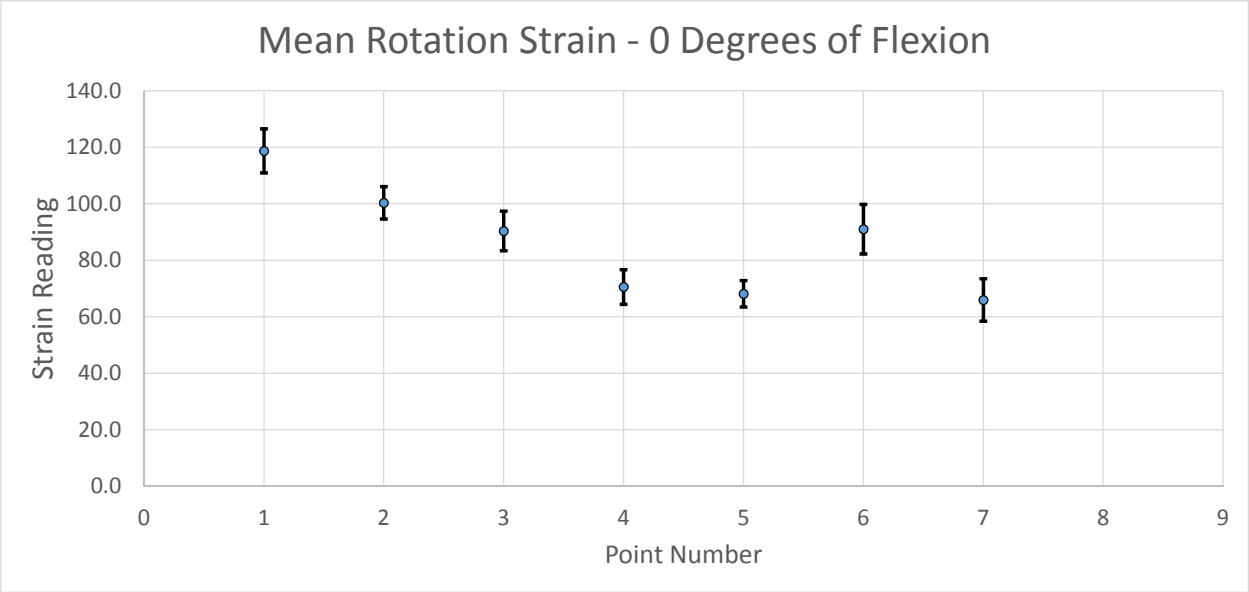

Figure 4.18: Mean strain for each point with standard error bars with arm at 0 degrees of flexion.

Figure 4.18 gives an indication of which points generated the most rotation strength in the study. This shows a simple comparison of the effectiveness of the points while giving an indication as to the statistical relevance of the difference between certain points. For example, it can be seen that the confidence intervals of point 3 and point 4 do not overlap, with point three having the higher value. This means that, with 95% confidence, point 3 generates more external rotation that point 4, making it a more effective solution.

To determine the exact significance and differences between the points, the means must be statistically compared. All 7 points were tested for normality using a set of Q-Q tests (shown in Appendix B) and were shown to be acceptably normal in distribution for a one-way ANOVA for comparison. The results of this comparison are summarised in Table 4.2 below with significance below 0.05 signifying statistically significant results. This analysis was done using IBM SPSS compare means, one-way ANOVA with a post-hoc Tukey analysis.

.

(I) Position	(J) Position	Mean Difference (I-J)	Std. Error	Sig.	95% Confidence Interval	
					Lower Bound	Upper Bound
Point 1	Point 2	18.39	5.05	0.006	3.35	33.43
	Point 3	28.34	4.89	0.000	13.78	42.90
	Point 4	48.18	4.89	0.000	33.62	62.75
	Point 5	50.59	4.89	0.000	36.03	65.15
	Point 6	27.71	4.89	0.000	13.15	42.28
	Point 7	52.78	4.89	0.000	38.21	67.34
Point 2	Point 1	-18.39	5.05	0.006	-33.43	-3.35
	Point 3	9.95	4.89	0.397	-4.62	24.51
	Point 4	29.79	4.89	0.000	15.23	44.35
	Point 5	32.20	4.89	0.000	17.63	46.76
	Point 6	9.32	4.89	0.479	-5.24	23.88
	Point 7	34.38	4.89	0.000	19.82	48.95
Point 3	Point 1	-28.34	4.89	0.000	-42.90	-13.78
	Point 2	-9.95	4.89	0.397	-24.51	4.62
	Point 4	19.84	4.73	0.001	5.77	33.91
	Point 5	22.25	4.73	0.000	8.18	36.32
	Point 6	-0.63	4.73	1.000	-14.69	13.44
	Point 7	24.44	4.73	0.000	10.37	38.51
Point 4	Point 1	-48.18	4.89	0.000	-62.75	-33.62
	Point 2	-29.79	4.89	0.000	-44.35	-15.23
	Point 3	-19.84	4.73	0.001	-33.91	-5.77
	Point 5	2.41	4.73	0.999	-11.66	16.48
	Point 6	-20.47	4.73	0.000	-34.54	-6.40
	Point 7	4.59	4.73	0.959	-9.48	18.66
Point 5	Point 1	-50.59	4.89	0.000	-65.15	-36.03
	Point 2	-32.20	4.89	0.000	-46.76	-17.63
	Point 3	-22.25	4.73	0.000	-36.32	-8.18
	Point 4	-2.41	4.73	0.999	-16.48	11.66
	Point 6	-22.88	4.73	0.000	-36.94	-8.81
	Point 7	2.19	4.73	0.999	-11.88	16.26
Point 6	Point 1	-27.71	4.89	0.000	-42.28	-13.15
	Point 2	-9.32	4.89	0.479	-23.88	5.24
	Point 3	0.63	4.73	1.000	-13.44	14.69
	Point 4	20.47	4.73	0.000	6.40	34.54
	Point 5	22.88	4.73	0.000	8.81	36.94
	Point 7	25.06	4.73	0.000	10.99	39.13
Point 7	Point 1	-52.78	4.89	0.000	-67.34	-38.21
	Point 2	-34.38	4.89	0.000	-48.95	-19.82
	Point 3	-24.44	4.73	0.000	-38.51	-10.37
	Point 4	-4.59	4.73	0.959	-18.66	9.48
	Point 5	-2.19	4.73	0.999	-16.26	11.88
	Point 6	-25.06	4.73	0.000	-39.13	-10.99

Table 4.2: One way Anova with a Tukey post hoc analysis to compare results for all cadaver tests at 0° of flexion.

From Table 4.2 it can be seen how any 2 points compare. For example, comparing point 3 with point 4, it can be seen that the difference in their means is 19.84 with a standard error of 4.73. This leads to a significance of 0.001 which is smaller than 0.05 (the standard marker for statistical significance and an indicator of 95% confidence). Similarly, if points 2 and 6 are compared, we can see that the significance is 0.479 which is greater than 0.05. This means that these two points, while having means which differ by 9.32, are not significantly different from one another to draw conclusions.

90° Flexion Results

The same process was followed to generate the results for the 90° flexion tests. Points 1 and 2 returned no results that were distinguishable from the noise in the system at 90° . All 32 tests were recorded as 0 values for these two points.

Figure 4.19 shows the data collected for all 32 data points (some data are missing due to low quality readings and cadaver decay) for all 7 points. The data used to populate these graphs is shown in the appropriate table in Appendix A.

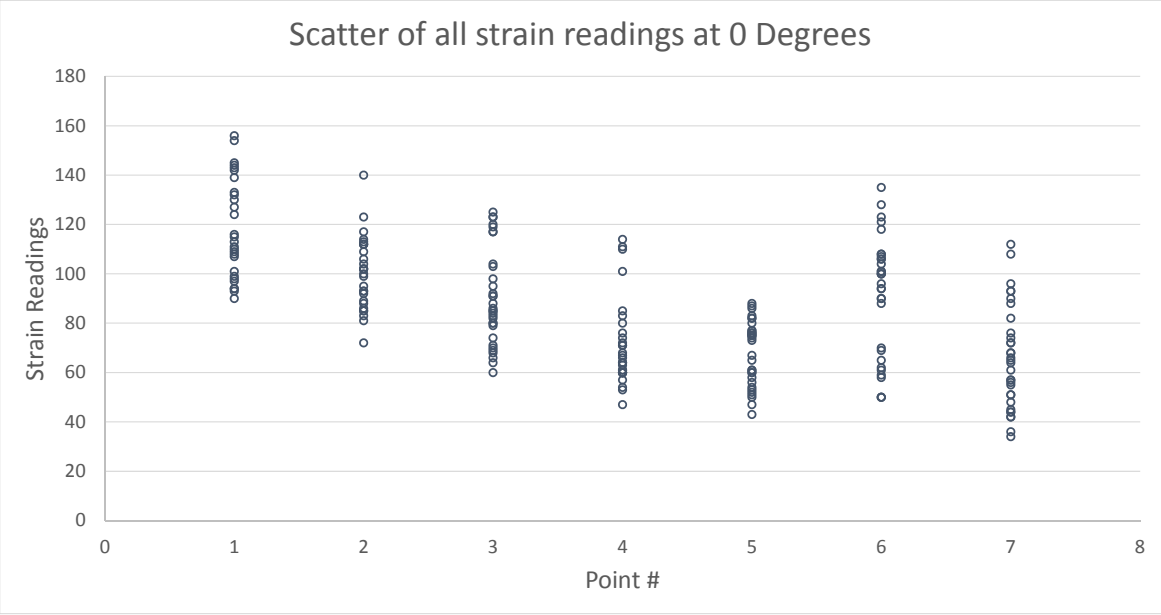

Figure 4.19: Scatter of all data points for the 90° flexion tests; The data used to populate this Graph can be found in Appendix A.

Figure 4.19 shows a large range of values measured for each point tested. This makes the results less robust, but it can still be seen that points 4-7 have returned higher strain measurements in rotaton that points 1-3. In order to better visualise the data, the means and 95% confidence intervals were plotted.These were determined in IBM SPSS with a one sample T-test. This is displayed as Figure 4.20

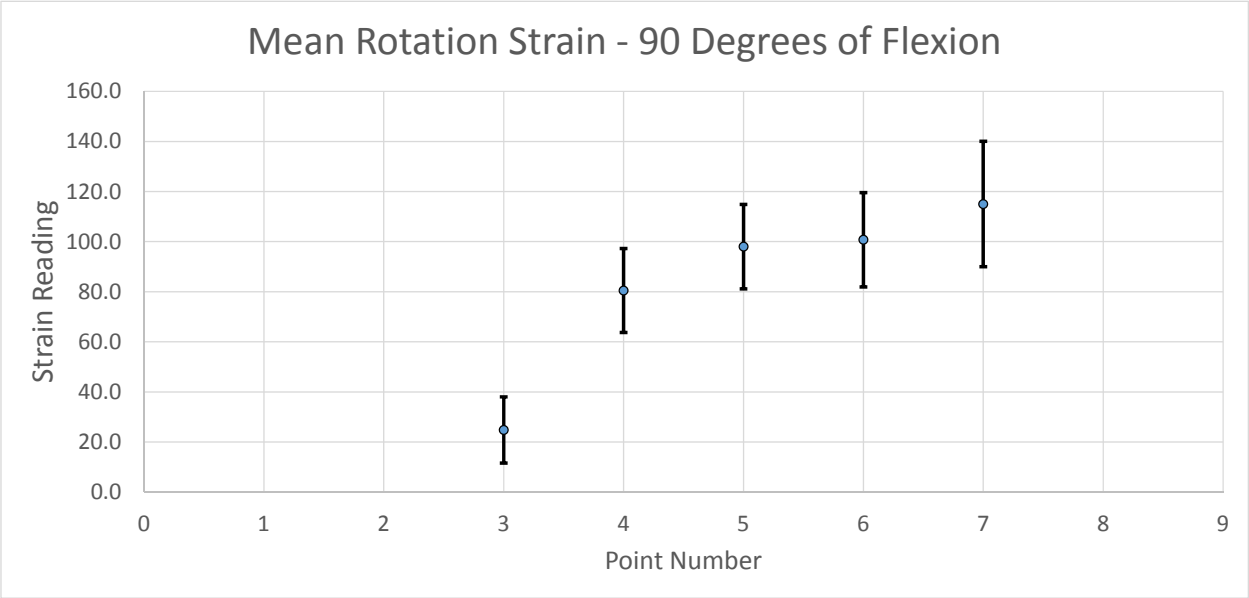

Figure 4.20: Mean strain for each point with standard error bars with arm at 90 degrees of flexion.

Figure 4.20 shows points 4-7 as being very similar, all of their means are included in the 95% confidence intervals of one another. This means they are likely not to be statistically different. They are clearly more effective at generating strain in rotation though, when compared to points 1-3.

In order to better analyse this data, a one-way ANOVA with post-hoc Tukey Test was done once the data for each point was shown to be normal using Q-Q plots. These can be found in Appendix B. The results of the ANOVA test are shown in Table 4.3. Looking at the comparison for point 5 in Table 4.3, it can be seen that the difference between point 5 and point 6 is only -2.74. This has a standard error of 10.44 and a significance of 1.00. This means that these points are statistically very similar. When point 5 is compared to point 3 however, the difference is 76.28 with a standard error of 10.11 and a significance of 0.000. This means that point 5 is statistically more effective, as it shows higher strain readings, than point 3 with a p value of 0.000. In this way, all 7 points are directly compared to one another and the statistical likelihood of their differing is recorded.

(I) Points	(J) Positon	Mean Difference (I-J)	Std. Error	Sig.	95% Confidence Interval	
					Lower Bound	Upper Bound
Point 1	Point 2	0.00	9.67	1.000	-28.82	28.82
	Point 3	-21.72	9.67	0.277	-50.53	7.10
	Point 4	-80.50	10.01	0.000	-110.33	-50.67
	Point 5	-98.00	10.01	0.000	-127.83	-68.17
	Point6	-100.74	10.11	0.000	-130.86	-70.62
	Point 7	-115.04	10.11	0.000	-145.16	-84.92
Point 2	Point 1	0.00	9.67	1.000	-28.82	28.82
	Point 3	-21.72	9.67	0.277	-50.53	7.10
	Point 4	-80.50	10.01	0.000	-110.33	-50.67
	Point 5	-98.00	10.01	0.000	-127.83	-68.17
	Point6	-100.74	10.11	0.000	-130.86	-70.62
	Point 7	-115.04	10.11	0.000	-145.16	-84.92
Point 3	Point 1	21.72	9.67	0.277	-7.10	50.53
	Point 2	21.72	9.67	0.277	-7.10	50.53
	Point 4	-58.78	10.01	0.000	-88.61	-28.95
	Point 5	-76.28	10.01	0.000	-106.11	-46.45
	Point6	-79.02	10.11	0.000	-109.14	-48.90
	Point 7	-93.32	10.11	0.000	-123.44	-63.20
Point 4	Point 1	80.50	10.01	0.000	50.67	110.33
	Point 2	80.50	10.01	0.000	50.67	110.33
	Point 3	58.78	10.01	0.000	28.95	88.61
	Point 5	-17.50	10.34	0.622	-48.31	13.31
	Point6	-20.24	10.44	0.457	-51.33	10.85
	Point 7	-34.54	10.44	0.019	-65.63	-3.45
Point 5	Point 1	98.00	10.01	0.000	68.17	127.83
	Point 2	98.00	10.01	0.000	68.17	127.83
	Point 3	76.28	10.01	0.000	46.45	106.11
	Point 4	17.50	10.34	0.622	-13.31	48.31
	Point6	-2.74	10.44	1.000	-33.83	28.35
	Point 7	-17.04	10.44	0.662	-48.13	14.05
Point6	Point 1	100.74	10.11	0.000	70.62	130.86
	Point 2	100.74	10.11	0.000	70.62	130.86
	Point 3	79.02	10.11	0.000	48.90	109.14
	Point 4	20.24	10.44	0.457	-10.85	51.33
	Point 5	2.74	10.44	1.000	-28.35	33.83
	Point 7	-14.30	10.53	0.824	-45.67	17.07
Point 7	Point 1	115.04	10.11	0.000	84.92	145.16
	Point 2	115.04	10.11	0.000	84.92	145.16
	Point 3	93.32	10.11	0.000	63.20	123.44
	Point 4	34.54	10.44	0.019	3.45	65.63
	Point 5	17.04	10.44	0.662	-14.05	48.13
	Point6	14.30	10.53	0.824	-17.07	45.67

Table 4.3: One-way anova with Tukey post hoc analysis to compare the results from the 90° cadaver tests.

4.5 Discussion of Cadaver Trial Results

The following section draws conclusions from, and discusses, the results presented in Section 4.4. The comparison of the results with the *in-silico* model results is presented in Chapter 5. This section will end with recomendations for future research in this area.

4.5.1 Conclusions From Cadaver Trials

From the results presented in Section 4.4, the following conclusions can be drawn. These conclusions can be used to improve surgical understanding of the effects of varying the insertion point of the LD tendon during transfer to treat posterior rotator cuff tears.

At 0° of flexion the conclusions drawn include:

- The maximum rotation load was generated at Point 1.
- The rotational loads generated at point 2 were not statistically different from those at point 3 and point 6.
- The second most optimal set of points for generating rotation were points 2,3, and 6.
- Points 4, 5, and 7 were not significantly different from one another. These three points were the least effective, but still generated significant amounts of strain in rotation as there was a large amount more variance in the readings.

At 90° of flexion the results were less clear, but the following conclusions can be drawn from them:

- Points 1 and 2 did not generate any rotational strain distiguishable from the noise of the system.
- Point 3 generated strain distiguishable from noise in most cases, but was significantly less effective than the remaining points. This did not allow it to be significantly greater than points 1 and 2 ($p = 0.277$).
- Points 4 - 6 were not significantly different from one another, but were all significantly different from points 1 - 3 ($p = 0.00$).

Overall this leads to the conclusion that: Points 1-3 are most effective at generating rotation at low angles of flexion (0° tests), but completely ineffective at high angles (90° tests). This means that if maximum flexion is required at low angles, these points would be prefered, if however, rotation is

required throughout the motion of flexion, then a sacrifice must be made at low angles to generate a rotational load at higher angles. To optimise rotation throughout the motion of flexion, point 6 makes the best compromise, with points 4 and 5 both also showing acceptable results.

4.5.2 Discussion of Results

The results for the 0° of flexion tests had considerably less variance than the results at 90° . This suggests that the 90° tests were more sensitive to slight changes in the system. These changes could have included slight variations in the amount of internal rotation applied as well as other human factors. The 90° tests could also have been more vulnerable to errors caused by friction in the clamp. This could possibly be seen in the difference between points 3, and 6. One would expect that they would be more similar as the only change is how distal the point is on the tuberosity. It could be hypothesised that the extra flexion affected the friction to cause this anomaly.

As mentioned in Chapter 2, the literature gives a number of potentially optimal insertion points. Figures 2.9 and 2.10 show these insertion points on the humerus. Point 6, which was found to be the optimal point for generating rotation for a wide range of flexion, was not tested in the literature and therefore cannot be compared. Bargoin et al. (2016) suggested the equivalent of point 2 as the optimal point. This is only valid at low angles of flexion and possibly for abduction (as tested by Bargoin et al. (2016)) according to this study. This study found points 4 and 5 to be the best of the points that can be compared to literature. This corroborates De Casas et al. (2014), Oh et al. (2013), and Gerber et al. (1988). When compared to the *in-silico* tests found in literature, this study agrees with Favre et al. (2008) at all angles and with Ling et al. (2009) (the secondary results at the lesser tuberosity) at low angles of flexion.

Overall the results for each test were conclusive and statistically significant differences were found suggesting that the insertion point does affect the surgical outcomes. This suggests that more research should be conducted to investigate these effects in additional circumstances. These results and conclusions are in line with much of the literature and help to build a more complex, complete understanding of the effects of various insertion points on the clinical outcomes of the surgery.

4.5.3 Recommendations for Future Cadaver Studies

As discussed above, this study has emphasized the importance of understanding the effects of moving the insertion point during LD tendon transfer. For this reason it is important that more studies are conducted to build on the insight gleaned from this study. Some recommendations of improvements to this study as well as suggestions on what future research should be conducted are listed below.

- Use bearings to ensure that non-sliding friction does not change results.
- Measure flexion loads to determine the effects of the various insertion points on flexion strength.
- Measure the rotation strength at various angles of abduction.
- Measure the effects of various insertion points on the glenohumeral joint contact force.

This chapter has described the cadaver trial that was conducted. The motivation and aims for this study have been described before the methods and design were outlined. The results were presented and discussed. The conclusions presented are compared to the *in-silico* model in Chapter 5.

Chapter 5

Overall Study Conclusions

This chapter outlines the comparison of the results from the *in-silico* and cadaver trials. Once the rotation results from the *in-silico* model are validated by the cadaver trial, this validation can be extended to the simulated flexion results. The importance of this validation is discussed briefly in Section 1.2, and extensively in Chapter 2. This chapter then compares the conclusions separately drawn from the two studies. To end, a discussion of the relevance and limitations of this research and the possible cause of discrepancies between the *in-silico* model and the cadaver trials.

5.1 Comparison of Results

The results from the two studies can be compared, point for point, using the 7 points of interest. These two studies did not measure the same parameters, merely directly related and proportional parameters. The best way to compare these results directly is by multiplying values of one study (the *in-silico* results) by a factor that aligns one of the relevant points in that study with the corresponding mean in the other study. When this same scaling factor is applied to all points, a comparison can be made between the results. This can be done because both sets of results represent quasi linear systems.

Figure 5.1 shows a comparison of the *in-silico* results in orange and the cadaver trial results in blue with error bars for 95% confidence. This comparison was generated using a scale factor of 1936 to align the scales at point 6.

In Figure 5.1 the differences between points in the simulation are smaller than those in the cadaver trials. Point 5 appears to be an outlier in that it performed similarly to points 2, 3, and 6 in the simulations when it was more similar to the lower points 4 and 7 in the cadaver trial. Point 1 was the optimal point in both trials, but was not as clearly optimal in the simulations as it was in the

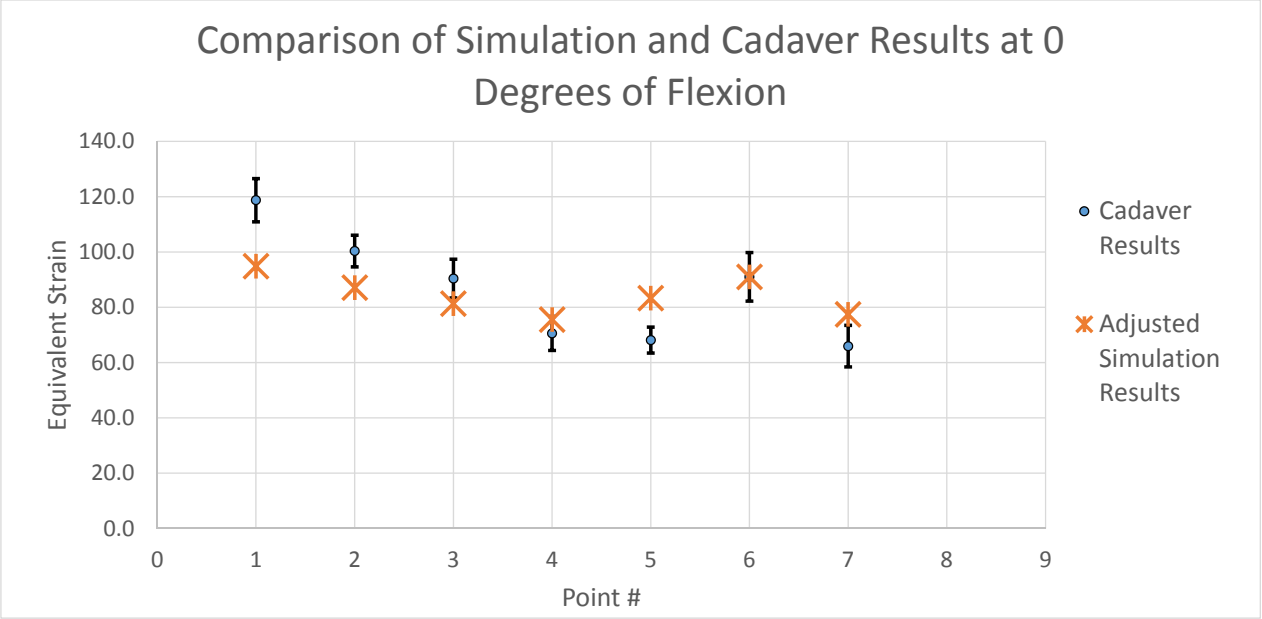

Figure 5.1: Comparison of simulation results (orange marker) and cadaver results (blue marker with error bar) using point 6 as the reference point for scaling at 0° of flexion.

cadaver trial. This could be because the wrapping objects aren't always able to accurately depict the amount that the tendon wraps around the humeral head to reach point 1.

Figure 5.2 shows the same comparison as Figure 5.1, but for the 90° tests. The *in-silico* results (orange) were scaled by the same factor of 1936 in order to compare them to the cadaver trial results shown in blue with error bars for 95% confidence.

Figure 5.2 shows a similar trend between the sets of points. Point 1 generates no flexion in either model. There is more of a difference for points 2 and 3, both of which generate little rotation in the cadaver trial, but some in the model. This could be due to the aforementioned sticking, caused by friction, or slight misalignment of the shoulder in rotation during the trials. Points 4-7 show a plateau in a similar range for both the cadaver and *in-silico* results.

Comparing the results from the two studies in this way shows that, with some error, the two studies are very similar. This allows us to use the cadaver study to validate the results in rotation for the simulation study, which in turn can be extended to the results for flexion as the basic mechanics of the model have been shown to be accurate and clinically relevant.

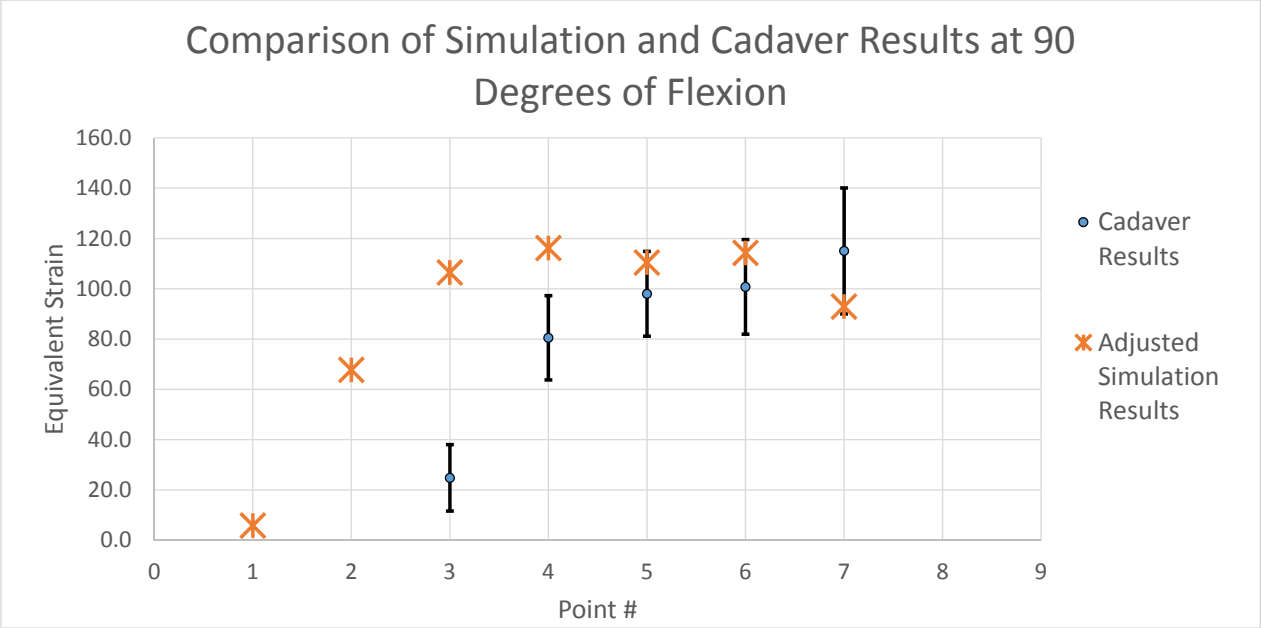

Figure 5.2: Comparison of simulation results (orange marker) and cadaver results (blue marker with error bar) using point 6 as the reference point for scaling at 90° of flexion.

5.2 Comparison of Conclusions

Because the comparison of results is inexact, it is important to compare the outcomes in another way in order to verify their relevance and accuracies. If the same conclusions can be drawn from two studies conducted in different mediums, with different, but related, parameters, then it can be interfered that both studies are more likely to be accurate as they will have corroborated one another.

At 0° of flexion, both studies show point 1 to be the optimal point. The conclusion is also drawn from both studies that the posterior edge of the greater tuberosity (points 4 and 7) generate the least rotation at 0 degrees of flexion, although point 5 appears to have an elevated effect in the simulation. Overall, while the simulation has smaller differences between the measured moment arms, the conclusions that were drawn were well corroborated by the cadaver trials.

Similarly, the 90° tests show similar conclusions. Both tests conclude that little to no rotation is generated at points 1 and 2. Point 3 is the major point of difference with the *in-silico* trial claiming it has a large effect in rotation and the cadaver concluding a very low effect. Points 4-7 show the same conclusion in both the *in-silico* study and the cadaver trial; that all 4 points (4, 5, 6, and 7) show good, and negligibly different external rotation capabilities at 90°.

5.3 Comparison with Literature

Figures 2.9 and 2.10, reproduced here as Figures 5.3a and 5.3b, show the optimal insertion points found in the literature for *in-silico* and cadaver studies respectively.

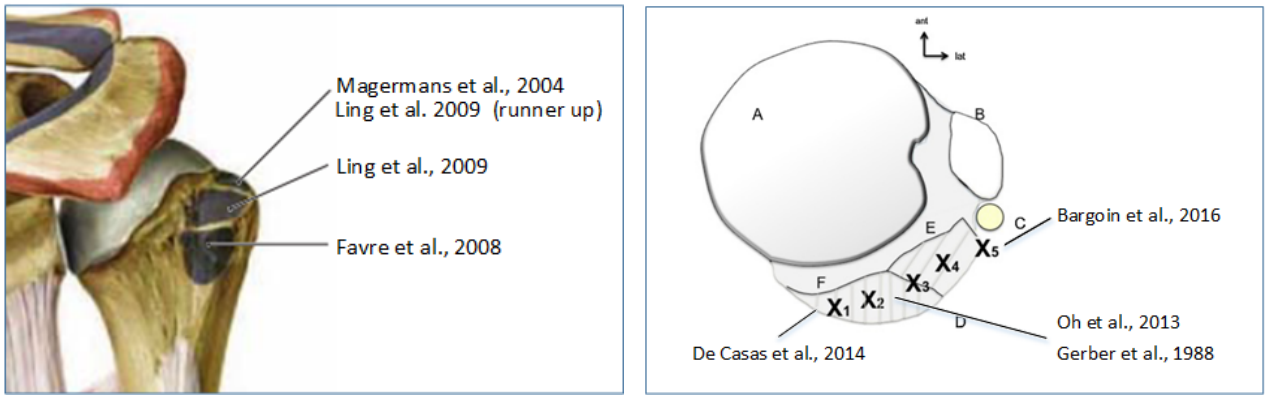

(a) Results of *in-silico* studies from literature reproduced from Figure 2.9

(b) Results of Cadaver studies in the literature, reproduced from Figure 2.10

Figure 5.3: Results from literature for comparison to the findings of this study

To restore rotation through a large range of flexion, point 6 in this study was found to be the optimal point. This was not tested in the literature. If flexion was required with this rotation over a large range, points 4 and 5 in this study were found to be superior. This is in line with the results found by De Casas et al. (2014), and Favre et al. (2008). It is also somewhat in line with Oh et al. (2013), Gerber et al. (1988) and the major finding by Ling et al. (2009).

The findings that points 1 and 2 in this study produce the most rotation are only applicable at low angles of flexion. This is in line with the results of Magermans et al. (2004) Bargoin et al. (2016) and the secondary results of Ling et al. (2009).

5.4 Discussion of Limitations and Discrepancies

The limitations of each study are specified in Section 3.1.4 and Section 4.1.4. These limitations generally describe the context of the study and emphasize that the results and conclusions may to be extended to other, untested applications. In order to broaden the relevance of the results, more studies should be done in abduction and at various angles of internal rotation.

There are some discrepancies between the results from the *in-silico* simulation and those from the cadaver study. The discrepancies for points 2 and 3 at 90° can be explained by interference from friction and from slight error in mounting of the specimens. This error does not compromise the

study as the results follow the same trend.

The variance in moment arms for the 7 points tested is larger in the cadaver trials. This is most likely due to the blunting and rounding off of sharp edges and peaks in the *in-silico* model due to the complexities of wrapping objects.

5.5 Final Surgical Conclusions

As these studies have been shown to produce similar results, a combined set of overall conclusions or surgical suggestions can be drawn. These conclusions should be taken in context with the work that precedes them and act merely as a summary of the most important results and conclusions drawn from the two studies. These conclusions, shown in Figure 5.4 are:

1. To generate rotation throughout the maximum range of flexion, with a neutral flexion generation, point 6 (near the middle of the greater tuberosity) is the optimal point. This is not tested by much of the previous literature.
2. To generate rotation throughout maximal flexion range and to generate flexion at low angles, the posterior edge of the greater tuberosity (points 4 and 5) are optimal. This is in line with the results of Favre et al. (2008)
3. To simply maximise rotation strength at low angles. Point 1, on the peak of the lesser tuberosity, is the optimal point.

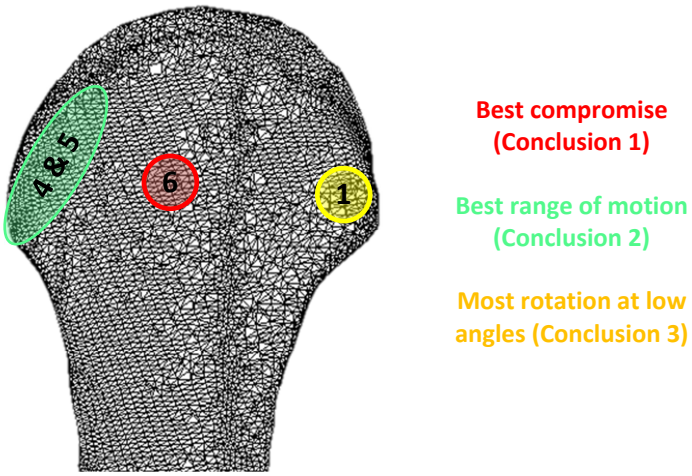

Figure 5.4: Graphical representation of final conclusions

Bibliography

Bargoin, K., Boissard, M., Kany, J., and Grimberg, J. (2016). Influence of fixation point of latissimus dorsi tendon transfer for irreparable rotator cuff tear on glenohumeral external rotation: A cadaver study. *Orthopaedics and Traumatology: Surgery and Research*, 102(8):971–975.

Bolsterlee, B., Veeger, D. H. E. J., and Chadwick, E. K. (2013). Clinical applications of musculoskeletal modelling for the shoulder and upper limb. *Medical and Biological Engineering and Computing*, 51(9):953–963.

Brigham and Women's Hospital (2007). Standard of Care : Latissimus Dorsi Tendon Transfer Case Type / Diagnosis :. In *Rehabilitation*, pages 1–11.

Cleeman, E., Hazrati, Y., Auerbach, J. D., Stein, K. S., Hausman, M., Flatow, E. L., and York, N. (2003). Latissimus dorsi tendon transfer for massive rotator cuff tears : A cadaveric study. 2746(03):539–543.

De Casas, R., Lois, M., Cidoncha, M., and Valadron, M. (2014). Clinic and electromyographic results of latissimus dorsi transfer for irreparable posterosuperior rotator cuff tears. *Journal of Orthopaedic Surgery and Research*, 9(1):83.

Drake, R. L., Vogl, W., Mitchell, A. W. M., and Vogl, A. W. (2012). *Gray's Basic Anatomy*.

Favre, P., Loeb, M. D., Helmy, N., and Gerber, C. (2008). Latissimus dorsi transfer to restore external rotation with reverse shoulder arthroplasty: A biomechanical study. *Journal of Shoulder and Elbow Surgery*, 17(4):650–658.

Gatti, C. J., Dickerson, C. R., Chadwick, E. K., Mell, A. G., and Hughes, R. E. (2007). Comparison of model-predicted and measured moment arms for the rotator cuff muscles. *Clinical Biomechanics*, 22(6):639–644.

Gerber, C., Maquieira, G., and Espinosa, N. (2006). Latissimus dorsi transfer for the treatment of irreparable rotator cuff tears. *The Journal of bone and joint surgery. American volume*, 88(1):113–20.

Gerber, C., Vinh, T. S., Hertel, R., and Hess, C. W. (1988). Latissimus dorsi transfer for the treatment of massive tears of the rotator cuff. A preliminary report. *Clinical orthopaedics and related research*, (232):51–61.

Gilroy, A. M. and Ross, L. M. (2009). *Atlas of Anatomy*. Thieme.

Grimberg, J. and Kany, J. (2014). Latissimus dorsi tendon transfer for irreparable postero-superior cuff tears: current concepts, indications, and recent advances. *Current Reviews in Musculoskeletal Medicine*, 7(1):22–32.

Habermeyer, P. (2006). Transfer of the tendon of latissimus dorsi for the treatment of massive tears of the rotator cuff: A New Single-incision Technique. *Journal of Bone and Joint Surgery - British Volume*, 88-B(2):208–212.

Hartzler, R. U., Barlow, J. D., An, K. N., and Elhassan, B. T. (2012). Biomechanical effectiveness of different types of tendon transfers to the shoulder for external rotation. *Journal of Shoulder and Elbow Surgery*, 21(10):1370–1376.

Henseler, J. F., Kolk, A., Zondag, B., Nagels, J., de Groot, J. H., and Nelissen, R. G. (2017). Three-dimensional shoulder motion after teres major or latissimus dorsi tendon transfer for posterosuperior rotator cuff tears. *Journal of Shoulder and Elbow Surgery*.

Holzbaur, K. R. S., Murray, W. M., and Delp, S. L. (2005). A model of the upper extremity for simulating musculoskeletal surgery and analyzing neuromuscular control. *Annals of Biomedical Engineering*, 33(6):829–840.

Iannotti, J. P., Hennigan, S., Herzog, R., Kella, S., Kelley, M., Leggin, B., and Williams, G. R. (2006). Latissimus dorsi tendon transfer for irreparable posterosuperior rotator cuff tears. Factors affecting outcome. *J Bone Joint Surg Am*, 88(2):342–348.

Ling, H. Y., Angeles, J. G., and Horodyski, M. B. (2009). Biomechanics of latissimus dorsi transfer for irreparable posterosuperior rotator cuff tears. *Clinical Biomechanics*, 24(3):261–266.

Magermans, D. J., Chadwick, E. K. J., Veeger, H. E. J., Rozing, P. M., and Van Der Helm, F. C. T. (2004). Effectiveness of tendon transfers for massive rotator cuff tears: A simulation study. *Clinical Biomechanics*, 19(2):116–122.

Neri, B. R., Chan, K. W., and Kwon, Y. W. (2009). Tendon transfers for irreparable rotator Cuff tears. *Bulletin of the NYU Hospital for Joint Diseases*, 67(1):15–21.

Oh, J. H., Tilan, J., Chen, Y. J., Chung, K. C., McGarry, M. H., and Lee, T. Q. (2013). Biomechanical effect of latissimus dorsi tendon transfer for irreparable massive cuff tear. *Journal of Shoulder and Elbow Surgery*, 22(2):150–157.

Pheasant, S. and Haslegrave, C. M. (2006). *Bodyspace: Anthropometry, Ergonomics, and the Design of Work*. Taylor and Francis Ltd., London, 2nd edition.

Quental, C., Folgado, J., Ambrósio, J., and Monteiro, J. (2013). Critical analysis of musculoskeletal modelling complexity in multibody biomechanical models of the upper limb. *Computer methods in biomechanics and biomedical engineering*, 5842(November 2014):37–41.

Saul, K. R., Hu, X., Goehler, C. M., Vidt, M. E., Daly, M., Velisar, A., and Murray, W. M. (2014). Benchmarking of dynamic simulation predictions in two software platforms using an upper limb musculoskeletal model.

Sherman, M. A., Seth, A., and Delp, S. L. (2015). Effectiveness in Biomechanical Models Using. In *Proc ASME Des Eng Tech Conf.*, pages 1–18.

Sim, F. H., Beaty, J. H., Canale, S. T., Ferlic, D. C., Helfet, D. L., and Warner, J. J. P. (2001). Management of Massive Irreparable Rotator Cuff Tears: The Role of Tendon Transfer *. *Instructional Course Lectures*, 50(50).

van der Helm, F. C. T. (1994). A finite element musculoskeletal model of the shoulder mechanism. *Journal of Biomechanics*, 27(5).

Wagner, D. W., Stepanyan, V., Shippen, J. M., Demers, M. S., Gibbons, R. S., Andrews, B. J., Creasey, G. H., and Beaupre, G. S. (2013). Consistency among musculoskeletal models: Caveat utilitor. *Annals of Biomedical Engineering*, 41(8):1787–1799.

Werner, C. M. L., Zingg, P. O., Lie, D., Jacob, H. A. C., and Gerber, C. (2006). The biomechanical role of the subscapularis in latissimus dorsi transfer for the treatment of irreparable rotator cuff tears. *Journal of Shoulder and Elbow Surgery*, 15(6):736–742.

Wu, G., Van Der Helm, F. C. T., Veeger, H. E. J., Makhsous, M., Van Roy, P., Anglin, C., Nagels, J., Karduna, A. R., McQuade, K., Wang, X., Werner, F. W., and Buchholz, B. (2005). ISB recommendation on definitions of joint coordinate systems of various joints for the reporting of human joint motion - Part II: Shoulder, elbow, wrist and hand. *Journal of Biomechanics*, 38(5):981–992.

Yamaguchi, K., Ditsios, K., Middleton, W. D., Hildebolt, C. F., Galatz, L. M., and Teefey, S. A. (2006). The Demographic and Morphological Features of Rotator Cuff Disease. A Comparison of Asymptomatic and Symptomatic Shoulders. *J Bone Joint Surg Am*, 88(8):1699–1704.

Appendix A

Cadaver Rig Parts Drawings

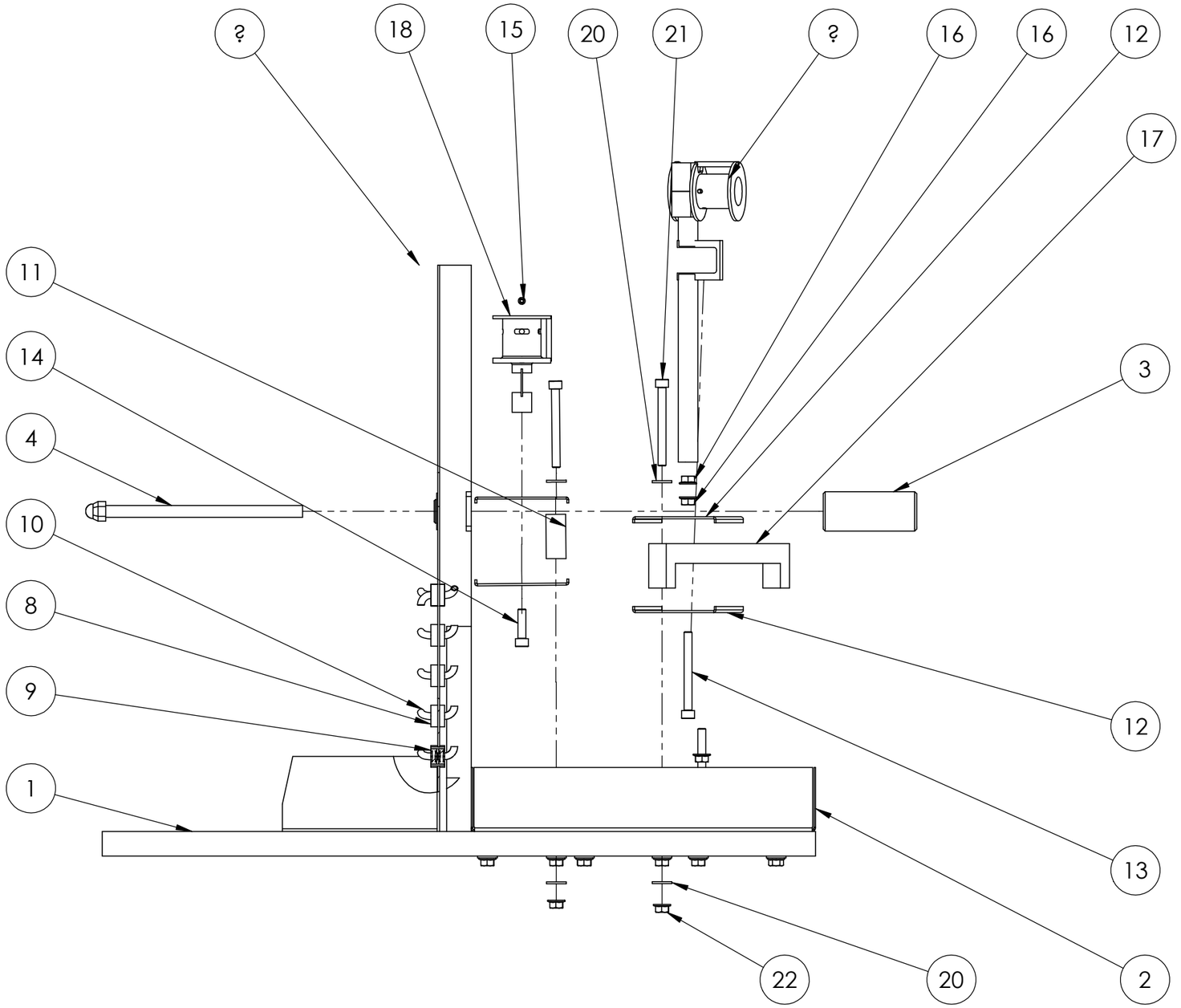

ITEM NO.	PART NUMBER	DESCRIPTION	QTY.
1	Frame	DONE (for previous studies)	1
2	Tray	DONE	1
3	Stopper	DONE	1
4	Bolt	DONE	1
5	plain washer large grade ac_iso		1
6	plain washer chamfered grade a_iso		1
7	Back Plate		1
8	Tube Attached to back plate		10
9	radial ball bearing_68_skf		20
10	Cable Guide		20
11	Runner		4
12	Plate	Bent steel plate	8
13	socket head cap screw_iso3		2
14	socket head cap screw_iso3		2
15	socket head cap screw_iso3		2
16	hex flange nut gradea_iso		4
17	Runner Long		4
18	Bottom brace		1
19	Long Brace Assem		1
20	ISO 10669-8.8-N		32
21	ISO 4762 M8 x 80 - 28N		16
22	ISO - 4161 - M8 - N		16

A3 Landscape	University of Cape Town Department of Mechanical Engineering			
	Title: Assembled Basics			
Assembly Drawing	Scale: 1:10	Date: 18/05/12	Sheet1	of 1
	Drawn By:		Drawing Number	

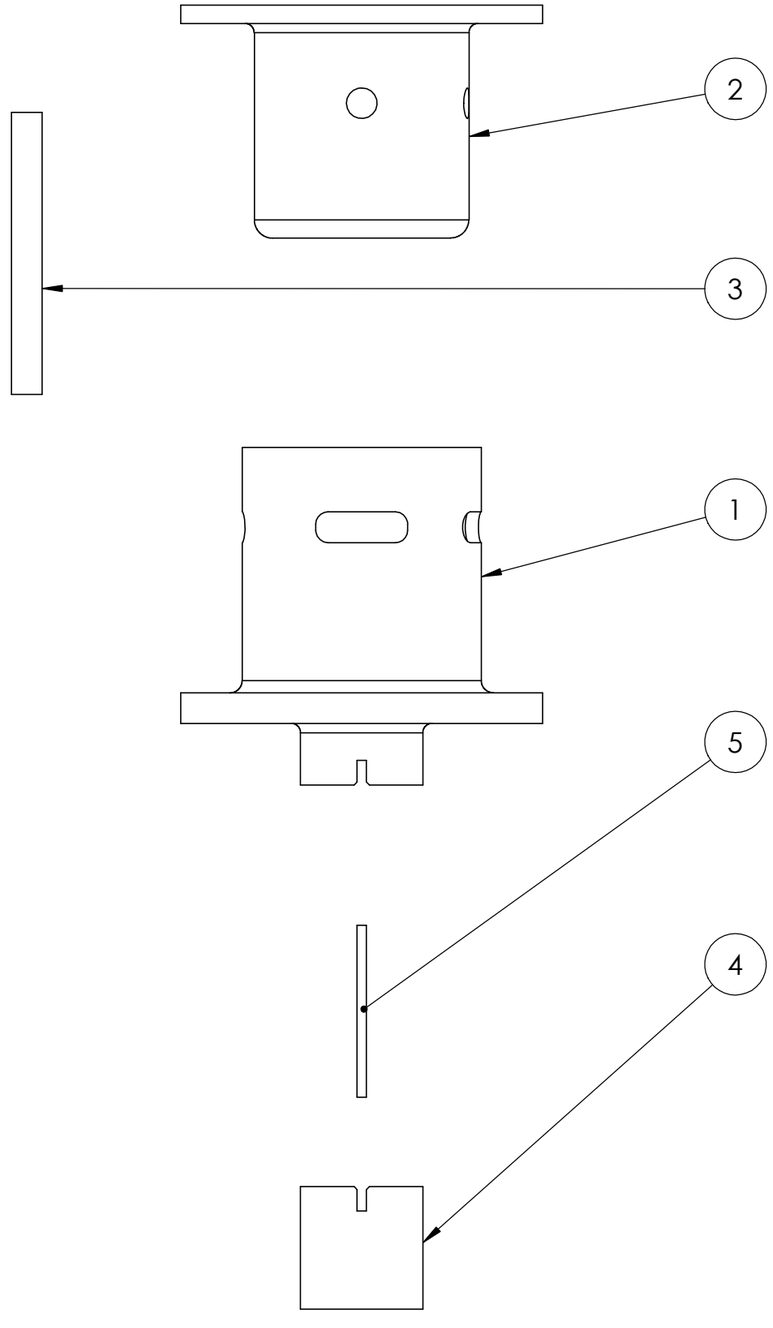

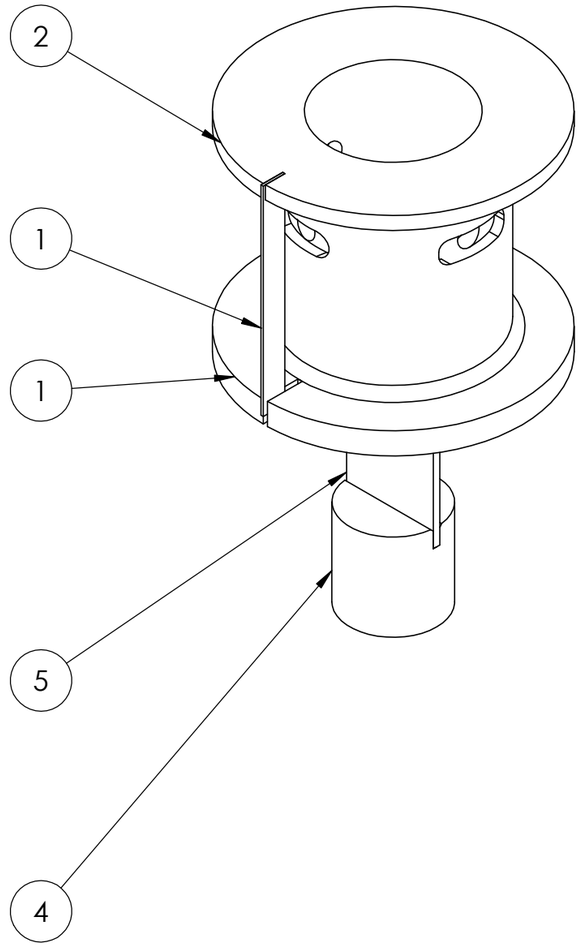

ITEM NO.	PART NUMBER	DESCRIPTION	QTY.
1	Bottom brace	STAINLESS STEEL	1
2	Bottom Brace Inner	STAINLESS STEEL	1
3	strain bar	ALUMINIUM	1
4	Bottom Brace Bottom	STAINLESS	1
5	Bottom Brace Load section	STAINLESS	1

A3 Landscape	University of Cape Town Department of Mechanical Engineering			
	Title: Bottom brace			
Assembly Drawing	Scale: 1:2	Date: 18/05/12	Sheet1	of 1
	Drawn By:		Drawing Number	

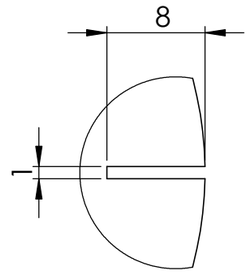

DETAIL A
SCALE 2 : 1

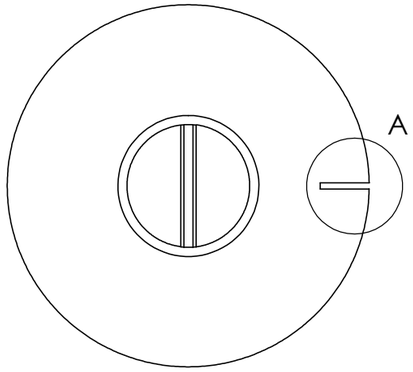

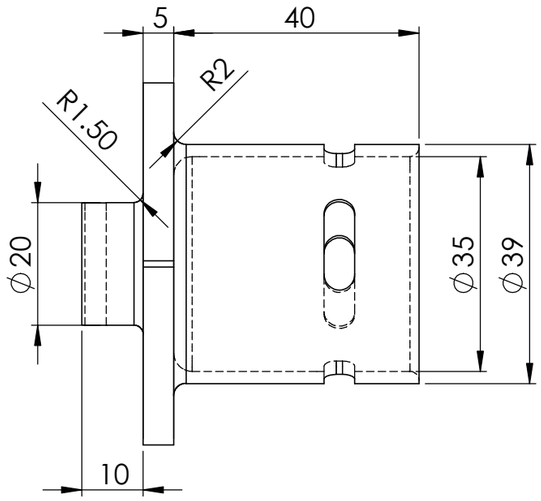

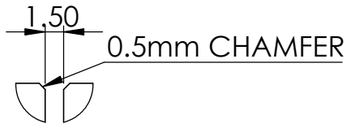

DETAIL B
SCALE 2 : 1

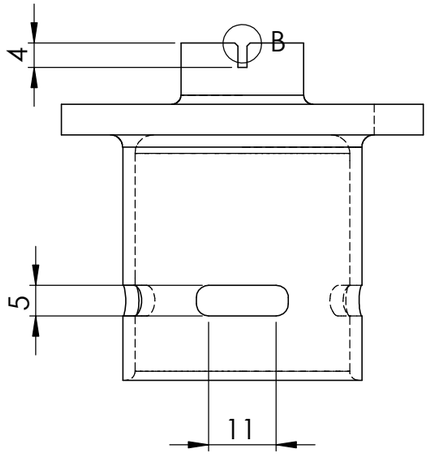

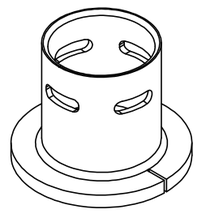

SIMILAR TO PREVIOUS VERSION.
BASE CHANGED
SLOT FOR STRAIN BAR SMALLER
QTY: 1
STAINLESS STEEL

A4 Portrait	University of Cape Town Department of Mechanical Engineering			
	Title: Bottom brace			
Part Finish	Scale: 1:2	Date: 18/05/12	Sheet1	of 1
Material:	Drawn By:		Drawing Number	

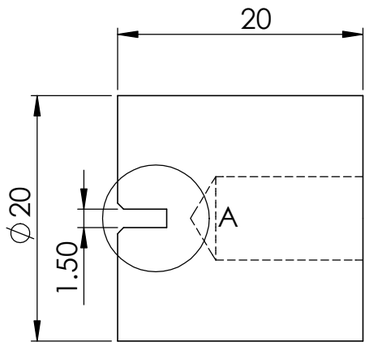

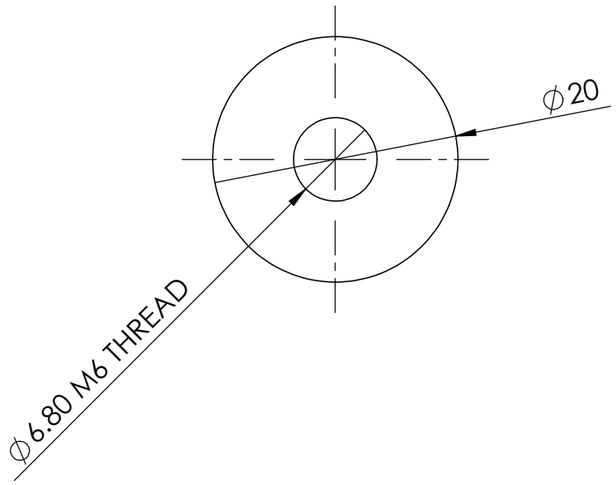

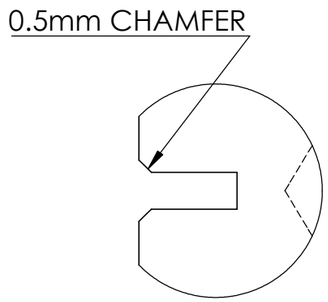

DETAIL A
SCALE 4 : 1

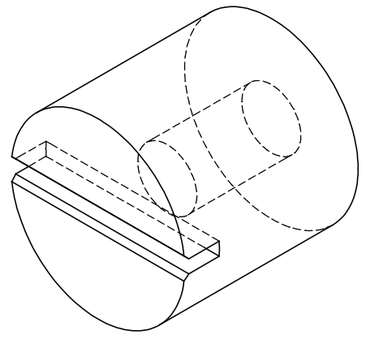

STAINLESS STEEL
QTY: 1

A4 Portrait	**University of Cape Town** Department of Mechanical Engineering			
	Title: Bottom Brace Bottom			
Part Finish	Scale: 2:1	Date: 18/05/12	Sheet1	of 1
Material:	Drawn By:		Drawing Number PART 4	

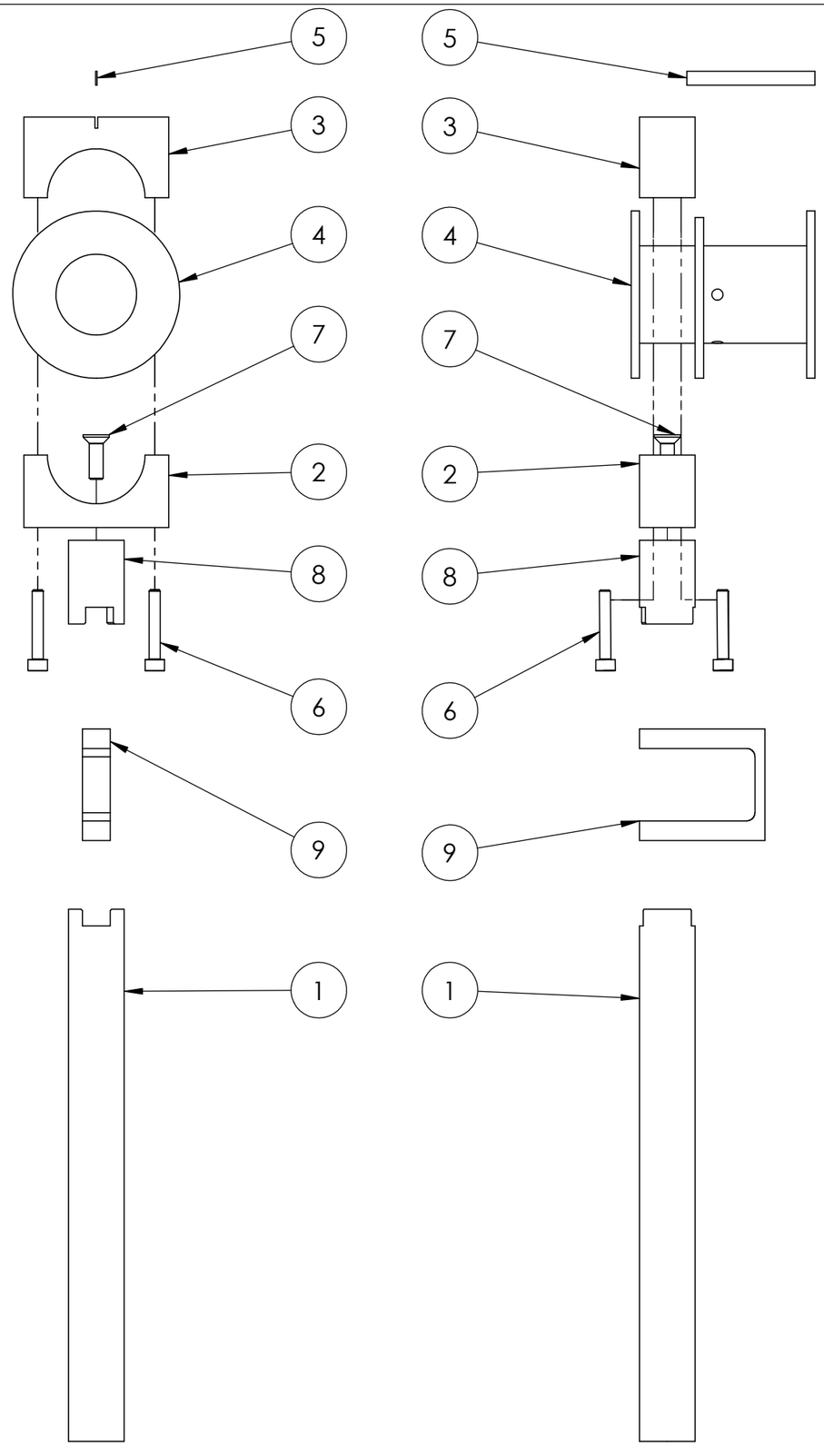

ITEM NO.	PART NUMBER	DESCRIPTION	QTY.
1	Long Rod	Stainless Steel	1
2	Long Bracket Bottom	Stainless Steel	1
3	Long Bracket Top	Stainless Steel	1
4	Long Brace Inner	Stainless Steel	1
5	strain bar	Aluminium	1
6	ISO 4762 M4 x 25 - 25N		4
7	ISO 10642 - M5 x 16 - 16N		1
8	Longrod Top	Stailess Steel	1
9	Top Gauge Amp	Aluminium	1

A3 Landscape	University of Cape Town Department of Mechanical Engineering			
	Title: Long Brace Assem			
Assembly Drawing	Scale: 1:5	Date: 18/05/12	Sheet1	of 1
	Drawn By:		Drawing Number	

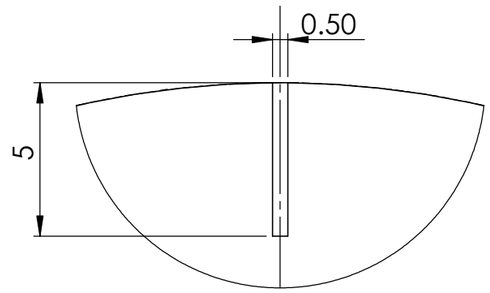

DETAIL A
SCALE 5 : 1

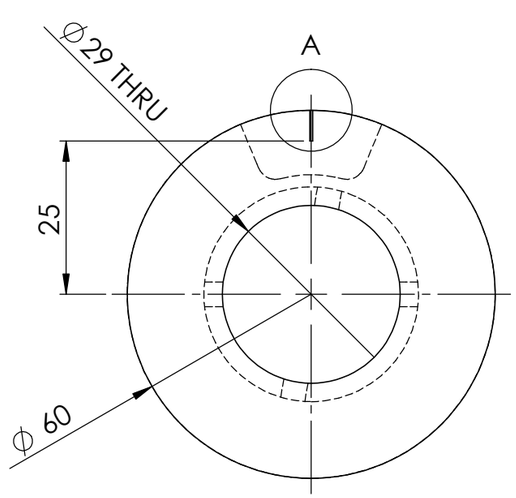

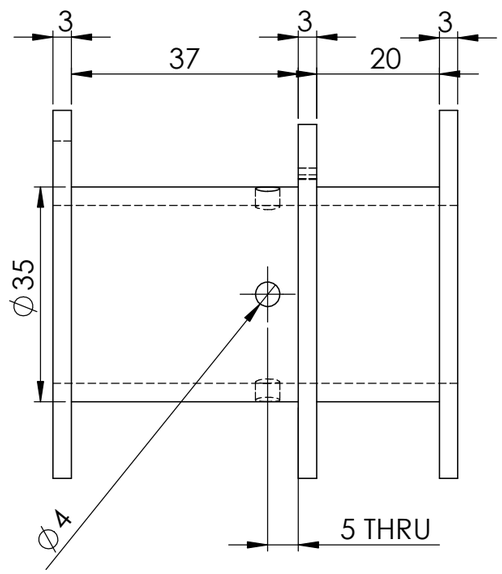

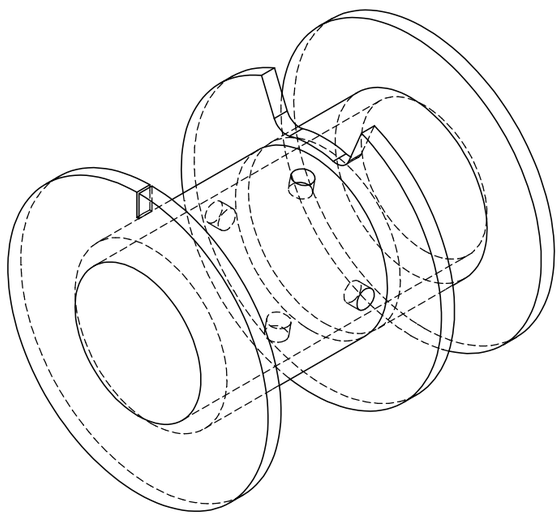

STAINLESS
QTY: 1

SAME AS BEFORE BUT SMALLER SLIT FOR SMALLER STRAIN PLATE

A4 Portrait	University of Cape Town Department of Mechanical Engineering			
	Title: Long Brace Inner			
Part Finish	Scale: 1:2	Date: 18/05/12	Sheet1	of 1
Material:	Drawn By:	Drawing Number		

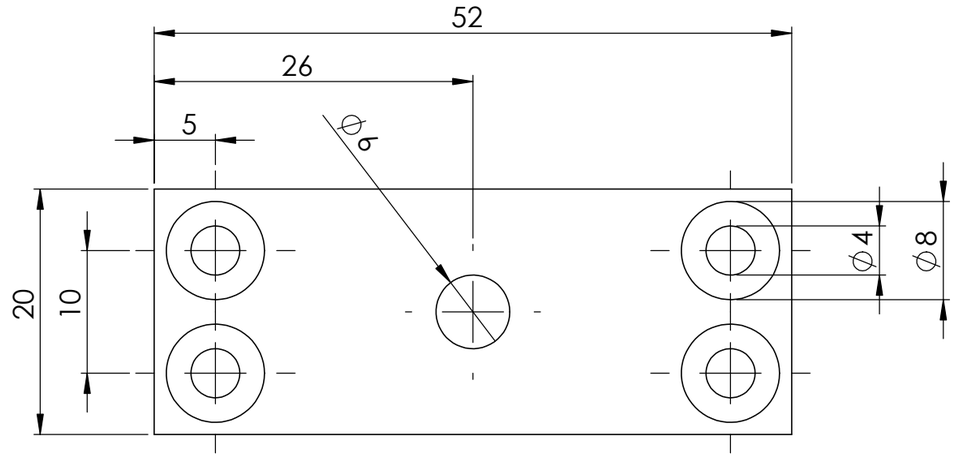

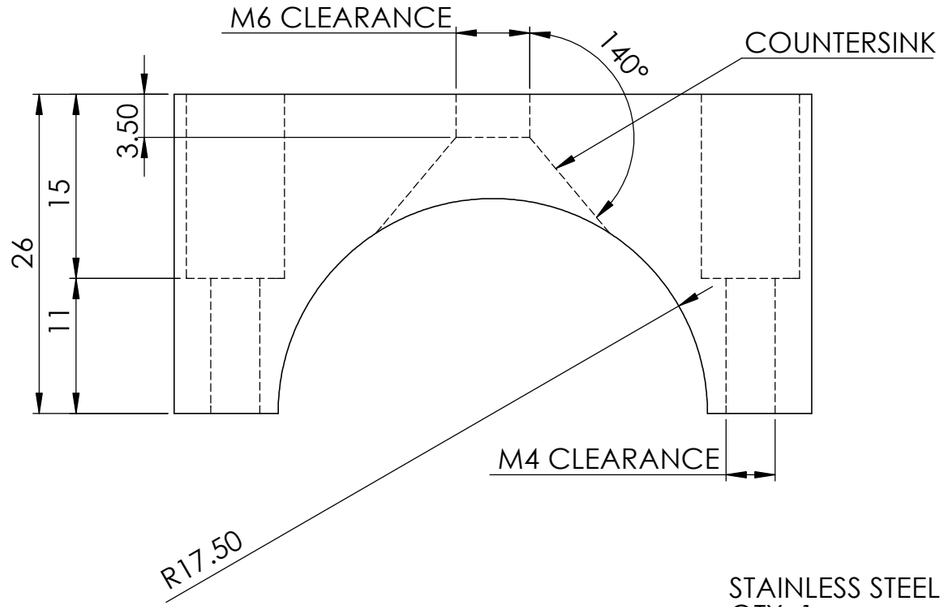

STAINLESS STEEL
QTY: 1

A4 Portrait	**University of Cape Town** **Department of Mechanical Engineering**			
	Title: **Long Bracket Bottom**			
Part Finish	**Scale:** **1:1**	**Date:** **18/05/12**	**Sheet1**	**of** **1**
Material:	Drawn By:		**Drawing Number** PART 2	

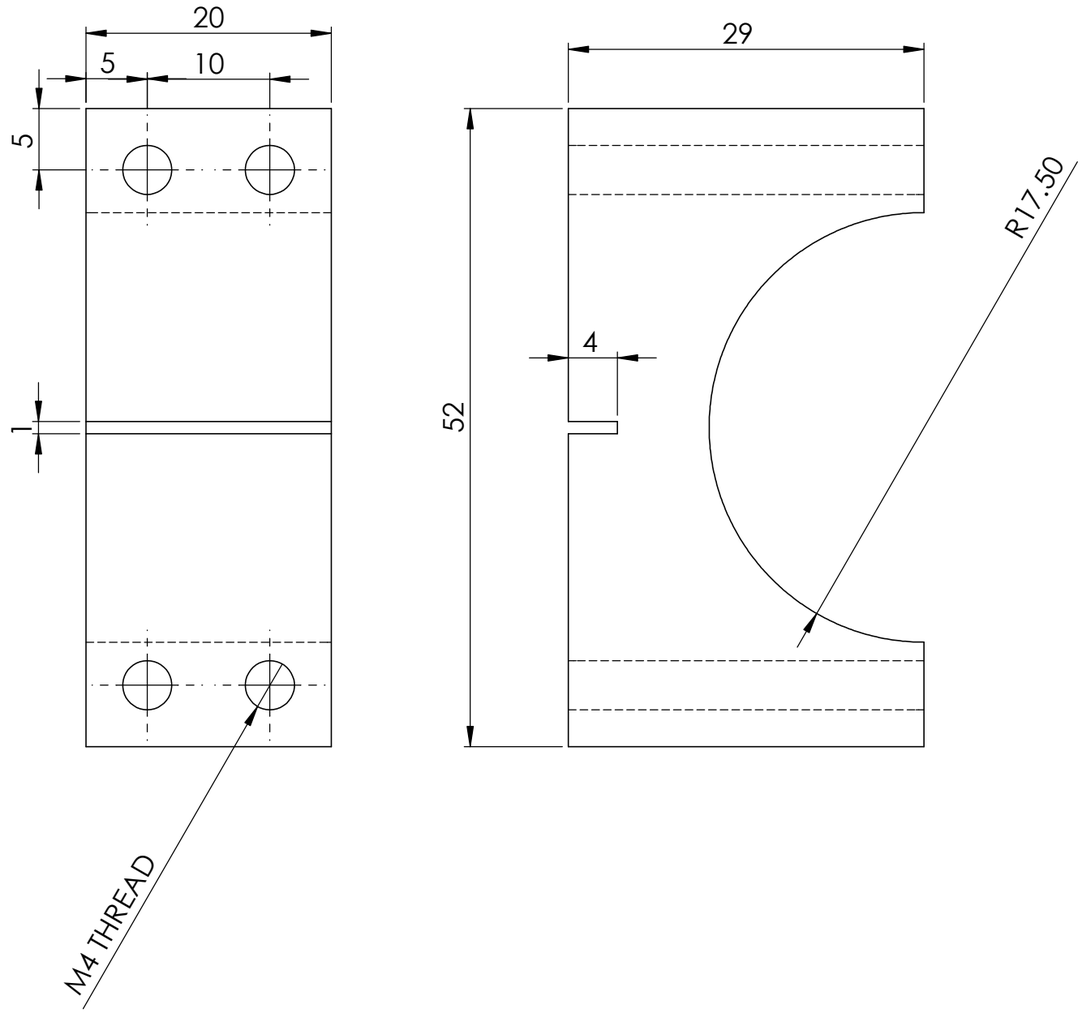

STAINLESS STEEL
QTY: 1

A4 Portrait	**University of Cape Town** **Department of Mechanical Engineering**			
	Title: **Long Bracket Top**			
Part Finish	**Scale:** 1:1	**Date:** 18/05/12	**Sheet1**	**of** 1
Material:	Drawn By:		**Drawing Number** Part 3	

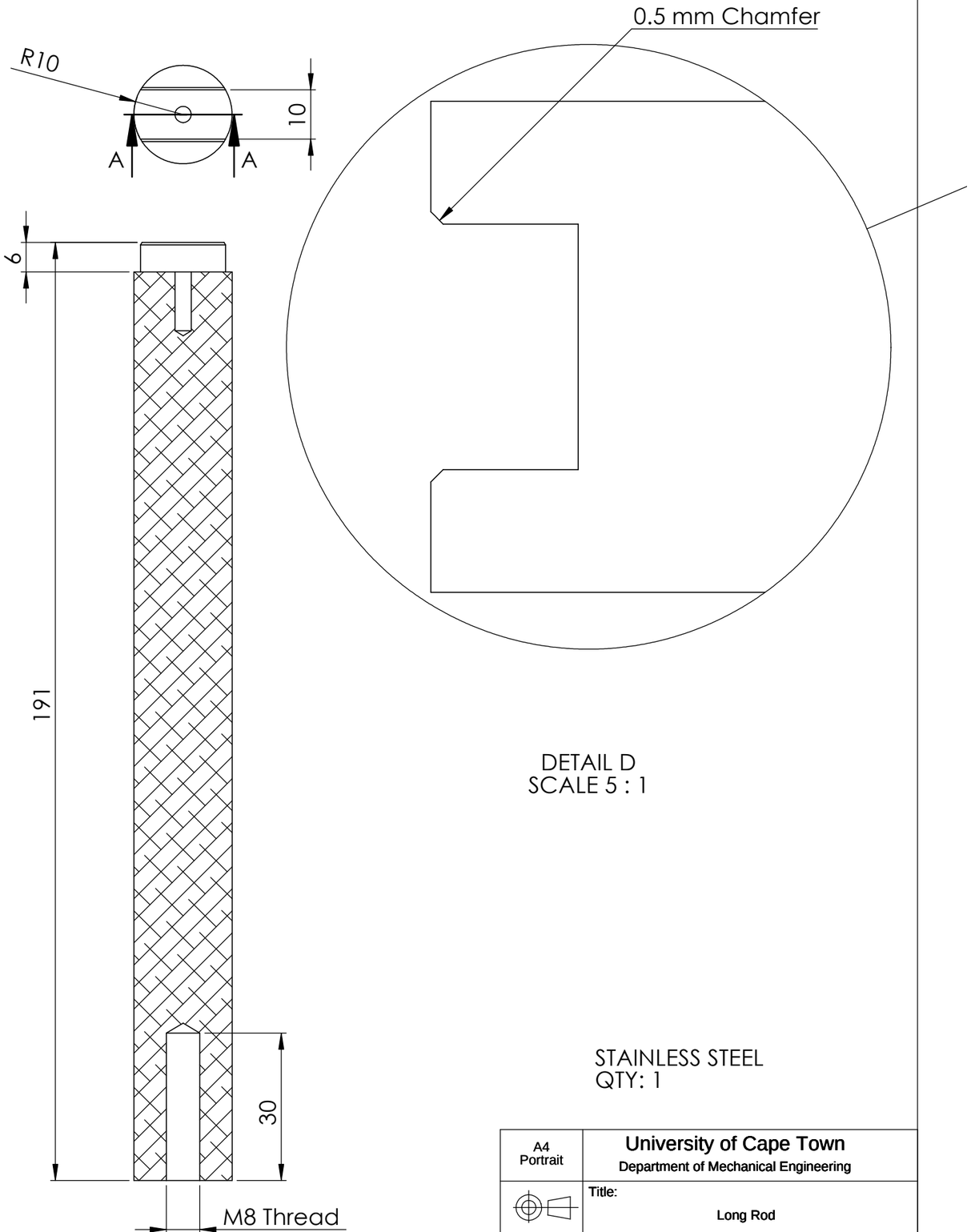

DETAIL D
SCALE 5 : 1

SECTION A-A
SCALE 1 : 1

STAINLESS STEEL
QTY: 1

A4 Portrait	**University of Cape Town** **Department of Mechanical Engineering**			
	Title: **Long Rod**			
Part Finish	**Scale:** **1:2**	**Date:** **18/05/12**	**Sheet1**	**of** **1**
Material:	Drawn By:		**Drawing Number** Part 1	

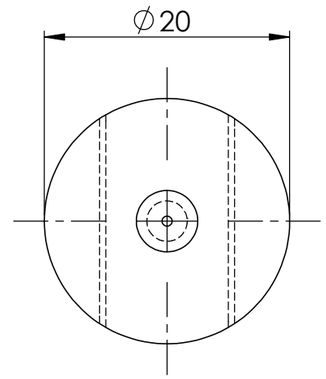

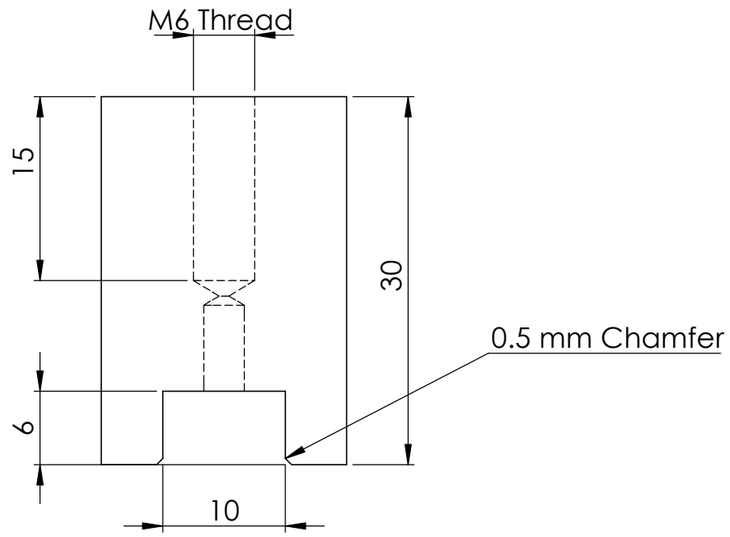

A4 Portrait	University of Cape Town Department of Mechanical Engineering			
	Title: Longrod Top			
Part Finish	Scale: 2:1	Date: 18/05/12	Sheet1	of 1
Material:	Drawn By:		Drawing Number Part 8	

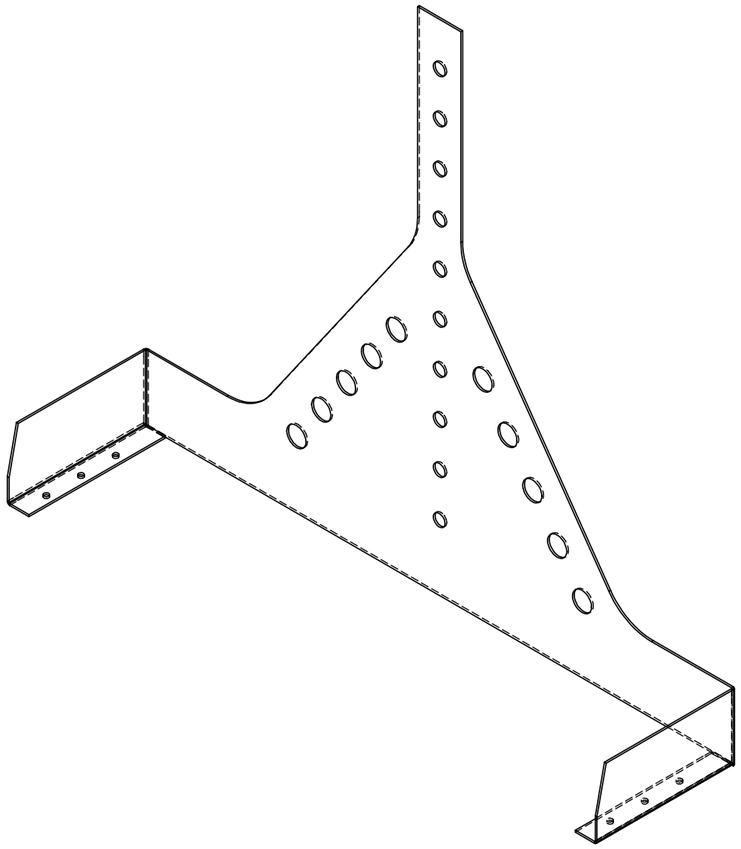

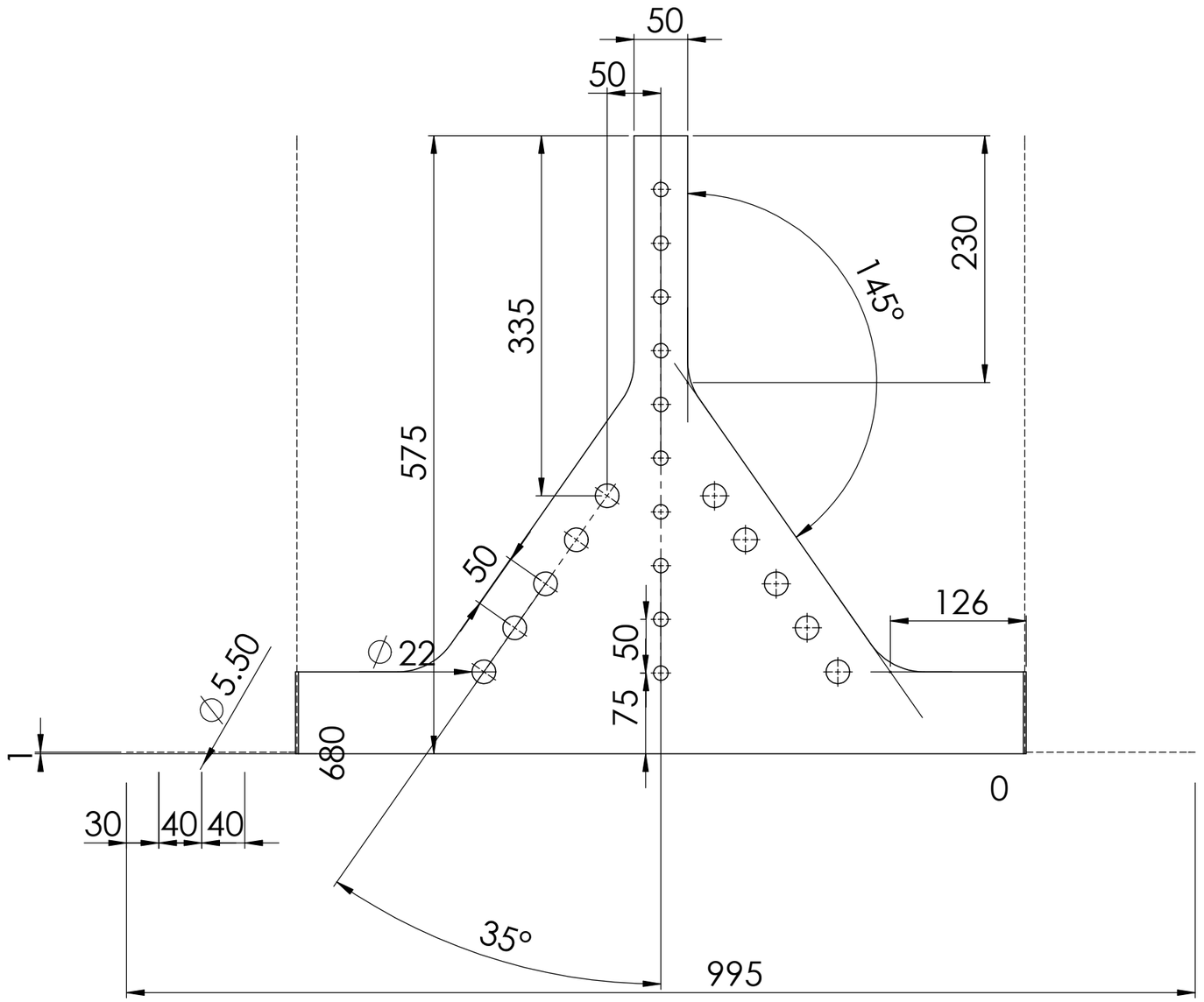

Athicker plate would be better. Around 2mm should work as this will need to be welded onto the frame

UNLESS OTHERWISE SPECIFIED: DIMENSIONS ARE IN MILLIMETERS SURFACE FINISH: TOLERANCES: LINEAR: ANGULAR:		FINISH:			DEBUR AND BREAK SHARP EDGES	DO NOT SCALE DRAWING	REVISION
	NAME	SIGNATURE	DATE			TITLE:	
DRAWN							
CHK'D							
APPV'D							
MFG							
Q.A				MATERIAL:		DWG NO. Part2	A3
				WEIGHT:		SCALE:1:10	SHEET 1 OF 1

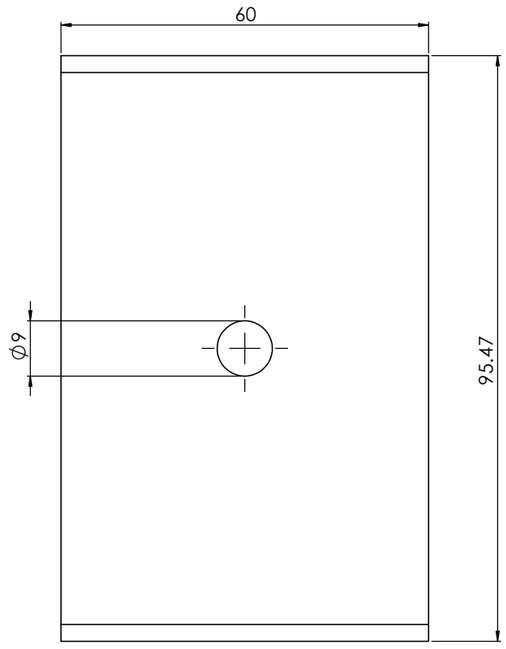

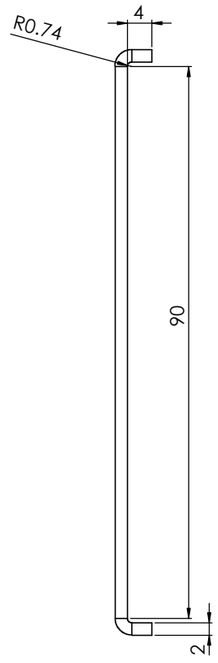

Plate thickness not specific. 1,5 and thicker should work. 2mm is preffered

UNLESS OTHERWISE SPECIFIED: DIMENSIONS ARE IN MILLIMETERS SURFACE FINISH: TOLERANCES: LINEAR: ANGULAR:	FINISH:		DEBUR AND BREAK SHARP EDGES	DO NOT SCALE DRAWING	REVISION
	NAME	SIGNATURE	DATE	TITLE: Bent steel plate	
DRAWN					
CHK'D					
APPV'D					
MFG					
Q.A.					
			MATERIAL:	DWG NO. Plate	A2
			WEIGHT:	SCALE:2:1	SHEET 1 OF 1

Appendix B

Cadaver Results

0 Degree Cadaver Results							
Specimen	Point 1	Point 2	Point 3	Point 4	Point 5	Point 6	Point 7
Cadaver 1 Right	143	83	123	60	61	128	90
	116	123	125	60	47	101	112
	142	113	119	60	51	135	76
	130	114	123	60	53	121	93
Cadaver 1 Left	107	109	74	61	65	100	93
	99	93	71	67	54	108	88
	156	106	83	72	52	101	108
	124	102	80	57	61	123	96
Cadaver 2 Right	90	88	69	85	75	96	45
	98	92	70	80	75	70	44
	94	86	80	74	77	88	51
	94	72	79	66	76	69	44
Cadaver 2 Left	132	112	64	64	74	62	42
	154	112	68	76	58	50	34
	145	140	66	60	82	50	36
	144	104	60	68	76	50	48
Cadaver 3 Right	133	81	98	60	43	65	57
	127	99	103	47	56	59	55
	115	85	84	53	50	58	42
	139	85	117	54	60	61	51
Cadaver 3 Left	No Data	No Data	92	71	82	94	74
	No Data	No Data	91	71	87	106	65
	No Data	No Data	86	64	73	104	68
	No Data	No Data	85	60	75	108	57
Cadaver 4 Right	109	89	91	61	67	106	72
	93	112	82	83	76	107	82
	97	93	85	63	83	118	68
	101	102	95	64	60	100	66
Cadaver 4 Left	110	117	104	114	80	90	72
	108	100	88	111	86	94	61
	111	95	120	110	77	90	56
	113	102	117	101	88	100	64

Table 5.1: Strain data collected at 0 degrees of flexion from all cadaver specimens

90 Degree Cadaver Results							
Specimen	Point 1	Point 2	Point 3	Point 4	Point 5	Point 6	Point 7
Cadaver 1 Right	0	0	8	28	20	34	37
	0	0	5	32	24	38	45
	0	0	5	26	24	38	46
	0	0	5	27	27	37	35
Cadaver 1 Left	0	0	10	39	55	46	38
	0	0	9	36	55	50	30
	0	0	8	34	49	45	36
	0	0	9	39	53	54	34
Cadaver 2 Right	0	0	32	90	99	99	111
	0	0	0	94	110	103	130
	0	0	0	96	128	109	108
	0	0	0	93	130	0	0
Cadaver 2 Left	No data due to cadaver decay						
Cadaver 3 Right	0	0	0	84	138	140	122
	0	0	0	97	132	149	123
	0	0	0	104	149	144	130
	0	0	0	104	137	133	125
Cadaver 3 Left	0	0	6	53	98	109	142
	0	0	5	49	86	104	165
	0	0	6	55	93	97	161
	0	0	5	50	96	101	152
Cadaver 4 Right	0	0	71	145	146	172	233
	0	0	95	161	143	173	228
	0	0	114	161	162	187	231
	0	0	94	156	140	181	204
Cadaver 4 Left	0	0	65	71	134	104	109
	0	0	50	98	112	81	105
	0	0	48	97	104	101	98
	0	0	45	135	100	91	128

Table 5.2: Strain measurements collected at 90 degrees for al cadaver specimen

Appendix C

Q - Q Plots of Cadaver Results at 0 and 90 Degrees

0 Degree Q-Q Plots

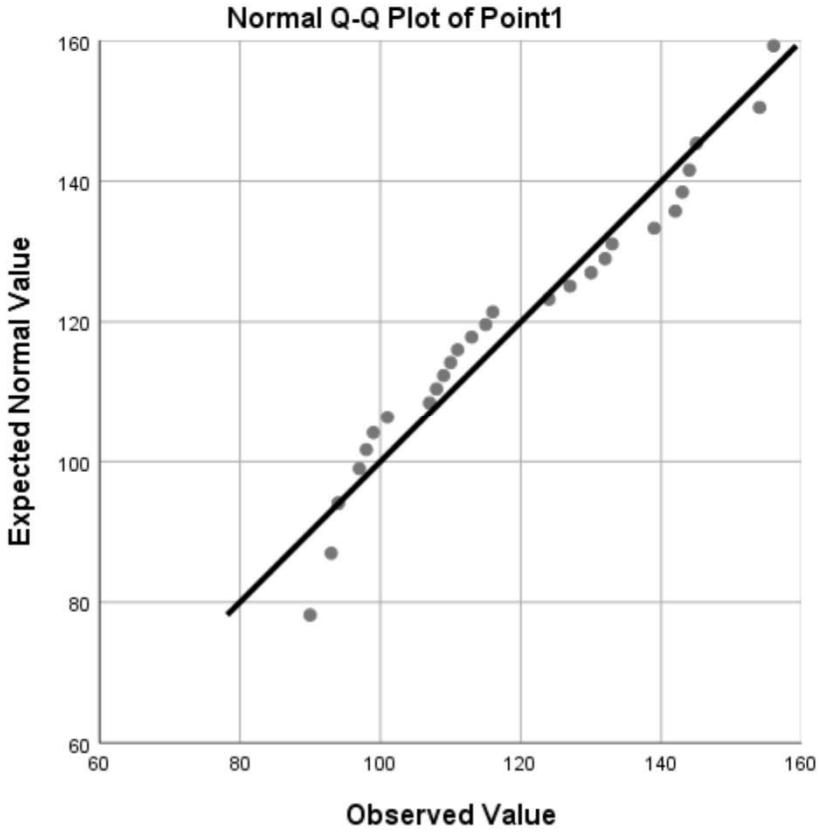

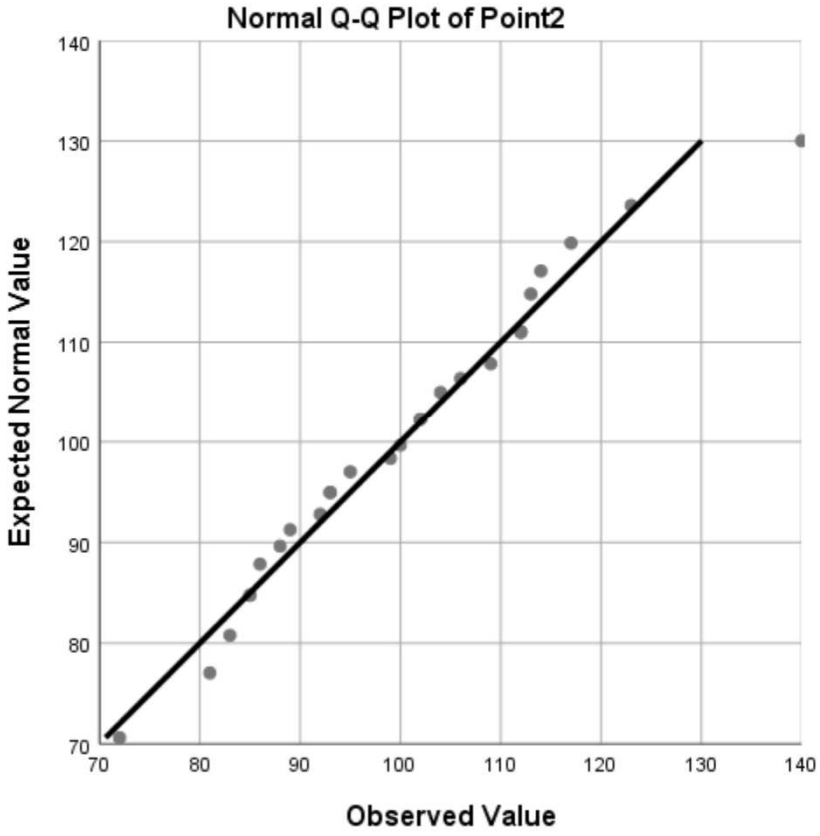

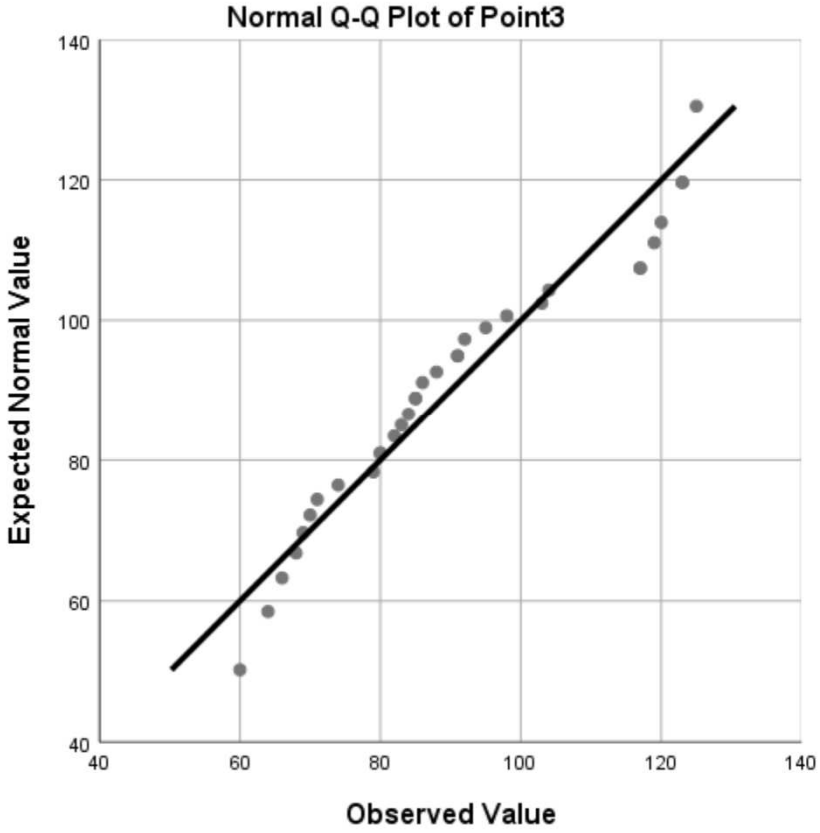
Normal Q-Q Plot of Point3
Expected Normal Value
Observed Value
140
120
100
80
60
40
40
60
80
100
120
140

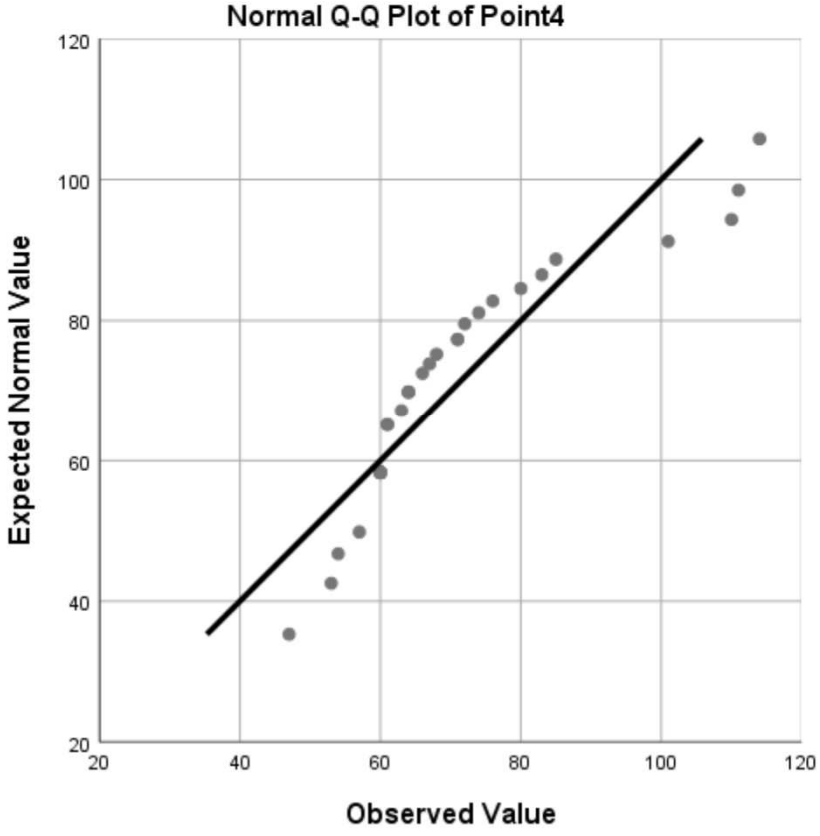
Normal Q-Q Plot of Point4
Expected Normal Value
Observed Value
120
100
80
60
40
20
20
40
60
80
100
120

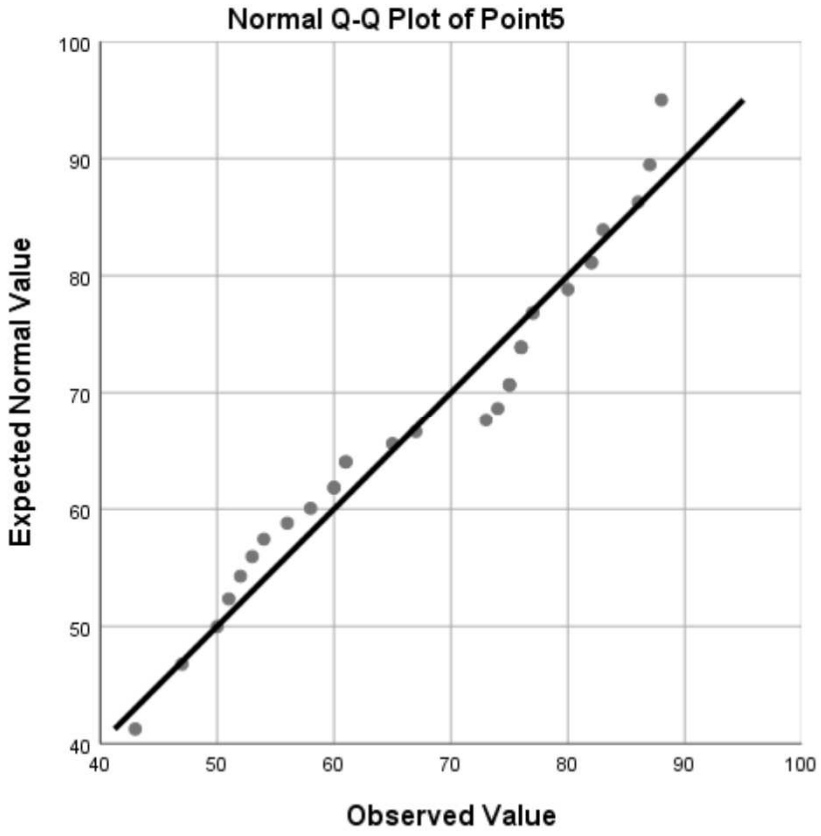
Normal Q-Q Plot of Point5
Expected Normal Value
Observed Value
100
90
80
70
60
50
40
40
50
60
70
80
90
100

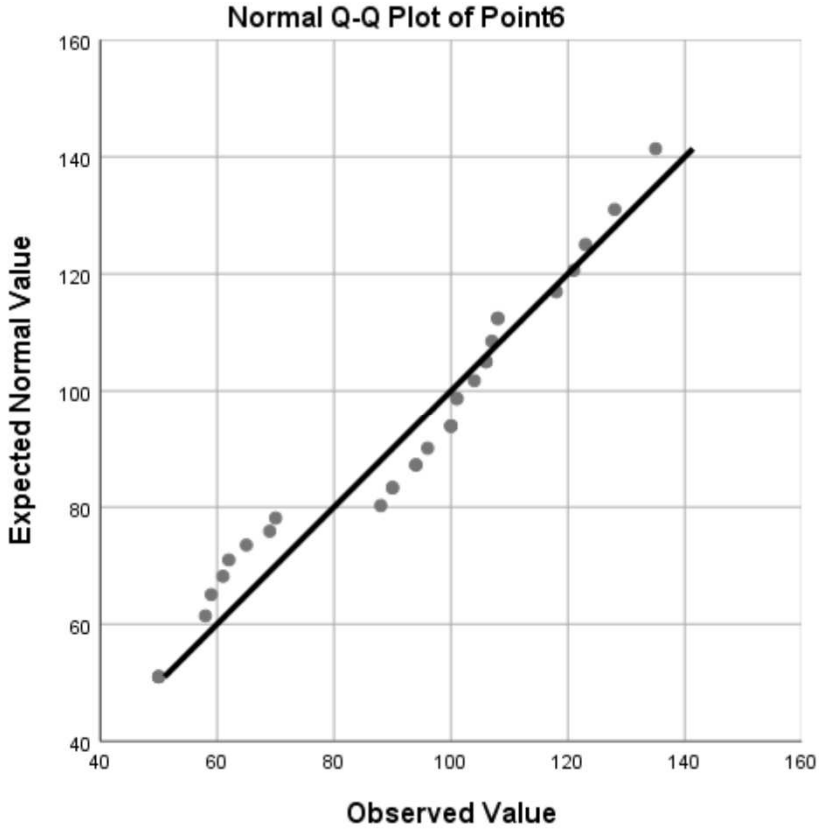
Normal Q-Q Plot of Point6
Expected Normal Value
Observed Value
160
140
120
100
80
60
40
40
60
80
100
120
140
160

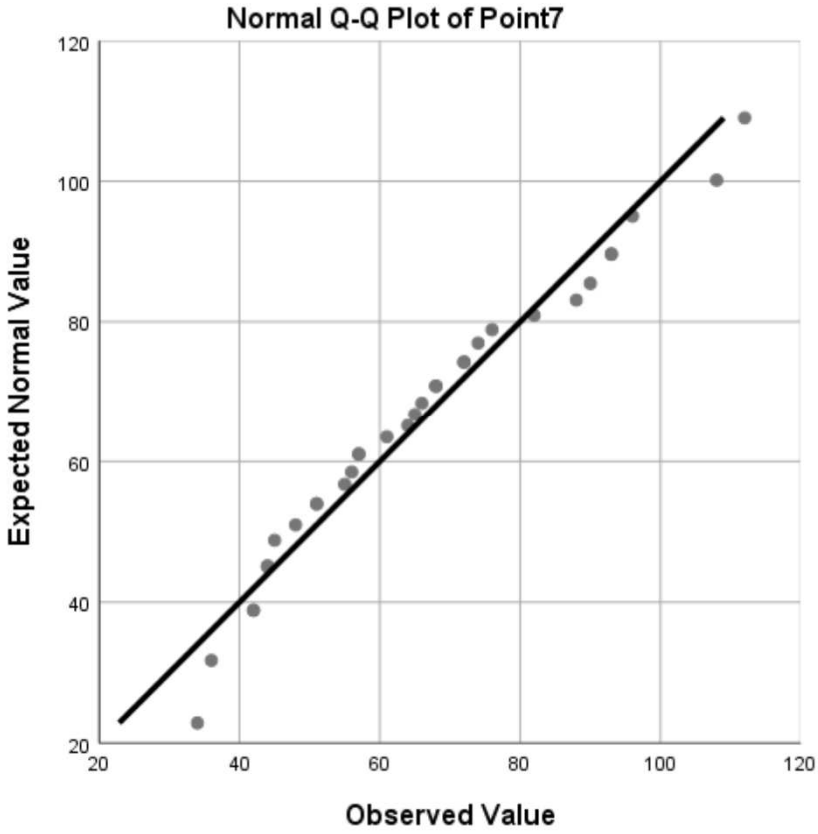
Normal Q-Q Plot of Point7
Expected Normal Value
Observed Value
120
100
80
60
40
20
20
40
60
80
100
120

90 Degree Q-Q Plots

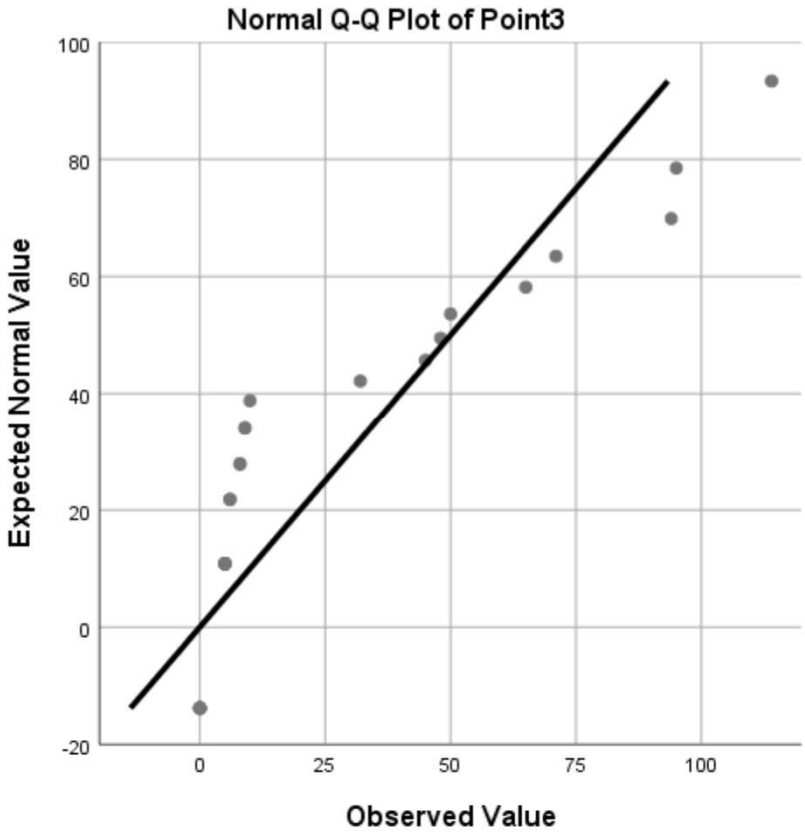

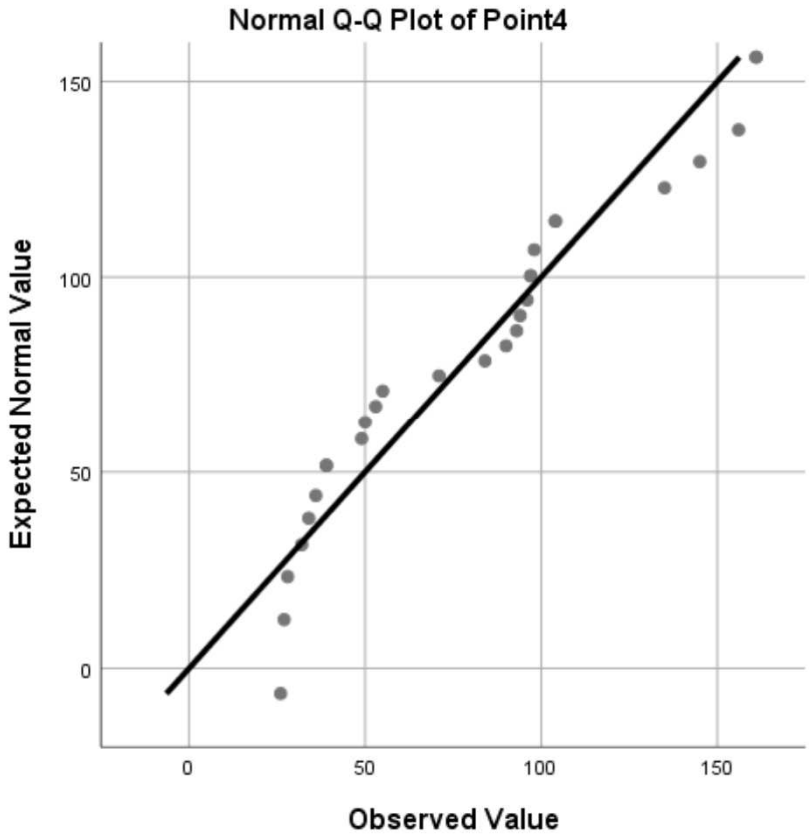

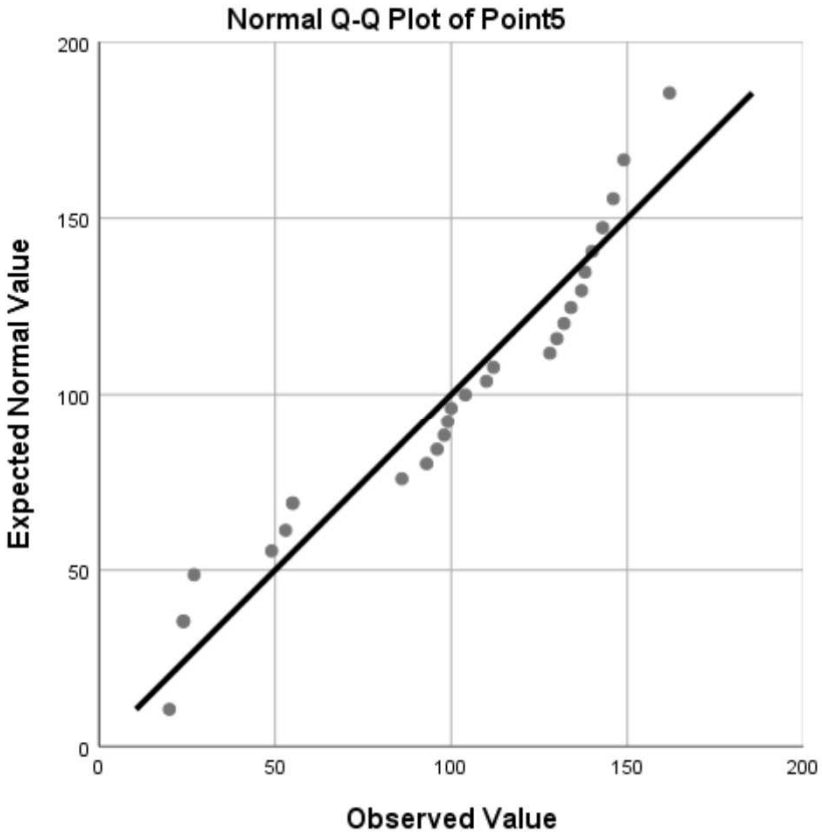
Normal Q-Q Plot of Point5
Expected Normal Value
Observed Value
0
50
100
150
200

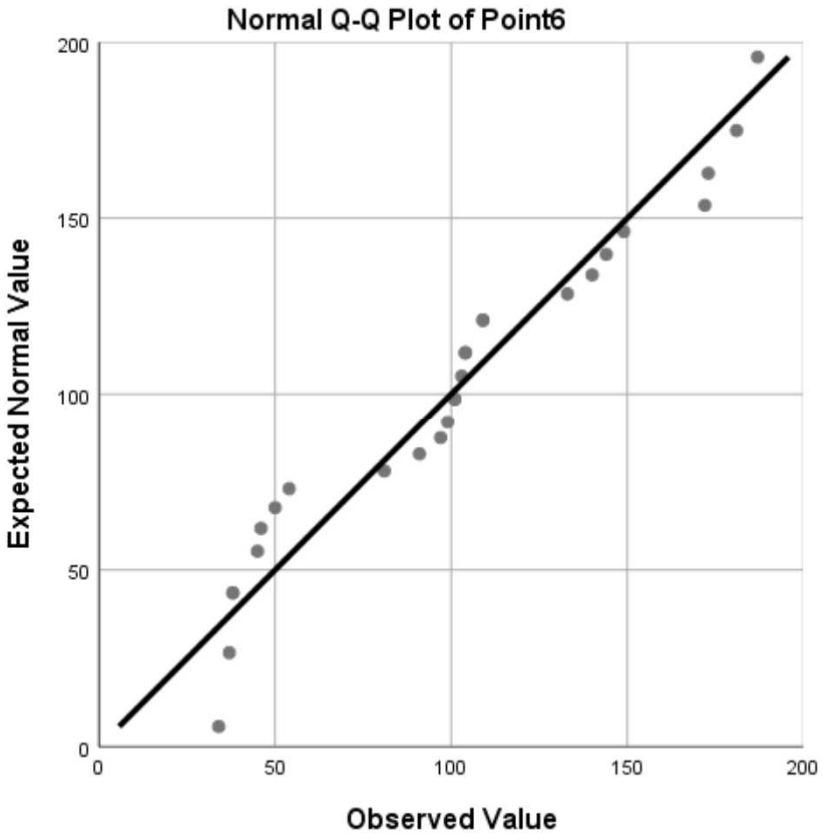
Normal Q-Q Plot of Point6
Expected Normal Value
Observed Value
0
50
100
150
200

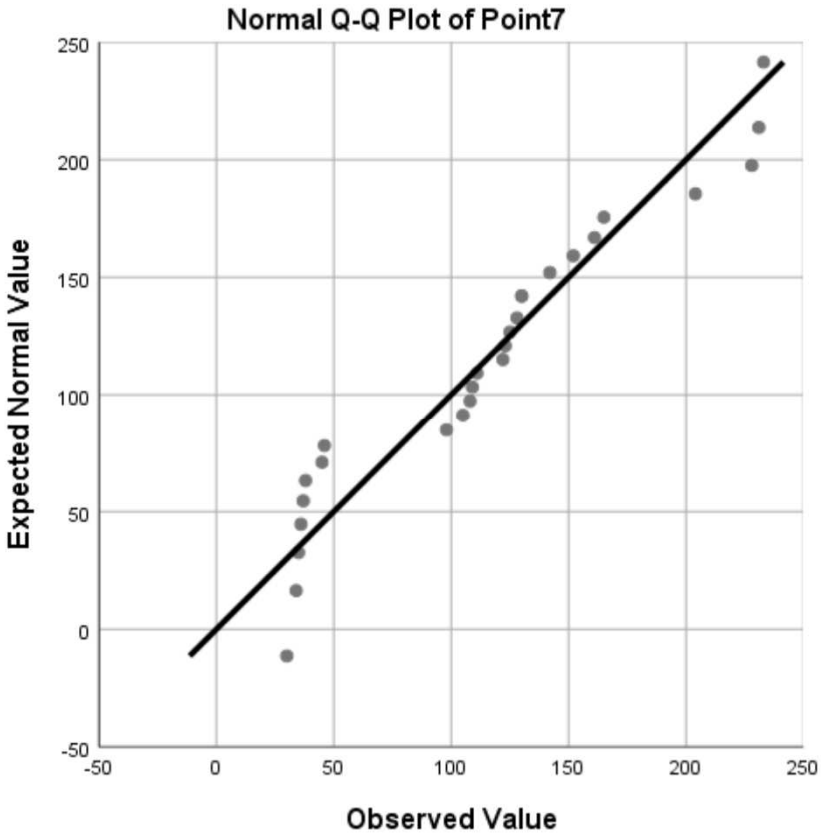
Normal Q-Q Plot of Point7
Expected Normal Value
Observed Value
250
200
150
100
50
0
-50
-50
0
50
100
150
200
250

Appendix D

Human Research Ethics Committee (HREC) Approval

UNIVERSITY OF CAPE TOWN
Faculty of Health Sciences
Human Research Ethics Committee

Room E52-24 Old Main Building
Groote Schuur Hospital
Observatory 7925
Telephone [021] 404 7682 • **Facsimile** [021] 406 6411
Email: nosi.tsama@uct.ac.za
Website: www.health.uct.ac.za/fhs/research/humanethics/forms

22 February 2017

HREC REF: 048/2017

Dr S Sivarasu
Human Biology
Biomedical Engineering
Anatomy Building

Dear Dr Sivarasu

PROJECT TITLE: SURGICAL INSERTION POINT OPTIMISATION OF THE LATISSIMUS DORSI USING BIOMECHANICAL VERIFICATION AND VALIDATION PROCESSES (M.Sc.-candidate-S Thompson)

Thank you for submitting your study to the Faculty of Health Sciences Human Research Ethics Committee for review

It is a pleasure to inform you that the HREC has **formally approved** the above-mentioned study.

Approval is granted for one year until the 28th February 2018. This is subject to the submission of an updated protocol reflecting changes that were communicated to the reviewer through your DRC Chair.

Please submit a progress form, using the standardised Annual Report Form if the study continues beyond the approval period. Please submit a Standard Closure form if the study is completed within the approval period.
(Forms can be found on our website: www.health.uct.ac.za/fhs/research/humanethics/forms)

We acknowledge that the student Seth Thompson will be involved in this study.

Please note that for all studies approved by the HREC, the principal investigator **must** obtain appropriate institutional approval before the research may occur.

Please quote the HREC REF in all your correspondence.

Please note that the ongoing ethical conduct of the study remains the responsibility of the principal investigator.

Yours sincerely

pp T Burgess
PROFESSOR M BLOCKMAN
CHAIRPERSON, FHS HUMAN RESEARCH ETHICS COMMITTEE

Federal Wide Assurance Number: FWA00001637.
Institutional Review Board (IRB) number: IRB00001938

This serves to confirm that the University of Cape Town Human Research Ethics Committee complies to the Ethics Standards for Clinical Research with a new drug in patients, based on the Medical Research Council (MRC-SA), Food and Drug Administration (FDA-USA), International Convention on Harmonisation Good Clinical Practice (ICH GCP), South African Good Clinical Practice Guidelines (DoH 2006), based on the Association of the British Pharmaceutical Industry Guidelines (ABPI),and Declaration of Helsinki (2013) guidelines.
The Human Research Ethics Committee granting this approval is in compliance with the ICH Harmonised Tripartite Guidelines E6: Note for Guidance on Good Clinical Practice (CPMP/ICH/135/95) and FDA Code Federal Regulation Part 50, 56 and 312.